National Library of Canada
Acquisitions and Bibliographic Services Branch
395 Wellington Street
Ottawa, Ontario
K1A 0N4

Bibliothèque nationale du Canada
Direction des acquisitions et des services bibliographiques
395, rue Wellington
Ottawa (Ontario)
K1A 0N4

Your file Votre référence

Our file Notre référence

NOTICE

The quality of this microform is heavily dependent upon the quality of the original thesis submitted for microfilming. Every effort has been made to ensure the highest quality of reproduction possible.

If pages are missing, contact the university which granted the degree.

Some pages may have indistinct print especially if the original pages were typed with a poor typewriter ribbon or if the university sent us an inferior photocopy.

AVIS

La qualité de cette microforme dépend grandement de la qualité de la thèse soumise au microfilmage. Nous avons tout fait pour assurer une qualité supérieure de reproduction.

S'il manque des pages, veuillez communiquer avec l'université qui a conféré le grade.

La qualité d'impression de certaines pages peut laisser à désirer, surtout si les pages originales ont été dactylographiées à l'aide d'un ruban usé ou si l'université nous a fait parvenir une photocopie de qualité inférieure.

Canada

Surface Loading of a Thin-walled Toroidal Shell

by

Fan Zhang

Thesis submitted to School of Graduate Studies
as partial fulfillment of the requirements
for the degree of M.A.Sc. in
Mechanical Engineering

UNIVERSITY OF OTTAWA

ISBN 0-315-80058-5

UNIVERSITÉ D'OTTAWA
UNIVERSITY OF OTTAWA

ABSTRACT

The present study is concerned with the series solution based on the Sanders shell theory for the linear elastic problems of the surface loading of thin-walled toroidal shells. The Sanders theory is considered to be one of the most accurate first order theories. For toroidal shells, series solutions have been given by several authors, using other theories and furthermore using a stress approach. In the present study a displacement approach is taken. The governing equations are first developed in toroidal coordinates. The loading case of a pad of uniform normal pressure is then considered in detail, and series expansions are written for the load, displacement and stress terms. Results are computed using the shell theory for sample problems. To check the accuracy of the theory, the results are compared with numerical results obtained using the Finite Element Method (FEM), the Mushtari-Vlasov–Donnel (MVD) and Flügge shell theories. There is a close agreement in the results. The Sanders shell theory is then applied to the problem of local loads on sectorial toroidal shells. The results are compared with results for corresponding cylindrical shells. Three tables are given summarizing results for characteristic displacements and stresses in a number of shells, covering a wide range of geometric parameters. The results given provide practical information for structural analysts and designers of piping and vessels, and furthermore give information about the Sanders shell theory and FEM solution characteristics.

ACKNOWLEDGEMENT

The author wishes to express her gratitude to Dr. D. Redekop for his continuous encouragement, invaluable suggestions, and patient guidance throughout the research.

Special thanks to the author's parents and husband for their moral support and encouragement during the study.

The financial support received from the University of Ottawa, and the Natural Sciences and Engineering Research Council of Canada is gratefully acknowledged.

Contents

List of Figures

List of Tables

Nomenclature

a, b, c, d	constant coefficients
D	bending rigidity, defined as $Et^3/[12(1-\nu^2)]$
E	Young's modulus
$\mathbf{e}_\theta, \mathbf{e}_\eta, \mathbf{e}_r$	base unit vectors at point P
K	extensional rigidity, defined as $Et/(1-\nu^2)$
$\overline{\mathrm{K}}$	pipe factor, defined as $[lt^{1/2}/r^{3/2}]^{1/2}$
$\mathbf{i}, \mathbf{j}, \mathbf{k}$	unit vectors
l	center-line length of shell
M, N	truncation integers
$M_\theta, M_\eta, M_{\theta\eta}$	bending stress resultants
$N_\theta, N_\eta, N_{\theta\eta}$	membrane stress resultants
p	magnitude of normal pressure
Q_θ, Q_η	normal shear resultants
r	cross-sectional radius of shell
$\mathbf{r}$	radius vector
R	mean toroidal radius of shell
R_1, R_2	radii of curvature
t	thickness of shell
u, v, w	displacement components

x, y, z	Cartesian coordinates
α	longitudinal angular distance to center of load region from shell mid-length
β	circumferential angular distance to center of load region from extrados
γ	radius ratio, defined as r/R
Γ	pipe factor, defined as r^2/Rt
δ	longitudinal angular length of load region
$\epsilon_\theta, \epsilon_\eta, \epsilon_{\theta\eta}$	strain components
ζ	$= 1 + \gamma cos\theta$
η	toroidal coordinate, defined as $\rho\phi$
θ	circumferential angular coordinate
$\kappa_\theta, \kappa_\eta, \kappa_{\theta\eta}$	change of curvature components
λ	circumferential angular length of load region
μ_m	$= m\pi\gamma/\psi$
ν	Poisson ratio
$\nu_1 - \nu_{41}$	coefficients for the Sanders theory
ξ_1, ξ_2	*Lamé* parameters
ρ	radius ratio, defined as R/r
$\sigma_\theta, \sigma_\eta$	direct stress components
ϕ	longitudinal angular coordinate
ψ	angular length of shell
ϕl	$= \psi/2$
Ω	pipe factor, defined as $lt^{1/2}/r^{3/2}$

Chapter 1

Introduction

1.1 Thin-walled Toroidal Shell

Because of its specific geometrical configuration, the toroidal shell is utilized in many areas of mechanical engineering. Thin-walled toroidal shells (sectorial or complete) are widely used in nuclear and other power industries. Examples include Tokamak-type fusion reactors, cooling towers, piping elbows and pipe bends (Figs. 1.1-1.4). Trunnion supports (Fig. 1.5), ram bending (Fig. 1.6), construction attachments, and accidental loads are among the causes of surface loading of toroidal shells. A toroidal shell is much more flexible in bending than a cylindrical shell. Therefore, it is of great importance to examine the effects of stress and displacement of a toroidal shell.

The general methods for resolving the problem of a toroidal shell are the series method and the finite element method. The series solution is generally more efficient and more accurate in calculations. Although the finite element method is often more convenient than the series method, it is only a discrete approximate value. In the present study,

a series solution is used based on the linear Sanders shell theory [1]. This theory is considered to be one of the most accurate first order theories [2].

1.2 The Sanders Shell Theory

This theory was originally derived by Sanders in 1959, on the basis of Love's [3] first-approximation theory, in which all of Love's original assumptions are preserved. In contrast to the results of Love's theory, all strains in the proposed theory vanish for rigid-body motions. This theory is recognized as one of the most accurate first order theories. The full theoretical development, in toroidal coordinates, is given in Chapter 3.

1.3 Mushtari-Vlasov-Donnel (MVD) Shell Theory

This theory was developed from Love's theory on the basis of order-of- magnitude considerations and is much easier to get results than the Sanders theory. It is therefore preferable in engineering applications if its accuracy is satisfactory for the purposes of engineering. The full displacement development, in toroidal coordinates, was given by Redekop [4].

1.4 Finite Element Method (FEM)

The finite element method is a powerful and popular technique for the numerical solution of a variety of problems in engineering. The fundamental concept of this method is

that any continuous quantity can be approximated by a discrete model having a finite number of degrees of freedom. The finite element method combines several mathematical concepts to produce a system of linear or non-linear equations. The number of equations is usually very large, anywhere from twenty thousand or more, and requires the computational power of the digital computer.

Numerous commercial software packages are now available for FEM implementation. The commercial program ADINA [5] is one of them. ADINA (Automatic Dynamic Incremental Non-linear Analysis) was developed at MIT (Massachusetts Institute of Technology) by Klaus-Jürgen Bathe. It is used in displacement and stress analysis. The isoparametric thin shell element and shell pressure loading are available in these computer programs. There are three displacement and two rotation degrees of freedom at each node. The element was used here as part of a linear elastic analysis.

In general, a proper finite element solution should converge and the accuracy of the calculation usually (but not always) increases as the number of degrees of freedom in the model increases.

The phenomenon of an element being much too stiff is referred to in the literature as element locking [5]. In essence, the phenomenon arises because the interpolation functions used for an element are not able to represent zero (or very small) shearing or membrane strains. If the element cannot represent zero shearing strains, but the physical situation corresponds to zero (or very small) shearing strains, then the element becomes very stiff as its thickness over length ratio decreases. Namely, for thin shells when full integration is used to evaluate the stiffness matrix, overstiff solutions are often produced owing to shear and membrane locking.

1.5 Outline of Present Investigation

The present study is concerned mainly with the series solution based on the Sanders shell theory. Attention is given to the problems of surface loading of a thin-walled toroidal shell. The study is carried out with two main objectives:

First, to develop Sanders shell theory in toroidal coordinates in a displacement form. In this study, the loading case of a pad of uniform normal pressure on the toroidal shell surface is considered in detail. The results are obtained by means of a computer program based on the Sanders shell theory. To check the accuracy of the theory, the results are compared with numerical results of some other method and shell theories.

Second, to provide practical information for toroidal shells, detailed displacement and stress results are given for a specific toroidal shell with loadings centered at three positions; the crown circles, the extrados, and the intrados. These results are compared with results for a corresponding cylindrical shell. Summaries of results are given for displacements and stresses in a number of toroidal shells, covering a wide range of geometric parameters.

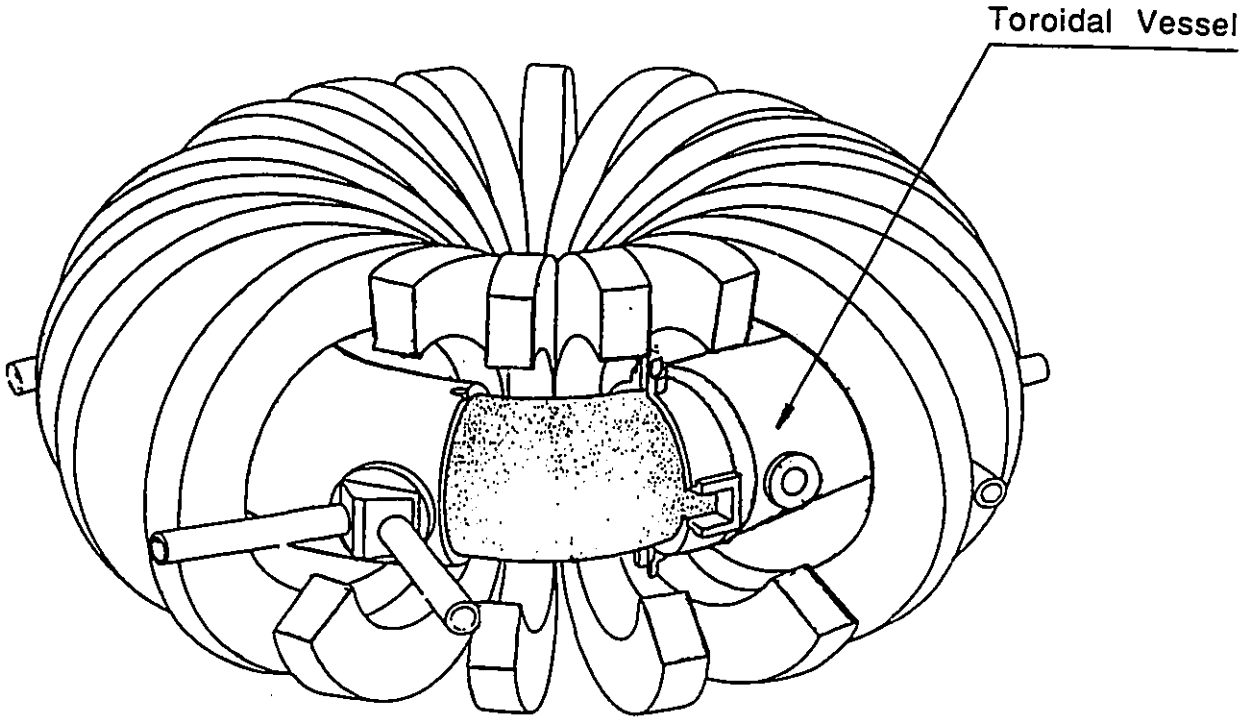

Figure 1.1: Tokamak-type fusion reactor

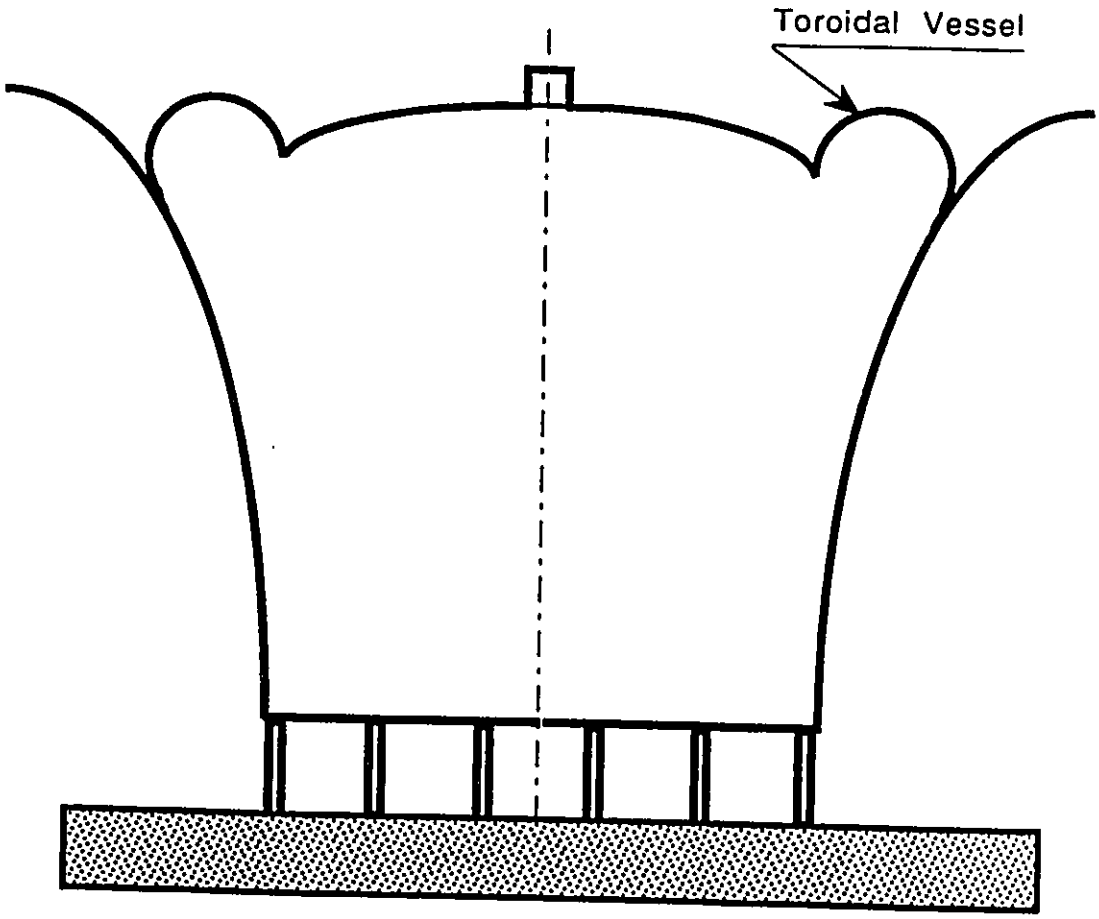

Figure 1.2: Schematic view of cooling tower

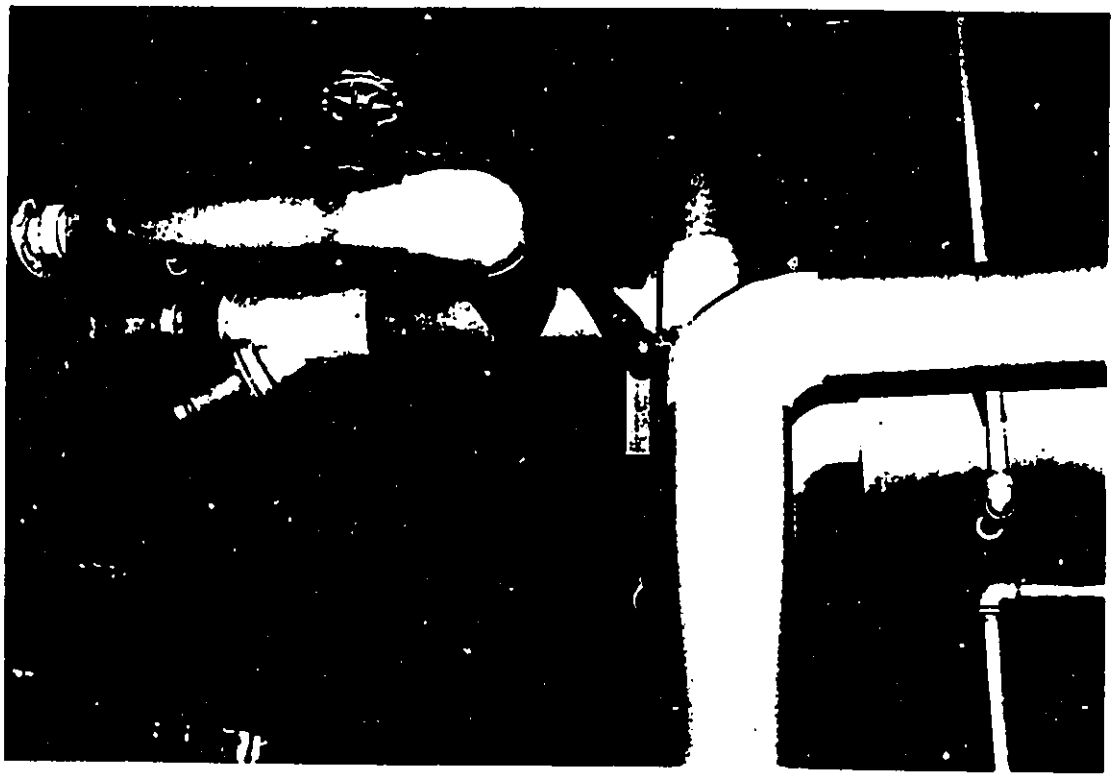

Figure 1.3: Piping elbows

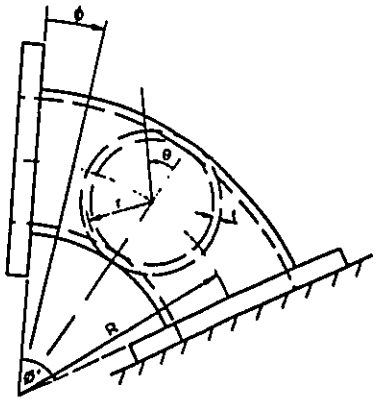

Figure 1.4: Flange-ended pipe bend

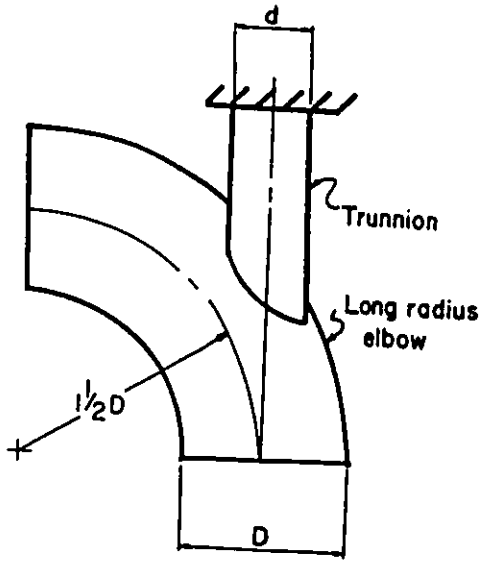

Figure 1.5: Trunnion elbow support

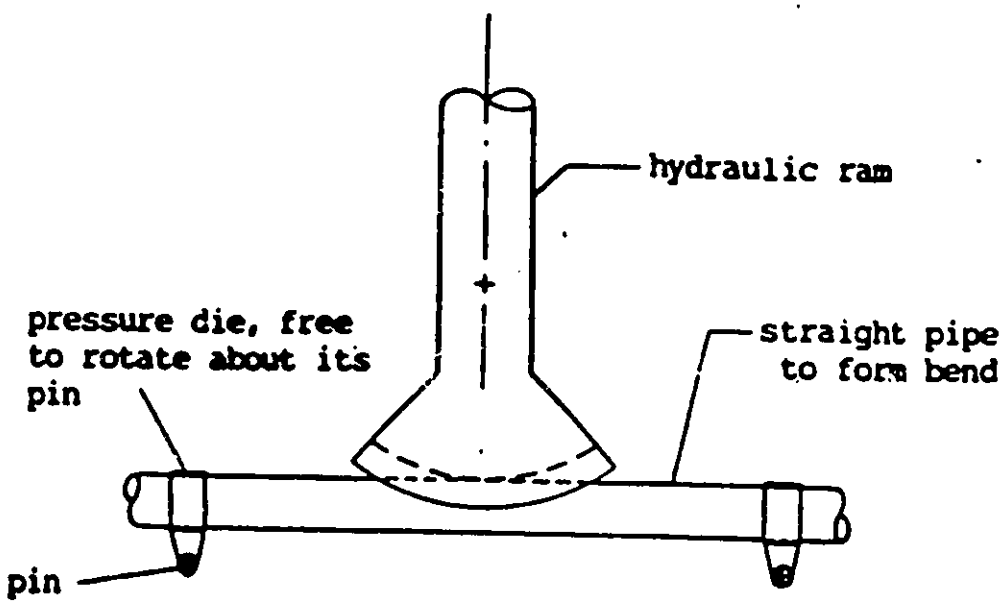

Figure 1.6: Schematic view of ram bending

Chapter 2

Literature Survey

In this chapter a survey of the literature of the linear thin-walled models of the state of stress and displacement in toroidal shells (sectorial or complete) is presented. Emphasis is placed on models using the shell bending theory and the FEM.

2.1 Previous Work on Thin Shell Theory Solutions

The early models developed were for thin-walled pipe bends, and were of the one-variable type accounting for variation of stress values in the circumferential direction (of the cross-section) only. Results thus could be exact only for complete, axisymmetric toroidal shells, as there is no treatment of end conditions.

Two-variable models are required to account for a longitudinal variation of stresses, in addition to circumferential. Such models can account for the effect of end restraints in sectorial toroidal shells, such as elbows and pipe bends with terminal flanges or tan-

gent pipes. For classical geometries involving circular cross-sections and constant wall thickness, series solutions are effective. An early such solution [6] covered U-bends with fixed ends and was based on the energy method. In Thailer and Cheng presented paper, a general solution for a thin-walled pipe bend containing rigid end constraints, subjected to in-plane bending moments. Inextensibility of the meridional center line is assumed. The displacements are expanded in series form and the equations of equilibrium are guaranteed by minimizing the total potential energy. The minimization is achieved in the manner of Rayleigh-Ritz.

Linear flexure of pipe bends with flanged tangents has been comprehensively studied by Whatham and Thompson [7]. Their original solution used as dependent variables a set of the stress functions. It included Fourier series expansion in the circumferential direction and computation of a substantial number of eigenvalues for the 'end' solution. The flexibility factor was represented in graphs for 90° and 180° bends. The same problem was treated by Thomson, Spence and Findlay [8-10] by means of a trigonometric-series solution, minimizing the total potential energy.

A complete set of series solutions, based on the Novozhilov [11] equations, has been presented by Whatham [12-15]. The system equations were presented in the first of these papers. This paper gives the equations, in a form suitable for computation, for the pressurizing of pipe bends and, by superposition, for any combination of forces and moments acting on the ends, neglecting end effects for the present. The 'end effect' was covered in the second paper. Where a number of solutions of the basic equations which represent the effect of self-equilibrating end loads, decaying with distance from the ends, were developed. These may be added to the earlier solution to enable the constraints imposed by the flanges to be satisfied and yield the complete flanged bend solution. Further results, and discussion of a general computer program based on the theory, were given in last two papers [14,15]. In the first of these latter two papers, thin shell

theory is applied to pipe bends terminated by flanges or flange-ended tangent pipes and subjected to any end loading, either in-plane or out-of-plane. Graphs of flexibility factor versus pipe bend characteristic are presented for in-plane bending of a wide range of pipe elbows terminated by flanges or short flange-ended tangents. Experimental results verify the thin shell solutions for in-plane and out-of-plane bending of a flanged pipe elbow.

Further shell theory solutions for cylindrical and toroidal shells have been reviewed by Axelrad and Emmerling [20], and Redekop, Colle, and Nguyen [21]. Recently, Whatham [22] conducted a series of studies using the semi-membrane theory to determine the effect of end loads on pipe bends and elbows. A considerable portion of his work was concerned with the determination of the flexibility in bending of a toroidal shell compared with a cylindrical shell. Thompson and Spence [23] have presented a solution employing the theorem of minimum potential energy, with suitable kinematically admissible displacements. Hui and Wei [24] have presented results for toroidal shells based on the Novozhilov equations for a number of problems involving end loadings.

The effect of local loads on cylindrical shells has been studied extensively [16-19]. In [17], a Fourier series solution was detailed which enabled displacement and stresses to be obtained in the region of local loads on cylindrical vessels. To facilitate the analysis of a general load system, in the radial, tangential and longitudinal directions, a compendium of 'loading term' solutions is presented. Redekop and Azar [19] have considered the ram bending of a straight cylindrical pipe using the shell theories and FEM. The loading is idealized as a set of pads of uniform radial pressure, and results are given for the elastic range. Results for local loads represent to varying degrees of accuracy the effect of attachments, lugs, supports, blast loading, or projectile impact on the surface of the shells.

Toroidal shells are also subject to local loads, although to a lesser extent than cylin-

drical shells. Trunnion supports, construction attachments, and accidental loads are among the causes of local loads on the surface of toroidal shells. In contrast to the case of cylindrical shells, the literature for toroidal shells subject to local loads is relatively sparse. Redekop [4] has used the Mushtari-Vlasov-Donnel (MVD) [2] shell theory to obtain solutions for local loads on a toroidal shell. The problem of ram bending of a curved pipe in the linear elastic range is considered in the study.

2.2 Finite Element Modeling for Thin Shell Element

With the development of fast and powerful digital computers in recent years, the FEM has played a predominant role in numerical solutions.

The linear two-variable FEM models for toroidal shells are of two main types. The first type, employing 'elbow' elements, features a shell-type variation of values in the circumferential direction and a beam-type variation in the longitudinal direction. The second type of model, employing 'shell' elements, features shell type behavior in both directions.

A number of elbow elements have been developed for practical use. The cost of an analysis using these elements is substantially reduced. However, the elements only provide moderate accuracy.

In view of the foregoing, shell elements have been chosen by a large number of researchers in recent years. There is greater accuracy of the results using these elements. The earlier attempts to develop a general shell element were made by, among others, Gallagher [25] in 1966. He presented a quadrilateral shell element with two constant

principal radii of curvature, and Connor and Brebbia [26] in 1967 introduced a rectangular element based on shallow shell theory. Both elements used only linear distributions for membrane displacements and consequently did not include all the required rigid body modes. The resulting elements are too stiff and not efficient enough. Brebbia and Deb Nath [27] in 1970 reviewed the shell finite elements and compared their relative convergence rates with an established finite difference solution for a clamped hypar shell under uniformly distributed normal load. Yang [28] in 1973 developed a high order shell finite element with two principal radii of curvature and a twist radius. Yang and Kapania [29] in 1983 extended this element to have the geometry of a quadrilateral defined by principal lines of curvature of the shell.

A significant contribution to shell analysis was the definition of geometry using variable order polynomials and rational B-spline functions [30]. This allowed the modeling of a wide variety of shell structures with arbitrary distributions of curvatures. Recently, Hansen and Heppler [31] presented a method to enable the shell-coordinate finite elements to exactly reproduce all of the six Cartesian rigid body modes. This was accomplished by forcing the rigid-body capability as an essential requirement for the derivation of the basis functions. The method was applied to shells of revolution with straight meridians. This work was extended by Heppler *et al.* [32] to include the more general situation of arbitrary shells of revolution.

Most of the quadrilateral elements published in the literature are limited to regular shapes. This may impose a limitation on the application for this kind of elements. Recently, tensor mathematics has been used in the formulation of curved quadrilateral shell elements to overcome such a limitation [33,34].

Kirchhoff shell theory has been widely used in the formulation of curved thin shell elements due to its well-established nature. However, such a formulation entails some limitations [35]. From the considerations of the principle of minimum potential energy,

Kirchhoff theory requires the continuity of the normal slope across the inter-element boundaries for the formulation of conforming shell elements. Irons and Draper [36] showed that it was impossible to use the Kirchhoff theory to formulate a conforming triangular plate or shell element with simple nodal connections.

Such limitations have led to the development of another type of popular shell element: the 'degenerated' shell elements, which are degenerated from the three-dimensional isoparametric formulations with additional consideration to incorporate the Kirchhoff hypothesis.

With a view to extending the isoparametric element concept, Ahmad *et al.* [37] first presented the degenerated shell element. Ahmad degenerated a three-dimensional brick element into a general curved shell element which has nodes only at the midsurface. The stress in the thickness direction is assumed to be equal to zero and the element displacement field is expressed in terms of three displacements of the midsurface, two rotations of the midsurface 'normal' and appropriate shape functions. Bathe [38], Crisfied [39] and Hughes [40] offer comprehensive overviews of the degenerated solid approach and related methodologies which involve some type of reduction to resultant form.

The original degenerated shell element performs reasonably well for moderately thick shell situations. However, for thin shells when full integration is used to evaluate the stiffness matrix, overstiff solutions are often produced due to shear or membrane locking.

Locking has been the subject of analysis by many authors in an attempt to both explain the phenomena and eventually remedy them. Attempts have been made to correct this behavior by use of reduced or selective integration techniques. Such schemes are not always successful in overcoming locking behaviour and the resulting solutions may still be overstiff for problems with highly constrained boundaries, and element mechanisms or spurious zero energy modes may form. These mechanisms can spread

from element to element causing either rank deficiency in the overall stiffness matrix and consequently no solution, or the even more dangerous situation in which the solution obtained may be polluted by a near mechanism.

Shear locking is the locking phenomenon associated with the development of spurious transverse shear strain. Shear locking in shell elements has been circumvented by the use of selective or reduced integration. This may, however, lead to matrices that are rank deficient and possess spurious (or zero-energy) modes called hourglass modes. Stabilization matrices are used to remove the spurious modes. The stabilization matrices are given by Jacquotte and Oden [41] for linear analysis.

In addition to using the selective or reduced integration scheme, some investigators utilized other techniques to overcome the shear locking problem.For example, Razzaque [42,43], Baldwin *et al.* [44] and Irons [45] applied discrete Kirchhoff constraints which enforced the Kirchhoff constraint only at discrete Gaussian points. Crisfield [46] utilized shear constraints to formulate a discrete Kirchhoff element in which the transverse shear strains are effectively zero. Bathe and Dvorkin [33,47] and Park and Stanley [48] used the assumed strain concept (both transverse shear and membrane strains) and the curvilinear natural coordinate system to formulate a curved quadrilateral shell element, respectively. Huang and Hinton [49,50] and Jang and Pinsky [34] utilized the same assumed strain concept and tensorial representations to formulate degenerated curved quadrilateral shell elements.

Membrane locking is the locking phenomenon associated with the development of non-zero membrane strain under a state of constant curvature. Stolarski and Belytschko [51] found that reduced shear integration in curved C^0 elements does also mitigate the effects of membrane locking. They also found that reduced integration in either the shear or the membrane energy expressions leads to improved accuracy in bending response. However, reduced shear integration is accompanied by a deterioration of membrane-

flexural coupling which is one of the essential features of the behavior of a curved element.

The assumed strain concept has been another technique used to avoid membrane locking. Huang and Hinton [49,50] used an enhanced interpolation of the membrane strains to formulate their nine-node degenerated shell element to avoid membrane locking. Stolarski and Belytschko [52] demonstrated that when low order middle surface displacement functions are used in the formulation of curved elements, an artificial constraint appears that causes a bending-dominated response to be replaced by a membrane-dominated response. This effect, due to the inability of an element to bend without stretching, is termed membrane locking. Membrane locking may also be avoided if the middle surface displacement field of the finite element is of sufficiently high order [52].

Chapter 3

The Sanders Shell Theory

3.1 Introduction

In this chapter a series solution based on the linear Sanders shell theory [1] is presented. At all times linear elastic small-displacement behavior is assumed. The governing equations are developed in toroidal coordinates in a convenient displacement form. They are solved for the case of a pad load of uniform normal pressure. Such a loading gives a first approximation of the effect of a trunnion pipe on an elbow [53]. Further applications are for the problems of the surface loading of a toroidal shell during construction or fabrication, and for the ram bending of curved pipes. In Chapter 4 numerical results, obtained from the Sanders theory, are compared with results from the isoparametric FEM [5,38,54]. These results define shell theory and FEM solution characteristics. In Chapter 5 further results from the Sanders theory are given which serve to provide information about elastic curved pipe displacement and stress characteristics.

3.2 Shell Geometry

The toroidal shell is assumed loaded by a pad of uniform normal pressure on the outside surface (Fig. 3.1). This loading is symmetrical about the horizontal $x-y$ plane and about a transverse plane bisecting the shell. The shell has a toroidal radius of R, a cross-sectional radius of r, and a thickness of t (Fig. 3.2). A general point P on the shell mid-surface is defined by the circumferential and longitudinal angular coordinates θ and ϕ. The radius vector $\mathbf{r}$ to P is given by

$$\mathbf{r} = (R + r cos\theta) sin\phi \mathbf{i} + (R + r cos\theta) cos\phi \mathbf{j} + r sin\theta \mathbf{k} \tag{3.1}$$

where $\mathbf{i}, \mathbf{j}, \mathbf{k}$ are unit vectors forming a base in the Cartesian x, y, z coordinate system. The first fundamental form of the middle surface is given by

$$ds^2 = A_1^2 d\xi_1^2 + A_2^2 d\xi_2^2 \tag{3.2}$$

Quantity ds is the differential line element, A_1 and A_2 are the *Lamé* parameters, while ξ_1 and ξ_2 are the base coordinates. Adopting the convention used by Whatham [22] the base coordinates are taken as

$$\xi_1 = \theta;\ \xi_2 = \eta = \rho\phi \tag{3.3}$$

where $\rho = R/r$. Both η and ϕ are used in the following as variables of the longitudinal direction. The *Lamé* parameters are

$$A_1 = r;\ A_2 = r\zeta \tag{3.4}$$

where

$$\zeta = 1 + \gamma cos\theta;\ \gamma = r/R = \rho^{-1} \tag{3.5}$$

The principal radius of curvatures for the circumferential (R_1) and longitudinal (R_2) directions are

$$R_1 = r;\ R_2 = r\zeta/(\gamma cos\theta) \tag{3.6}$$

The set of base unit vectors at P (Fig. 3.2) is given by

$$\begin{aligned}
\mathbf{e}_\theta &= -sin\theta sin\phi\mathbf{i} - sin\theta cos\phi\mathbf{j} + cos\theta\mathbf{k} \\
\mathbf{e}_\eta &= cos\phi\mathbf{i} - sin\phi\mathbf{j} \\
\mathbf{e}_r &= cos\theta sin\phi\mathbf{i} + cos\theta cos\phi\mathbf{j} + sin\theta\mathbf{k}
\end{aligned} \tag{3.7}$$

The subscripts θ and η in eqn. (3.7) and in the following indicate respectively the shell circumferential and longitudinal directions, while r indicates the outward normal direction.

3.3 The Sanders Shell Theory

The shell theory of Sanders [1] is considered one of the most accurate first order theories. Mainly due to its relative complexity it has not been used previously in toroidal coordinates. The governing equations are written in terms of the three displacement components u, v, and w (Fig. 3.3). Membrane stress resultants $N_\theta, N_\eta, N_{\theta\eta}$, and bending stress resultants, $M_\theta, M_\eta, M_{\theta\eta}$, are defined in the theory, as well as normal shear resultants Q_θ, Q_η (Fig. 3.3).

The five equilibrium equations of this theory may be reduced, by eliminating the normal shear stress resultants, to the following:

$$\begin{aligned}
&\frac{\partial(\zeta N_\theta)}{\partial\theta} + \frac{\partial N_{\theta\eta}}{\partial\eta} + \gamma sin\theta N_\eta \\
&+\frac{1}{r}\frac{\partial(\zeta M_\theta)}{\partial\theta} + \frac{1+(2\zeta)^{-1}}{r}\frac{\partial M_{\theta\eta}}{\partial\eta} + \frac{\gamma sin\theta M_\eta}{r} = 0 \\
&\frac{\partial(\zeta N_{\theta\eta})}{\partial\theta} + \frac{\partial N_\eta}{\partial\eta} - \gamma sin\theta N_{\theta\eta} + \frac{\gamma cos\theta}{r\zeta}\frac{\partial M_\eta}{\partial\eta} \\
&+\frac{2\gamma cos\theta - 1}{2r}\frac{\partial M_{\theta\eta}}{\partial\theta} - \frac{2\gamma^2 sin2\theta + \gamma sin\theta}{2r\zeta}M_{\theta\eta} = 0
\end{aligned} \tag{3.8}$$

$$\frac{N_\theta}{r} + \frac{\gamma cos\theta}{\zeta r} N_\eta - \frac{1}{r^2}\frac{\partial^2 M_\theta}{\partial \theta^2} - \frac{1}{(r\zeta)^2}\frac{\partial^2 M_\eta}{\partial \eta^2} - \frac{2}{(r\zeta)^2}\frac{\partial}{\partial \theta}(\zeta \frac{\partial M_{\theta\eta}}{\partial \eta})$$
$$-\frac{\gamma sin\theta}{r^2\zeta}\frac{\partial(M_\eta - 2M_\theta)}{\partial \theta} - \frac{\gamma cos\theta(M_\eta - M_\theta)}{r^2\zeta} = q_r$$

where $q_r = q_r(\theta, \eta)$ is the normal surface loading (positive outward). Surface loadings in the circumferential and longitudinal directions are taken as zero in the present study.

The constitutive equations relating the stress resultants with the mid-surface strain and curvature functions are

$$\begin{aligned} N_\theta &= K(\epsilon_\theta + \nu\epsilon_\eta);\ M_\theta = D(\kappa_\theta + \nu\kappa_\eta) \\ N_\eta &= K(\epsilon_\eta + \nu\epsilon_\theta);\ M_\eta = D(\kappa_\eta + \nu\kappa_\theta) \\ N_{\theta\eta} &= K(1-\nu)\epsilon_{\theta\eta};\ M_{\theta\eta} = D(1-\nu)\kappa_{\theta\eta} \end{aligned} \tag{3.9}$$

where

$$D = Et^3/[12(1-\nu^2)];\ K = Et/(1-\nu^2) \tag{3.10}$$

and E = Young's modulus; ν = Poisson ratio; $\epsilon_\theta, \kappa_\theta$ = circumferential strain, curvature; $\epsilon_\eta, \kappa_\eta$ = longitudinal strain, curvature; and $\epsilon_{\theta\eta}, \kappa_{\theta\eta}$ = shear strain, curvature.

The shear stress resultants Q_θ, Q_η are available from the other resultants through

$$\begin{aligned} Q_\theta &= \frac{1}{r}\frac{\partial M_\theta}{\partial \theta} + \frac{1}{r\zeta}\frac{\partial M_{\theta\eta}}{\partial \eta} + \frac{\gamma sin\theta(M_\eta - M_\theta)}{r\zeta} \\ Q_\eta &= \frac{1}{r}\frac{\partial M_{\theta\eta}}{\partial \theta} + \frac{1}{r\zeta}\frac{\partial M_\eta}{\partial \eta} - \frac{2\gamma sin\theta M_{\theta\eta}}{r\zeta} \end{aligned} \tag{3.11}$$

The circumferential and longitudinal normal stress components $\sigma_\theta, \sigma_\eta$, on the surfaces of the shell, are found from the stress resultants by

$$\begin{aligned} \sigma_\theta &= N_\theta/t \pm M_\theta(6/t^2) \\ \sigma_\eta &= N_\eta/t \pm M_\eta(6/t^2) \end{aligned} \tag{3.12}$$

The plus sign in these relations applies to points on the shell outside surface, while the minus sign to points on the inside surface. The first term of the right hand members indicates in each case the membrane stress contribution and the second term the bending stress contribution.

The strain-displacement and curvature-displacement relations in the theory of Sanders [1], expressed in toroidal coordinates, are

$$
\begin{aligned}
\epsilon_\theta &= \frac{1}{r}(\frac{\partial u}{\partial \theta} + w) \\
\epsilon_\eta &= \frac{1}{r\zeta}(-\gamma sin\theta u + \frac{\partial v}{\partial \eta} + \gamma cos\theta w) \\
\epsilon_{\theta\eta} &= \frac{1}{2r\zeta}(\frac{\partial u}{\partial \eta} + \gamma sin\theta v) + \frac{1}{2r}\frac{\partial v}{\partial \theta} \\
\kappa_\theta &= \frac{1}{r^2}(\frac{\partial u}{\partial \theta} - \frac{\partial^2 w}{\partial \theta^2}) \\
\kappa_\eta &= -\frac{sin\theta}{rR\zeta}(u - \frac{\partial w}{\partial \theta}) + \frac{cos\theta}{rR\zeta^2}\frac{\partial v}{\partial \eta} - \frac{1}{(r\zeta)^2}\frac{\partial^2 w}{\partial \eta^2} \\
\kappa_{\theta\eta} &= \frac{(1+2\zeta)}{(2r\zeta)^2}\frac{\partial u}{\partial \eta} + \frac{1}{2r^2\zeta}(\gamma cos\theta - \frac{1}{2})\frac{\partial v}{\partial \theta} \\
&\quad + \frac{2\gamma^2 sin2\theta + (1-2\zeta)\gamma sin\theta}{(2r\zeta)^2}v - \frac{1}{r^2\zeta}\frac{\partial^2 w}{\partial \theta \partial \eta} - \frac{1}{rR\zeta^2}\frac{\partial w}{\partial \eta}
\end{aligned}
\tag{3.13}
$$

By combining eqns. (3.13), (3.9), and (3.8) one obtains a set of three equations which govern the system. These equations which are in terms of the three displacement components are

$$
\begin{aligned}
&[\nu_1\frac{\partial^2}{\partial\theta^2} + \nu_2\frac{\partial^2}{\partial\eta^2} + \nu_3\frac{\partial}{\partial\theta} + \nu_4]u + [\nu_5\frac{\partial^2}{\partial\theta\partial\eta} + \nu_6\frac{\partial}{\partial\eta}]v \\
&+[\nu_7\frac{\partial^3}{\partial\theta^3} + \nu_8\frac{\partial^3}{\partial\theta\partial\eta^2} + \nu_9\frac{\partial^2}{\partial\theta^2} + \nu_{10}\frac{\partial^2}{\partial\eta^2} + \nu_{11}\frac{\partial}{\partial\theta} + \nu_{12}]w = 0 \\
&[\nu_{13}\frac{\partial^2}{\partial\theta\partial\eta} + \nu_{14}\frac{\partial}{\partial\eta}]u + [\nu_{15}\frac{\partial^2}{\partial\theta^2} + \nu_{16}\frac{\partial^2}{\partial\eta^2} + \nu_{17}\frac{\partial}{\partial\theta} + \nu_{18}]v \\
&+[\nu_{19}\frac{\partial^3}{\partial\eta^3} + \nu_{20}\frac{\partial^3}{\partial\theta^2\partial\eta} + \nu_{21}\frac{\partial^2}{\partial\theta\partial\eta} + \nu_{22}\frac{\partial}{\partial\eta}]w = 0
\end{aligned}
\tag{3.14}
$$

$$
\begin{aligned}
&[\nu_{23}\frac{\partial^3}{\partial\theta^3}+\nu_{24}\frac{\partial^3}{\partial\theta\partial\eta^2}+\nu_{25}\frac{\partial^2}{\partial\eta^2}+\nu_{26}\frac{\partial^2}{\partial\theta^2}+\nu_{27}\frac{\partial}{\partial\theta}+\nu_{28}]u\\
&+[\nu_{29}\frac{\partial^3}{\partial\eta^3}+\nu_{30}\frac{\partial^3}{\partial\theta^2\partial\eta}+\nu_{31}\frac{\partial^2}{\partial\theta\partial\eta}+\nu_{32}\frac{\partial}{\partial\eta}]v\\
&+[\nu_{33}\frac{\partial^4}{\partial\theta^4}+\nu_{34}\frac{\partial^4}{\partial\eta^4}+\nu_{35}\frac{\partial^4}{\partial\theta^2\partial\eta^2}-\nu_{36}\frac{\partial^3}{\partial\theta^3}+\nu_{37}\frac{\partial^3}{\partial\theta\partial\eta^2}\\
&+\nu_{38}\frac{\partial^2}{\partial\eta^2}+\nu_{39}\frac{\partial^2}{\partial\theta^2}+\nu_{40}\frac{\partial}{\partial\theta}+\nu_{41}]w=-(r^4/D)\zeta^4 q_r
\end{aligned}
$$

where the $\nu_i, i = 1, 41$ are given in the Appendix A.

Fourier series expansions are written for the displacement components and the normal load as follows

$$
\begin{aligned}
u &= \sum_{n=1}^{\infty}\sum_{m=1}^{\infty} u_{mn} sinn\theta sin\mu_m\eta\\
v &= \sum_{n=0}^{\infty}\sum_{m=1}^{\infty} v_{mn} cosn\theta cos\mu_m\eta\\
w &= \sum_{n=0}^{\infty}\sum_{m=1}^{\infty} w_{mn} cosn\theta sin\mu_m\eta\\
q_r &= \sum_{n=0}^{\infty}\sum_{m=1}^{\infty} q_{mn} cosn\theta sin\mu_m\eta
\end{aligned}
\tag{3.15}
$$

where

$$\mu_m = m\pi\gamma/\psi \tag{3.16}$$

and ψ equals the shell angular length (Fig. 3.1). Quantities N and M (unsubscripted) are the series truncation integers. These are selected large enough to ensure convergence of the solution.

The selection of the series expansions in eqn. (3.15) implies that simply supported conditions exist at the ends of the shell. Thus the following boundary conditions are satisfied at the shell ends $\phi = 0°$ and $\phi = \psi$

$$N_\eta = u = w = M_\eta = 0 \tag{3.17}$$

Furthermore selection of the $cos\ n\theta$ term instead of the $sin\ n\theta$ term in the series for q_r restricts the loading to cases of in-plane bending for the toroidal shell.

The Fourier series expansions of eqns. (3.15) are next substituted into the governing equations (3.14), and the coefficients of like products of trigonometric terms are collected. The resulting algebraic expressions for the coefficients are cumbersome. They were developed with the aid of the algebraic computation software MAPLE [55]. The resulting expressions have the form

$$\begin{aligned}
&\sum_{n=1}^{\infty}\sum_{m=1}^{\infty}[(a_{19m,n-4}u_{m,n-4} + a_{29m,n-4}v_{m,n-4} + a_{39m,n-4}w_{m,n-4} \\
&+a_{18m,n-3}u_{m,n-3} + a_{28m,n-3}v_{m,n-3} + a_{38m,n-3}w_{m,n-3} \\
&+a_{17m,n-2}u_{m,n-2} + a_{27m,n-2}v_{m,n-2} + a_{37m,n-2}w_{m,n-2} \\
&+a_{16m,n-1}u_{m,n-1} + a_{26m,n-1}v_{m,n-1} + a_{36m,n-1}w_{m,n-1} \\
&+a_{15mn}u_{mn} + a_{25mn}v_{mn} + a_{35mn}w_{mn} \\
&+a_{14m,n+1}u_{m,n+1} + a_{24m,n+1}v_{m,n+1} + a_{34m,n+1}w_{m,n+1} \\
&+a_{13m,n+2}u_{m,n+2} + a_{23m,n+2}v_{m,n+2} + a_{33m,n+2}w_{m,n+2} \\
&+a_{12m,n+3}u_{m,n+3} + a_{22m,n+3}v_{m,n+3} + a_{32m,n+3}w_{m,n+3} \\
&+a_{11m,n+4}u_{m,n+4} + a_{21m,n+4}v_{m,n+4} + a_{31m,n+4}w_{m,n+4})sinn\theta]sin\mu_m\eta = 0
\end{aligned} \tag{3.18}$$

$$\begin{aligned}
&\sum_{n=0}^{\infty}\sum_{m=1}^{\infty}[(b_{19m,n-4}u_{m,n-4} + b_{29m,n-4}v_{m,n-4} + b_{39m,n-4}w_{m,n-4} \\
&+b_{18m,n-3}u_{m,n-3} + b_{28m,n-3}v_{m,n-3} + b_{38m,n-3}w_{m,n-3} \\
&+b_{17m,n-2}u_{m,n-2} + b_{27m,n-2}v_{m,n-2} + b_{37m,n-2}w_{m,n-2} \\
&+b_{16m,n-1}u_{m,n-1} + b_{26m,n-1}v_{m,n-1} + b_{36m,n-1}w_{m,n-1} \\
&+b_{15mn}u_{mn} + b_{25mn}v_{mn} + b_{35mn}w_{mn} \\
&+b_{14m,n+1}u_{m,n+1} + b_{24m,n+1}v_{m,n+1} + b_{34m,n+1}w_{m,n+1} \\
&+b_{13m,n+2}u_{m,n+2} + b_{23m,n+2}v_{m,n+2} + b_{33m,n+2}w_{m,n+2} \\
&+b_{12m,n+3}u_{m,n+3} + b_{22m,n+3}v_{m,n+3} + b_{32m,n+3}w_{m,n+3}
\end{aligned} \tag{3.19}$$

$$+b_{11m,n+4}u_{m,n+4} + b_{21m,n+4}v_{m,n+4} + b_{31m,n+4}w_{m,n+4})cosn\theta]cos\mu_m\eta = 0$$

$$\sum_{n=0}^{\infty}\sum_{m=1}^{\infty}[(c_{19m,n-4}u_{m,n-4} + c_{29m,n-4}v_{m,n-4} + c_{39m,n-4}w_{m,n-4}$$
$$+c_{18m,n-3}u_{m,n-3} + c_{28m,n-3}v_{m,n-3} + c_{38m,n-3}w_{m,n-3}$$
$$+c_{17m,n-2}u_{m,n-2} + c_{27m,n-2}v_{m,n-2} + c_{37m,n-2}w_{m,n-2}$$
$$+c_{16m,n-1}u_{m,n-1} + c_{26m,n-1}v_{m,n-1} + c_{36m,n-1}w_{m,n-1}$$
$$+c_{15mn}u_{mn} + c_{25mn}v_{mn} + c_{35mn}w_{mn} \qquad (3.20)$$
$$+c_{14m,n+1}u_{m,n+1} + c_{24m,n+1}v_{m,n+1} + c_{34m,n+1}w_{m,n+1}$$
$$+c_{13m,n+2}u_{m,n+2} + c_{23m,n+2}v_{m,n+2} + c_{33m,n+2}w_{m,n+2}$$
$$+c_{12m,n+3}u_{m,n+3} + c_{22m,n+3}v_{m,n+3} + c_{32m,n+3}w_{m,n+3}$$
$$+c_{11m,n+4}u_{m,n+4} + c_{21m,n+4}v_{m,n+4} + c_{31m,n+4}w_{m,n+4})cosn\theta]sin\mu_m\eta =$$
$$\sum_{n=0}^{\infty}\sum_{m=1}^{\infty}[d_9q_{m,n-4} + d_8q_{m,n-3} + d_7q_{m,n-2} + d_6q_{m,n-1} + d_5q_{mn}$$
$$+d_4q_{m,n+1} + d_3q_{m,n+2} + d_2q_{m,n+3} + d_1q_{m,n+4}]cosn\theta sin\mu_m\eta$$

where the coefficients $a_{ijmn}, b_{ijmn}, c_{ijmn}$ and d_i are lengthy, but known, functions of n, μ_m, ν, and K. These generic expressions involve negative-indexed terms for $n = 0, 1, 2, 3$ which are not present in the original expansions. It is necessary to modify the equations for these values of n, setting the appropriate terms to zero and employing the identities

$$cos(-n\theta) = cosn\theta;\ sin(-n\theta) = -sinn\theta \qquad (3.21)$$

for the cases of negative arguments of the *cos* and *sin* functions. The quantities q_{mn} are related to the loading, and are prescribed in eqns. (3.23-3.24) below.

By equating coefficients of like trigonometric terms on the two sides of the equations, one obtains $M' = (M-1)/2+1$ sets of simultaneous equations, each consisting of $3N+2$ equations. By neglecting coefficients of order higher than N, there are in each set, also $3N+2$ unknowns. Each of the M' sets of equations is banded, consisting of one group

of two equations and N groups of three equations. The band-width is uniform at 27 terms. A customized band solution algorithm was developed to solve such an equation set efficiently.

The solution is developed for a normal pressure q_r on the shell surface which is everywhere zero, except in the following four regions where the pressure is uniform at a value of $-p$ (i.e. radially inwards):

$$\begin{aligned}
&(-\beta-\lambda) \le \theta \le (-\beta+\lambda);\ (\phi\prime-\alpha-\delta) \le \phi \le (\phi\prime-\alpha+\delta)\\
&(\beta-\lambda) \le \theta \le (\beta+\lambda);\ (\phi\prime-\alpha-\delta) \le \phi \le (\phi\prime-\alpha+\delta)\\
&(-\beta-\lambda) \le \theta \le (-\beta+\lambda);\ (\phi\prime+\alpha-\delta) \le \phi \le (\phi\prime+\alpha+\delta)\\
&(\beta-\lambda) \le \theta \le (\beta+\lambda);\ (\phi\prime+\alpha-\delta) \le \phi \le (\phi\prime+\alpha+\delta)
\end{aligned} \tag{3.22}$$

The four regions (3.22) are symmetric with respect to the planes $z = 0$ and $\phi = \phi\prime$ (Fig. 3.1). Quantity β is the circumferential angle to the center of the load pad, while 2λ is the angular length of the pad in the circumferential direction. Quantity α is the longitudinal angle measured from the transverse plane of symmetry to the center of the load pad, while 2δ is the angular length of the pad in the longitudinal direction. In considering the loading to be applied in four regions it is possible to represent a single load, two loads, or four loads with a single theoretical expression, by simply specifying the regions to be adjacent or separated with respect to each other. In the present study only the first two of these capabilities were used.

The Fourier series for such a bisymmetric set of four uniform pad loads is given by eqn.

$$q_r = \sum_{n=0}^{\infty}\sum_{m=1}^{\infty} q_{mn} cosn\theta sin\mu_m\eta \tag{3.23}$$

where the q_{mn} are constants to be determined for a specified loading.

$$q_{mo} = -(16p/\pi^2)(\lambda/m)k_m \sin\mu_m\eta$$

$$q_{mn} = -(16p/\pi^2)(2/mn)k_m \cos n\beta \sin n\lambda \cos n\theta \sin \mu_m \eta, \ (n > 0) \tag{3.24}$$
$$k_m = \sin(m\pi/2) \cos m\pi\alpha/\psi \sin m\pi\delta/\psi$$

The following series expansions are written for the strain and curvature functions

$$\begin{aligned}
\epsilon_\theta &= \sum_{n=0}^{\infty}\sum_{m=1}^{\infty} \epsilon_{\theta mn} cosn\theta sin\mu_m\eta \\
\epsilon_\eta &= \sum_{n=0}^{\infty}\sum_{m=1}^{\infty} \epsilon_{\eta mn} cosn\theta sin\mu_m\eta \\
\epsilon_{\theta\eta} &= \sum_{n=1}^{\infty}\sum_{m=1}^{\infty} \epsilon_{\theta\eta mn} sinn\theta cos\mu_m\eta \\
\kappa_\theta &= \sum_{n=0}^{\infty}\sum_{m=1}^{\infty} \kappa_{\theta mn} cosn\theta sin\mu_m\eta \\
\kappa_\eta &= \sum_{n=0}^{\infty}\sum_{m=1}^{\infty} \kappa_{\eta mn} cosn\theta sin\mu_m\eta \\
\kappa_{\theta\eta} &= \sum_{n=1}^{\infty}\sum_{m=1}^{\infty} \kappa_{\theta\eta mn} sinn\theta cos\mu_m\eta
\end{aligned} \tag{3.25}$$

Expressions are required for the strain and curvature coefficients of the right hand members in terms of the displacement coefficients. By substituting the series (3.15) into the eqns. (3.13) and equating coefficients of like terms one obtains

$$\begin{aligned}
\epsilon_{\theta mn} &= (nu_{mn} + w_{mn})/r \\
\epsilon_{\eta mn} &= -(u_{m,n+1} - u_{m,n-1})/(2\rho r\zeta) - \mu_m v_{mn}/(r\zeta) \\
&\quad +(w_{m,n+1} + w_{m,n-1})/(2\rho r\zeta) \\
\epsilon_{\theta\eta mn} &= \mu_m u_{mn}/(2r\zeta) + (v_{m,n-1} - v_{m,n+1})/(4\rho r\zeta) - nv_{mn}/(2r)
\end{aligned} \tag{3.26}$$

and

$$\begin{aligned}
\kappa_{\theta mn} &= n(u_{mn} + nw_{mn})/r^2 \\
\kappa_{\eta mn} &= -(u_{m,n+1} - u_{m,n-1})/(2\rho r^2\zeta) \\
&\quad -\mu_m(v_{m,n+1} + v_{m,n-1})/(2\rho r^2\zeta^2) \\
&\quad +\mu_m^2 w_{mn}/(r\zeta^2) - n(w_{m,n+1} - w_{m,n-1})/(2\rho r^2\zeta)
\end{aligned} \tag{3.27}$$

$$
\begin{aligned}
\kappa_{\theta\eta mn} \;=\; & \mu_m u_{mn}(1+2\zeta)/(2r\zeta)^2 - n(v_{m,n-1}+v_{m,n+1})/(4rR\zeta) \\
& + n v_{mn}/(4r^2\zeta) + (v_{m,n-2}-v_{m,n+2})/(2R\zeta)^2 \\
& + (1-2\zeta)(v_{m,n-1}-v_{m,n+1})/(8rR\zeta^2) \\
& + n\mu_m w_{mn}/(2r^2\zeta) - \mu_m(w_{m,n-1}-w_{m,n+1})/(2rR\zeta^2)
\end{aligned}
$$

Terms with negative indices are understood to be zero.

To summarize, the displacement coefficients for a loading specified by the eqns. (3.23)-(3.24), are found by solving the eqn. set (3.18)-(3.20), while the total displacement components are found from eqns. (3.15a-c). The strain-curvature coefficients are from the relations (3.26)-(3.27), while the total strain and curvature components are found from eqn. (3.25). The stress resultants are found from eqn. (3.9), while the normal stress components on the shell surface are found from eqn. (3.12).

The theory presented in this section was coded in a FORTRAN computer program labelled TORSAN, and it is given in Appendix B. Results from this section are presented in Chapters 4 and 5.

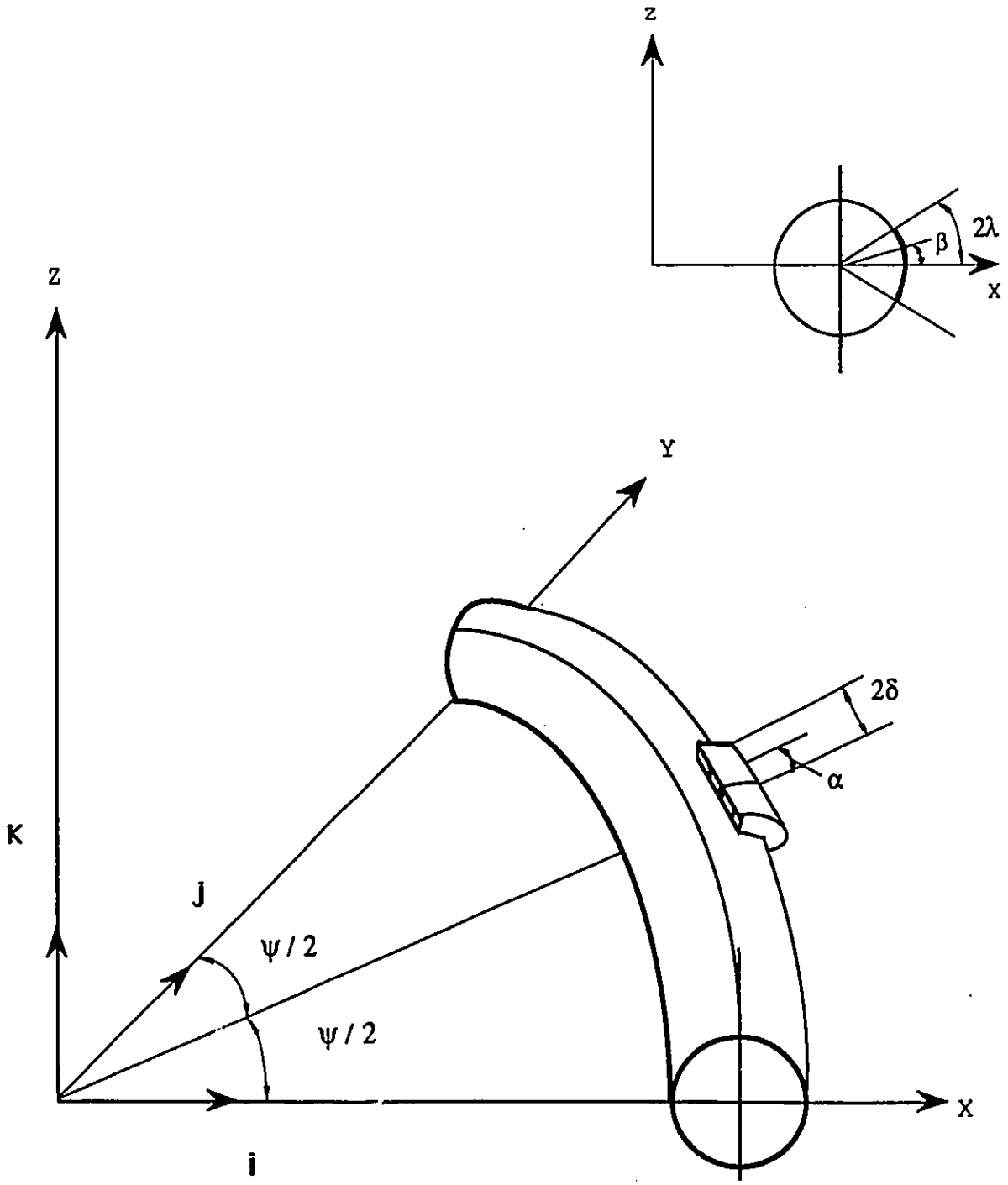

Figure 3.1: Surface loading of a toroidal shell.

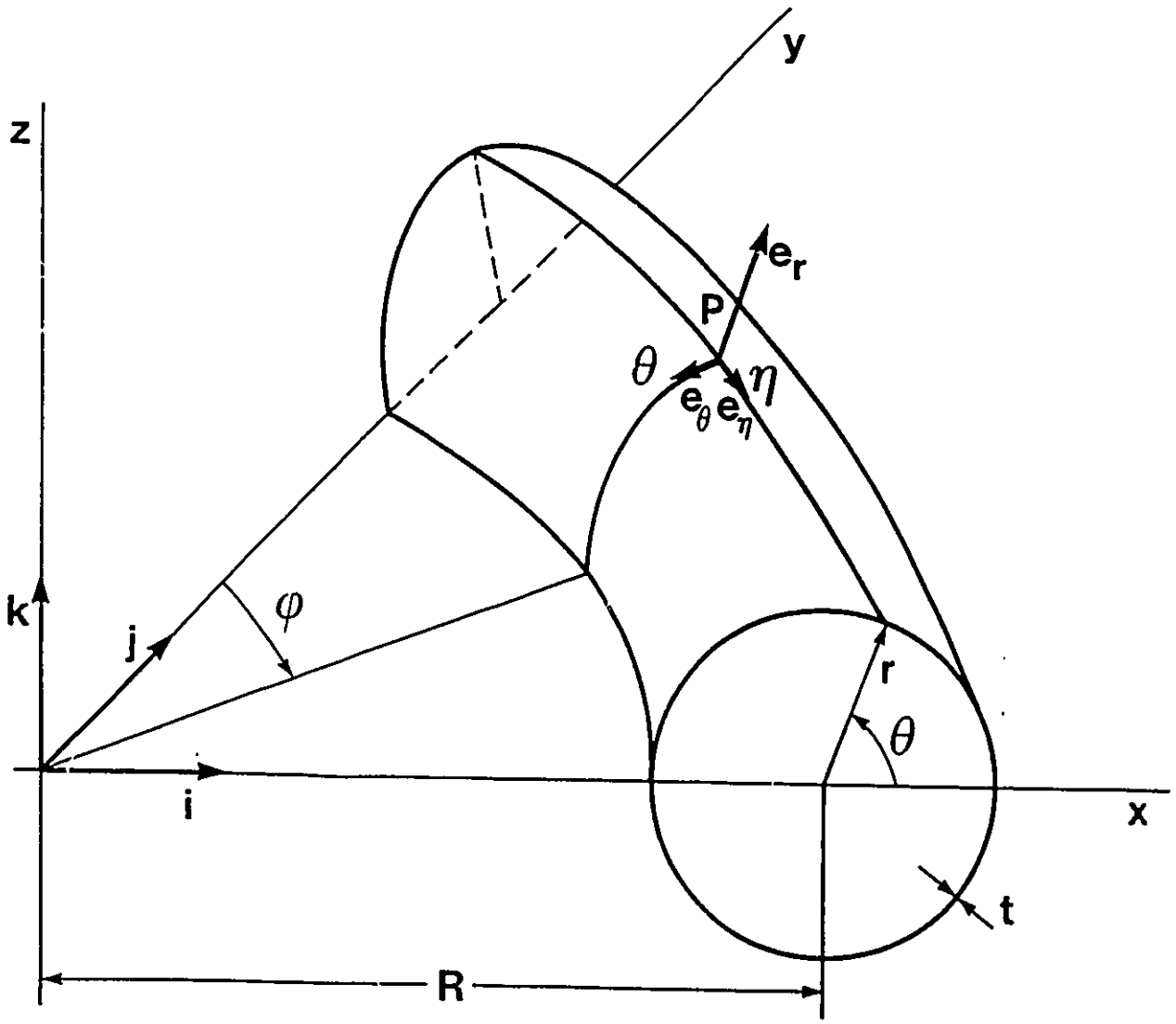

Figure 3.2: Toroidal coordinate system.

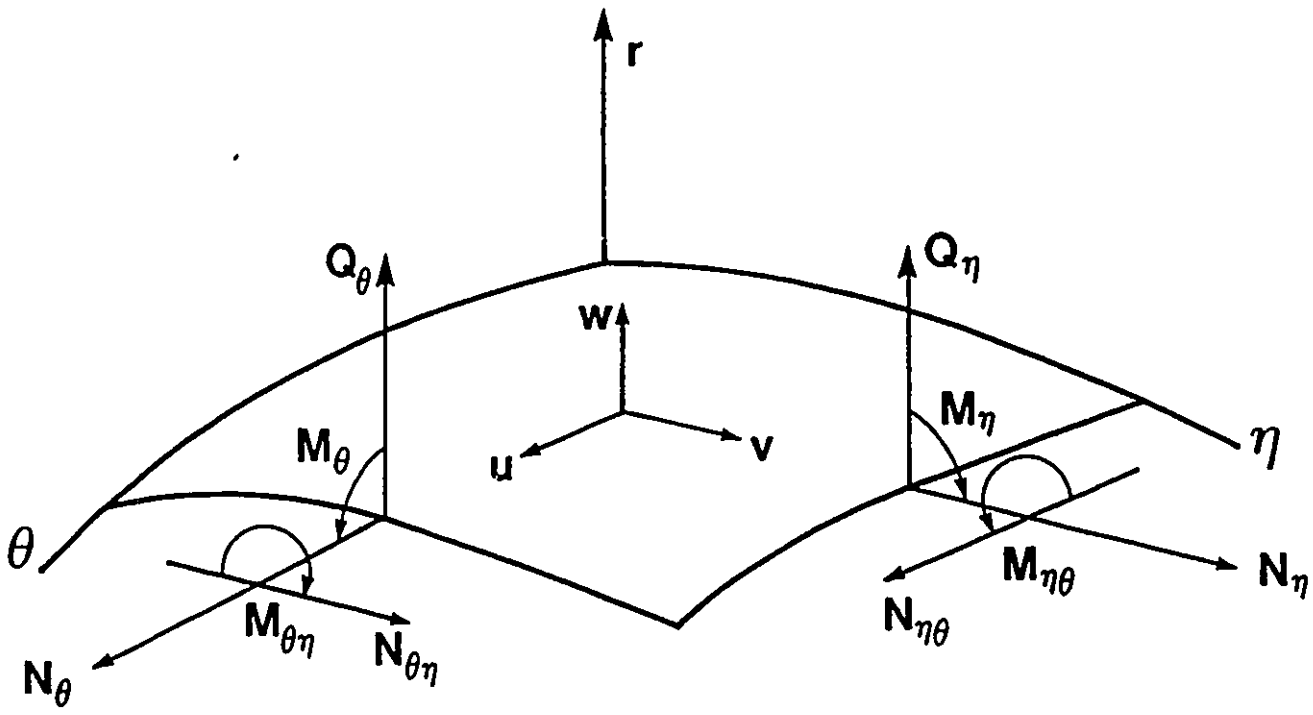

Figure 3.3: Displacement components and stress resultants.

Chapter 4

Comparison of The Sanders Shell Theory Results with Other Results

4.1 Introduction

In this chapter, the solution of the Sanders shell theory for three problems is compared with solutions from either the FEM method or other shell theories. The first two problems cover cases of local loads on sectorial toroidal shells. The first problem is for a small R/r ratio while the second for a large R/r ratio. The final problem concerns the case of a half-filled cylindrical vessel. Efforts are made to assess the accuracy of the Sanders shell theory by comparison with the other results.

4.2 Local Load on a 90°-Elbow

Results obtained using the Sanders theory are compared in this section with results obtained from the FEM (ADINA package). The problem considered has relevance to the problem of an elbow connected to a trunnion pipe [53]. The loading corresponds to a single pad of inward uniform normal pressure centered at the extrados ($\theta = 0°$), on the $\phi = 45°$ plane (Fig. 3.1). The pad extends for 60° in the circumferential direction and 30° in the longitudinal direction. The numerical values for the geometric, material and loading parameters are as follows (Fig. 3.2)

$$\begin{aligned} & r = 84.15\,mm;\ E = 207,000\,MPa \\ & R = 252.45\,mm;\ \nu = 0.3 \\ & t = 7.1\,mm;\ p = 1\,MPa \\ & \beta = 15°;\ \lambda = 15° \\ & \alpha = 7.5°;\ \delta = 7.5° \\ & \psi = 90°;\ \phi\prime = 45° \end{aligned} \tag{4.1}$$

Two sets of results from the Sanders theory are given. The first set, represented by SAN in the figures, is considered to be very close to the converged solution, and corresponds to truncation integers of $M = 51$, $N = 25$. The second set, represented by SANU in the figures, is an unconverged approximation, corresponding to truncation integers of $M = 11$, $N = 7$. The finite element results, represented by FEM in the figures, correspond to the 80-element mesh and a total of 775 nodal points (Fig. 4.1). There are three displacement and two rotation degrees of freedom at each node. Fig. 4.1 shows a projected view of FEM mesh. The projected view is easy to draw and clearly indicates the mesh.

A comparison of results for the radial displacement component w at the extrados is

given in Fig. 4.2. The deflection pattern indicates a localized bulging under the load, superimposed on a beam bending mode. The three sets of results (SAN, FEM, and SANU) show very good agreement over the entire length of the elbow. At $\phi = 45°$, where the deflection is the largest, the SAN values differ by only 0.23% from the FEM values.

A comparison of the results for the radial displacement component w on the transverse plane $\phi = 45°$ is given in Fig. 4.3. There is a relatively large inward deflection of the shell under the load pad near the extrados and a smaller outward deflection elsewhere. It is observed that the pad load is located in a positive curvature portion of the toroidal shell and the deflection pattern in the immediate vicinity approximates that in a spherical shell. There is very good agreement among the three sets of results.

Fig. 4.4 shows a comparison of the results for the longitudinal stress σ_η at the extrados. The stress is shown for the inside surface of the shell. A variation of stress is observed which corresponds to a superposition of beam bending and local bending at the pad edges. There is a sharp rise and drop in stress near the pad edges, as was observed in the study by Redekop for a slightly curved toroidal shell [4]. There is good agreement in the SAN and FEM set of values over the entire length of the elbow. At $\phi = 45°$, where the stress is largest, the agreement is to two figures. The SANU values do not closely represent the variation of stress near the pad edges.

Fig. 4.5 shows a comparison of results for the longitudinal stress σ_η on the transverse plane $\phi = 45°$. There is good agreement in the three sets of results. The absolute maximum stress occurs on the outside surface at the extrados. The SAN value here is 27.3 MPA while the FEM value is 26.9 MPa. The maximum stress on the inside surface also occurs at the extrados.

In Fig. 4.6 a comparison of results is given for the circumferential stress σ_θ for the

transverse plane $\phi = 45°$. The stress shows oscillatory variation, with the maximum values located at $\theta = 0°$, and nodes located at approximately $\theta = 30°$ and $\theta = 90°$. The membrane stresses are compressive from the extrados to approximately $\theta = 90°$ and tensile thereafter. Good agreement is observed in the three sets of values. The overall maximum absolute stress occurs on the outside surface at the extrados. The SAN value is 21.8 MPa while the FEM value is 21.3 MPa.

Table 4.1 shows a comparison of predicted changes in the horizontal and vertical cross-sectional diameters at various positions along the length of the elbow. The three sets of values show very close agreement. At the central transverse plane, where the largest changes in diameter take place, the SAN values are 1.3% smaller for the horizontal direction, and 0.1% smaller for the vertical direction, compared to the FEM values.

The commercial program ADINA was used to obtain the FEM results. Taking into account the symmetry about the horizontal xy plane of the toroidal shell, only a half of it needs to be considered. This portion is modelled by a mesh of 80 unequal-sized 16-noded shell elements and a total of 775 nodal points. In order to obtain a useful approximate solution for stress concentrations, a finer subdivision is necessary in regions where stress concentrations are expected. Therefore, the elements span respectively, 15°, 22.5° and 30° in the circumferential direction and 7.5° and 11.25° in the longitudinal direction. A representation of the mesh of elements is given in Fig. 4.1. Element matrices were evaluated using Gaussian integration based on a $4 \times 4 \times 2$(r-s-t) grid, and a total of 3605 equilibrium equations were solved in the numerical solution.

The ADINA information for CPU time was not available but believed to be of the same order as a FEM computer program SHELL FORTRAN. CPU times in sec. are 3.2, 40.8 and 225.8, respectively for SANU, SAN and FEM on an AMDAHL 5860/CMS mainfram computer.

4.3 Ram Bending of a Sectorial Toroidal shell

In this section the problem of the ram bending of a sectorial toroidal shell in the elastic range is considered. The loading is idealized as a set of pads of uniform normal pressure. Numerical results for displacements and stresses are obtained using the MVD [2] and Sanders [1] shell theories, and these are compared with results from the FEM.

The curved pipe is assumed bent by three dies which impart a uniform normal pressure on the shell outside surface at three positions (Fig. 4.7). The loading is symmetrical about the horizontal plane $z = 0$, and about a vertical transverse plane which divides the shell into two equal parts of angular length $\psi/2$. This satisfies the symmetrical conditions inherent in equation (3.15).

Numerical results are presented in this section for the following values of the geometric, material, and load parameters (Fig. 3.2)

$$
\begin{aligned}
& r = 57.5\,mm;\ E = 207{,}000\,MPa \\
& R = 5750\,mm;\ \nu = 0.3 \\
& t = 3.6\,mm;\ p = 6\,MPa \\
& \beta' = 135°;\ \beta'' = 45° \\
& \lambda' = 45°;\ \lambda'' = 45° \\
& \alpha' = 0.28648°;\ \alpha'' = 2.5783° \\
& \delta' = 0.28648°;\ \delta'' = 0.28648° \\
& \psi = 5.7296°;\ \phi\prime = 2.8648°
\end{aligned}
\tag{4.2}
$$

This loading corresponds to the case where the ram and reactive dies extend respectively through one-fifth and one-tenth of the shell length, and wrap half-way around the circumference.

Three sets of results are given in Fig. 4.9-4.13 and Table 4.2 below. The first two sets, labelled MVD and SAN, were obtained respectively using the MVD and Sanders shell theories. These results are from solutions for which the truncation integers of equations (3.15-3.16) were $M = 101$ and $N = 51$. The displacements in these solutions agreed to at least two figures with results from solutions for which the truncation integers were $M = 51$ and $N = 25$. They thus can be considered to be the converged values. The third set of results was obtained using the program ADINA, with a mesh as depicted in Fig. 4.8. To make some comparisons at specific positions results were also computed using elementary straight beam theory. A simply supported beam was assumed with a transverse point load applied at the mid-span. The assumed beam length was 517.5 mm representing the distance between the centers of the two outer dies.

Fig. 4.9 shows a comparison of results for the radial displacement w on the intrados ($\theta = 180°$), on the right side of the transverse plane of symmetry. The deflection pattern corresponds to a beam bending mode onto which is superimposed a localized bulging due to the pad load. The SAN and FEM values agree to within 1%, while the MVD values are consistently lower. At the transverse plane of symmetry where the displacement is the largest, the MVD value is 4.9% below the FEM value. For the comparable cylindrical shell (ref. [19], Fig. 4.8) the maximum deflection on the intrados was 0.61 mm. The current maximum value of 0.690 mm exceeds this value by 11.5%. From the beam theory a prediction of 0.515 mm was obtained for the mid-span deflection. The comparable MVD value, found by taking the mean of the absolute deflections on the intrados and extrados ($\theta = 0°$) is 0.590 mm, while the FEM result is 0.593 mm.

A comparison of results for the radial displacement w on the transverse plane of symmetry $\phi = \psi/2$ is shown in Fig. 4.10. The SAN and FEM results again show close agreement (maximum difference less than 1%). The MVD results are 5.4% greater than

the FEM results on the extrados and 4.9% smaller on the intrados.

Fig. 4.11 shows a comparison of the results for the longitudinal stress σ_η at the intrados on the right side of the transverse plane of symmetry. The SAN and FEM results for this stress show close agreement, while the MVD values are consistently smaller. The absolute maximum stress predicted by the MVD theory is 241.1 MPa, by the Sanders theory 253.1 MPa, while by the FEM 265.5 MPa. The straight beam theory predicts a maximum bending stress of 274.4 MPa. The comparable maximum stress for a cylindrical shell (ref. [19], Fig. 3.3) using the MVD theory is 214.9 MPa.

A comparison of results for the longitudinal stress σ_η on the transverse plane of symmetry is shown in Fig. 4.12. There is close agreement in the SAN and FEM results. The absolute maximum stress predicted by MVD is 241.1 MPa, that by the Sanders theory 253.1 MPa, while that by the FEM 265.5 MPa. This maximum occurs on the inside surface at the intrados. The maximum stress on the outside surface occurs approximately at $\theta = 125°$. Finally the comparable maximum stress for a cylindrical shell (ref. [19], Fig. 4.11) using the MVD theory is 239.3 MPa.

Fig. 4.13 shows a comparison of results for the circumferential stress σ_θ on the transverse plane of symmetry. The agreement in the SAN and FEM results is not as close as for the longitudinal stress. The overall maximum absolute stress predicted by MVD is 232.5 MPa, that by the Sanders theory 253.0 Mpa, while that by FEM 283.5 MPa. This maximum occurs on the outside surface at approximately $\theta = 112°$. Finally the comparable maximum stress for a cylindrical shell (ref. [19], Fig. 4.10) using the MVD theory is 295.0 MPa.

A comparison of the predicted changes in the horizontal and vertical diameters of the shell is shown in Table 4.2. The MVD, SAN, and FEM results are given using the longitudinal coordinate ϕ. The agreement between the SAN and FEM results is good.

Quantitatively, the maximum value predicted by the MVD theory is 30.4% below that predicted by the FEM for the horizontal diameter, and 34.0% below for the vertical diameter. The maximum value predicted by the Sanders theory is 6.8% above the value predicted by the FEM for the horizontal diameter, and 10.8% above for the vertical diameter.

Finally the prediction, for the current loading, of the rotation of the end section with respect to the transverse plane of symmetry is 0.167° using the MVD theory, 0.177° for the Sanders theory, and 0.175° using the FEM. The beam theory predicts a rotation of 0.171°.

The ADINA program was used to determine the FEM solution. Taking into account the symmetry about the horizontal xy plane of the toroidal shell, only a half of it needs to be considered. This portion is again modelled by a mesh of 80 unequal-sized 16-noded shell elements and a total of 775 nodal points. In order to obtain a useful approximate solution for stress concentrations, a finer subdivision is necessary in regions where stress concentrations are expected. Therefore, the elements span respectively, 22.5° in the circumferential direction and 0.17°, 0.28° and 0.4° in the longitudinal direction. A representation of the mesh of elements is given in Fig. 4.8. Element matrices were evaluated using Gaussian integration based on a $4 \times 4 \times 2$(r-s-t) grid, and a total of 3605 equilibrium equations were again solved in the numerical solution.

In the previous work on a cylindrical shell with this element [19] a converged solution was obtained with a mesh containing the same number of nodes and distributed in the same pattern.

4.4 Half-filled Cylindrical Vessel

Consider an end supported circular cylindrical vessel half-filled with fluid. The height of the fluid is indicated by the angle $\overline{\alpha} = 90°$ measured from the bottom of the vessel (Fig. 4.14). It is assumed that the radial pressure remains constant along the length and is directly proportional to the depth at the point of consideration.

In this section, results obtained using the Sanders theory are compared with results obtained from the Flügge theory. These problems are considered (Fig. 4.15); a straight cylindrical vessel, and two similar slightly curved toroidal vessels. There are equal radii, thickness and center-line length in three cases. The dimensions of the cylindrical vessel used here are; length $l = 12.19\,m$, mean diameter $2r = 2.44\,m$ and thickness $t = 12.7\,mm$.

Fig. 4.16 presents circumferential bending stresses ($6M_\theta/t^2$) and longitudinal membrane stresses (N_x/t) predicted around the central profile (x=l/2). For each stress four sets of results are presented. Three sets of results from the Sanders theory are given. The first set, represented by CYL-SAN in the figures, corresponds to a half-filled cylindrical vessel. The second and third sets, respectively represented by TOR-SAN-DEFL. 3T and TOR-SAN-DEFL. 6T in the figures, correspond to half-filled toroidal vessels whose deflections are three times and six times the thickness (Fig. 4.15). Flügge results represented by CYL-FLG, correspond to a half-filled cylindrical vessel. It is noted that the depth of fluid was not quite constant everywhere along the length of toroidal vessels. As only the stresses around the central profile are considered, the fact that the vessels were slightly curved has a negligible effect.

The results labelled SAN were obtained using the FORTRAN program TORSAN, which was discussed in Chapter 3. The Flügge theory results are from ref. [17].

The agreement of the two sets of results (CYL-FLG, CYL-SAN) in the Fig. 4.16 is considered very satisfactory for both stresses. The maximum longitudinal membrane stress occurs on the datum generator ($\overline{\phi} = 0°$). The maximum circumferential bending stress is located at the fluid surface ($\overline{\phi} = 90°$). Both sets of stress values for the toroidal vessel are in general smaller than the values for the corresponding cylindrical vessel. The larger the deflection, the smaller both stress values for the toroidal vessel. The circumferential bending stress values decrease faster than the longitudinal stress values. The quantitative results for the stresses indicate that a cylindrical vessel is more highly stressed under the fluid loading than a toroidal vessel.

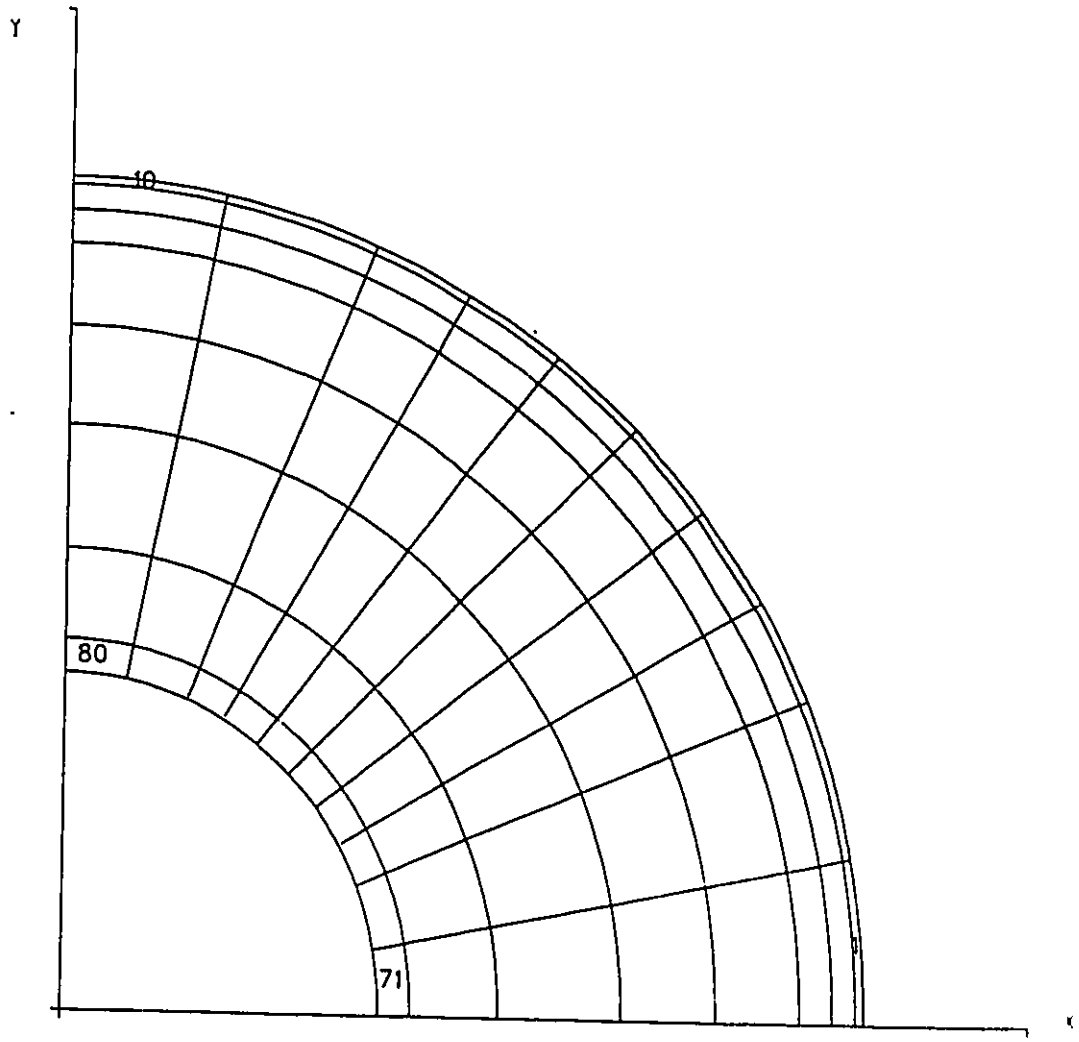

Figure 4.1: Projected view of FEM mesh for the case of the surface loading, showing some element numbers.

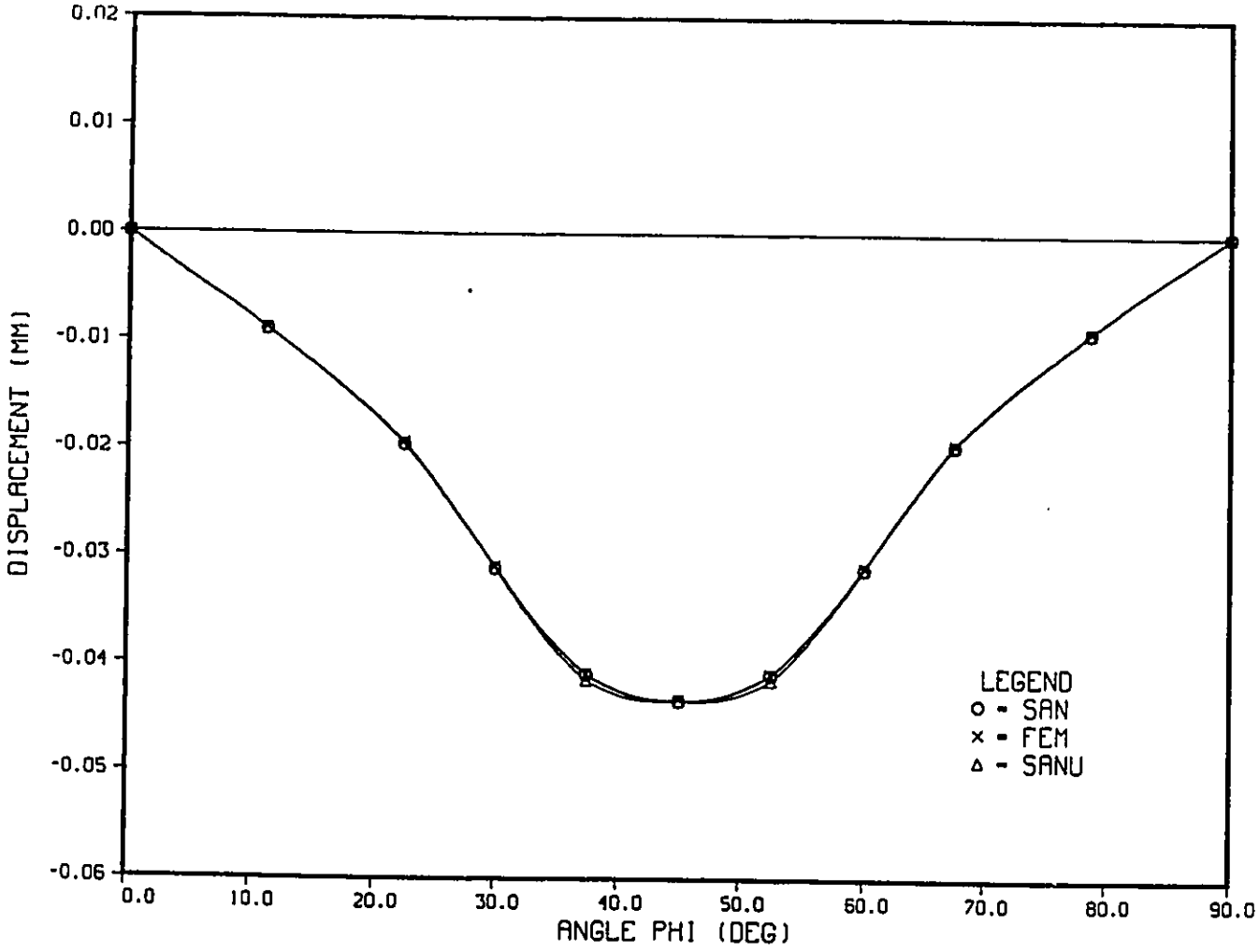

Figure 4.2: Comparison of results for radial displacement w on plane $\theta = 0°$.

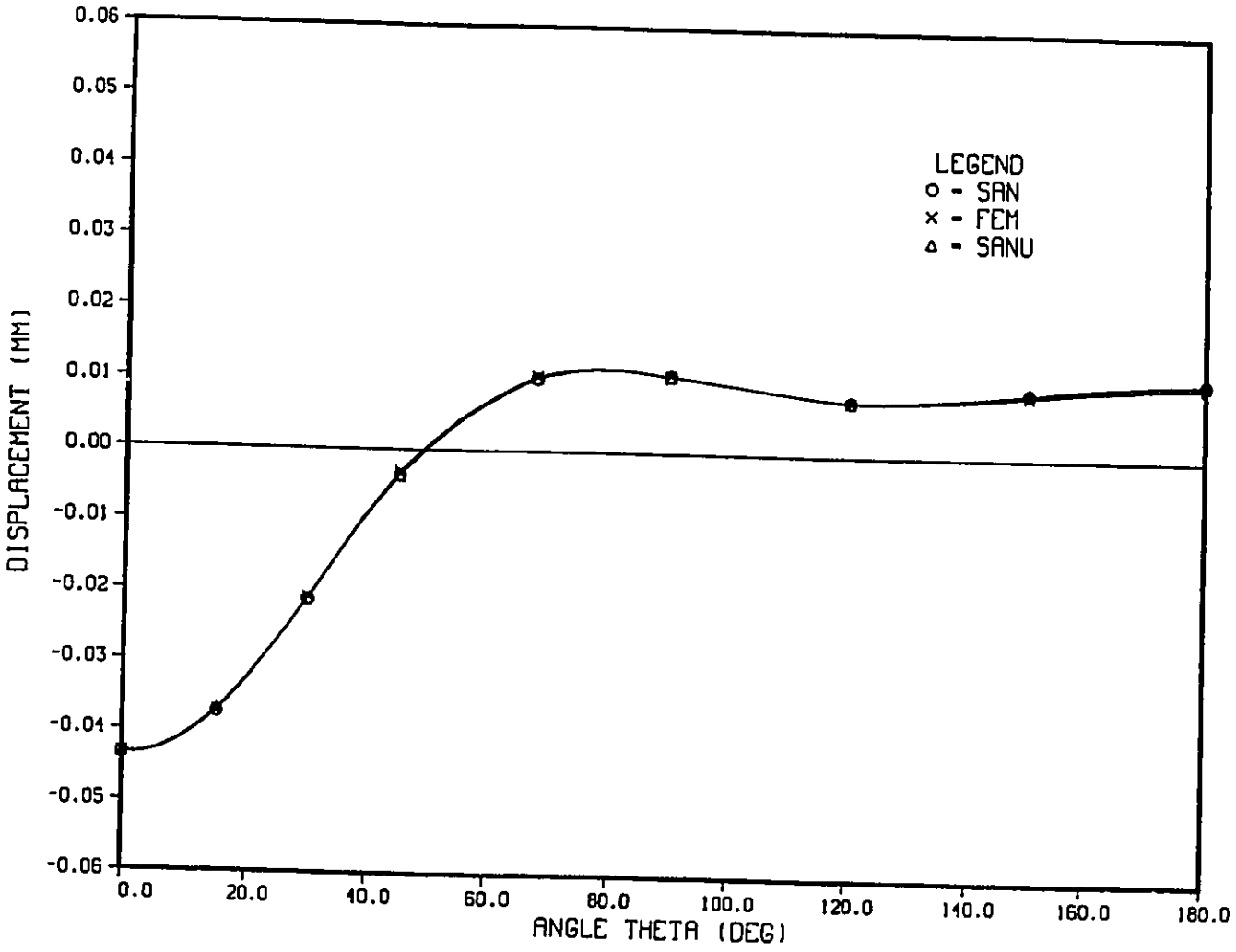

Figure 4.3: Comparison of results for radial displacement w on plane $\phi = 45°$.

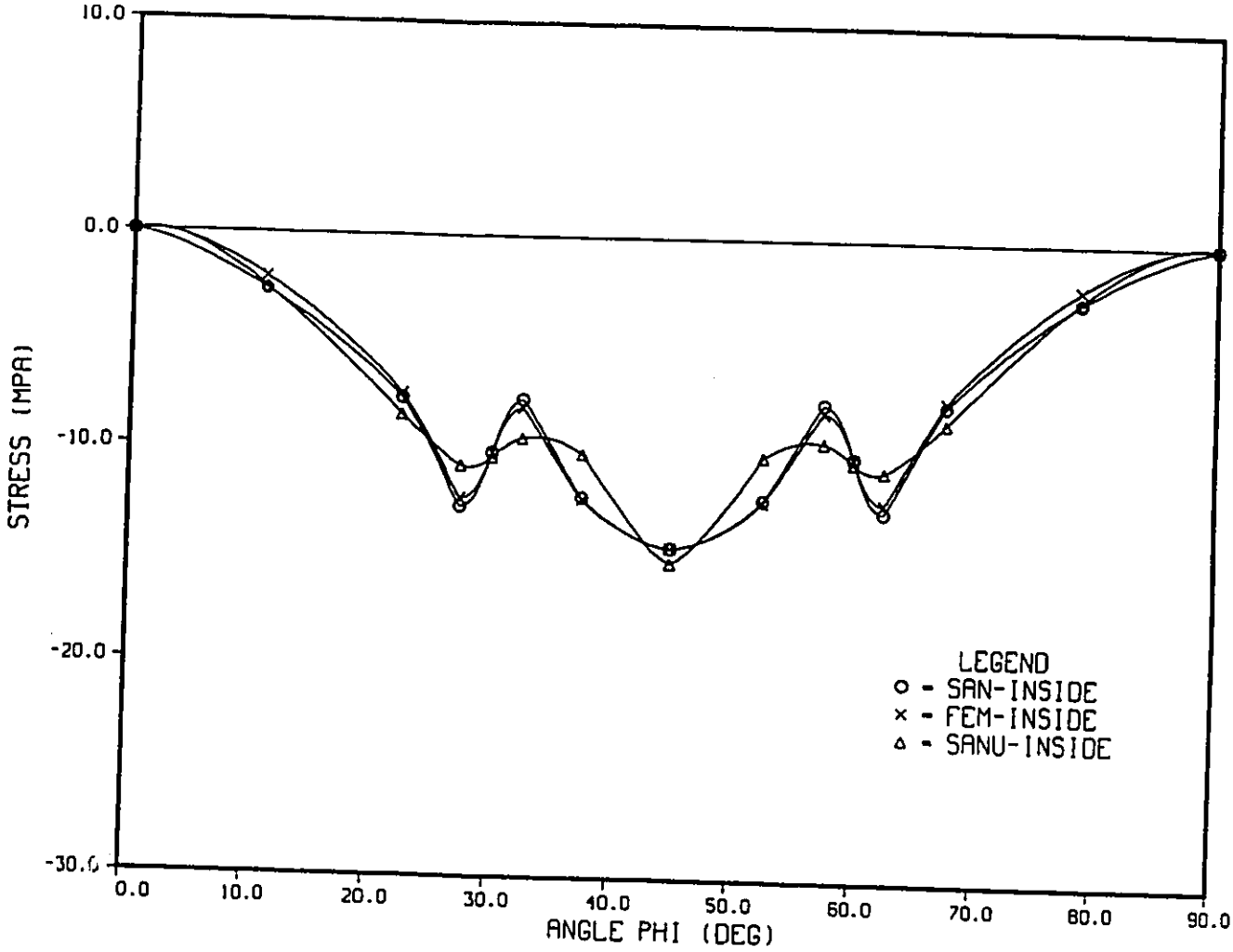

Figure 4.4: Comparison of results for longitudinal stress σ_η on plane $\theta = 0°$.

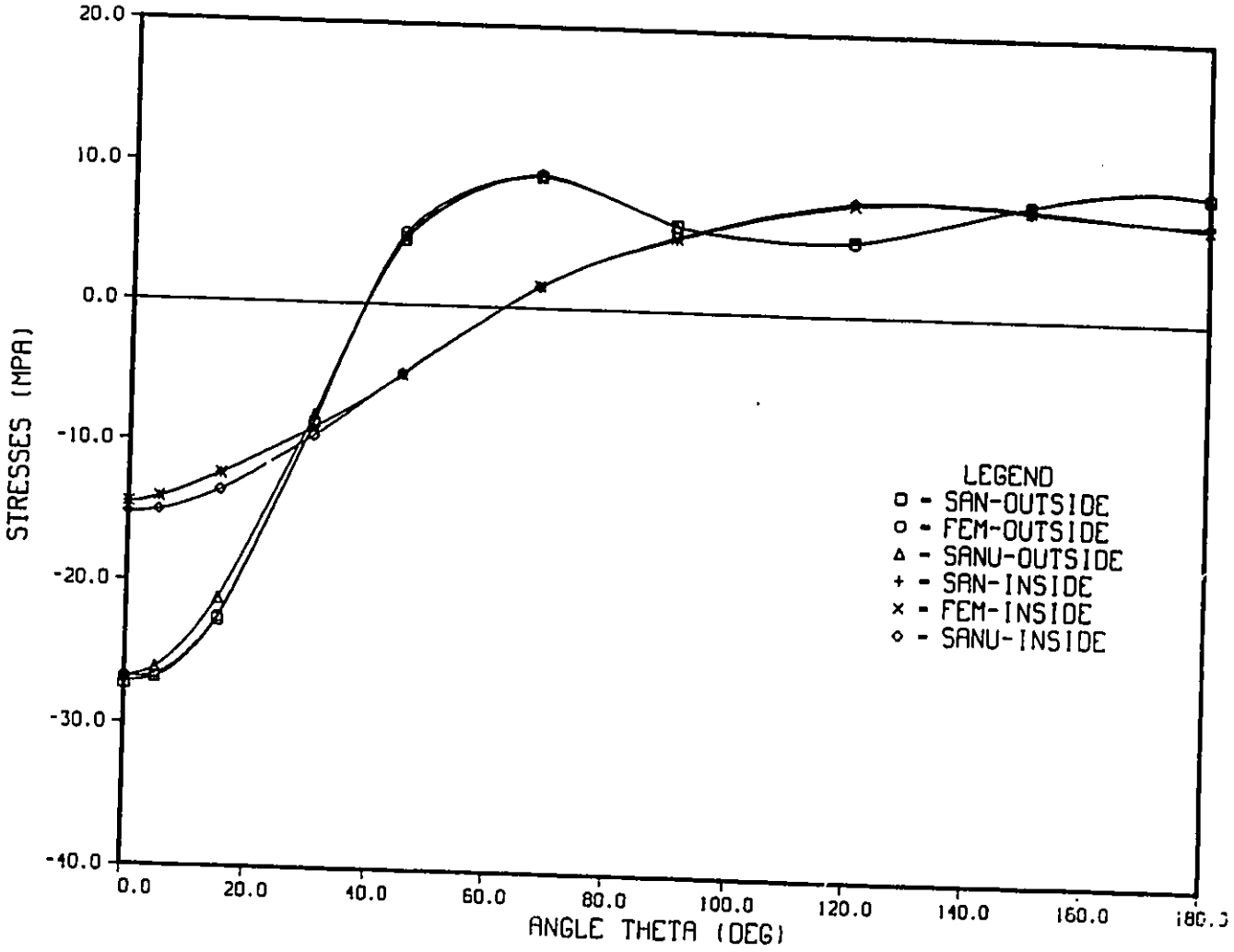

Figure 4.5: Comparison of results for longitudinal stress σ_η on plane $\phi = 45°$.

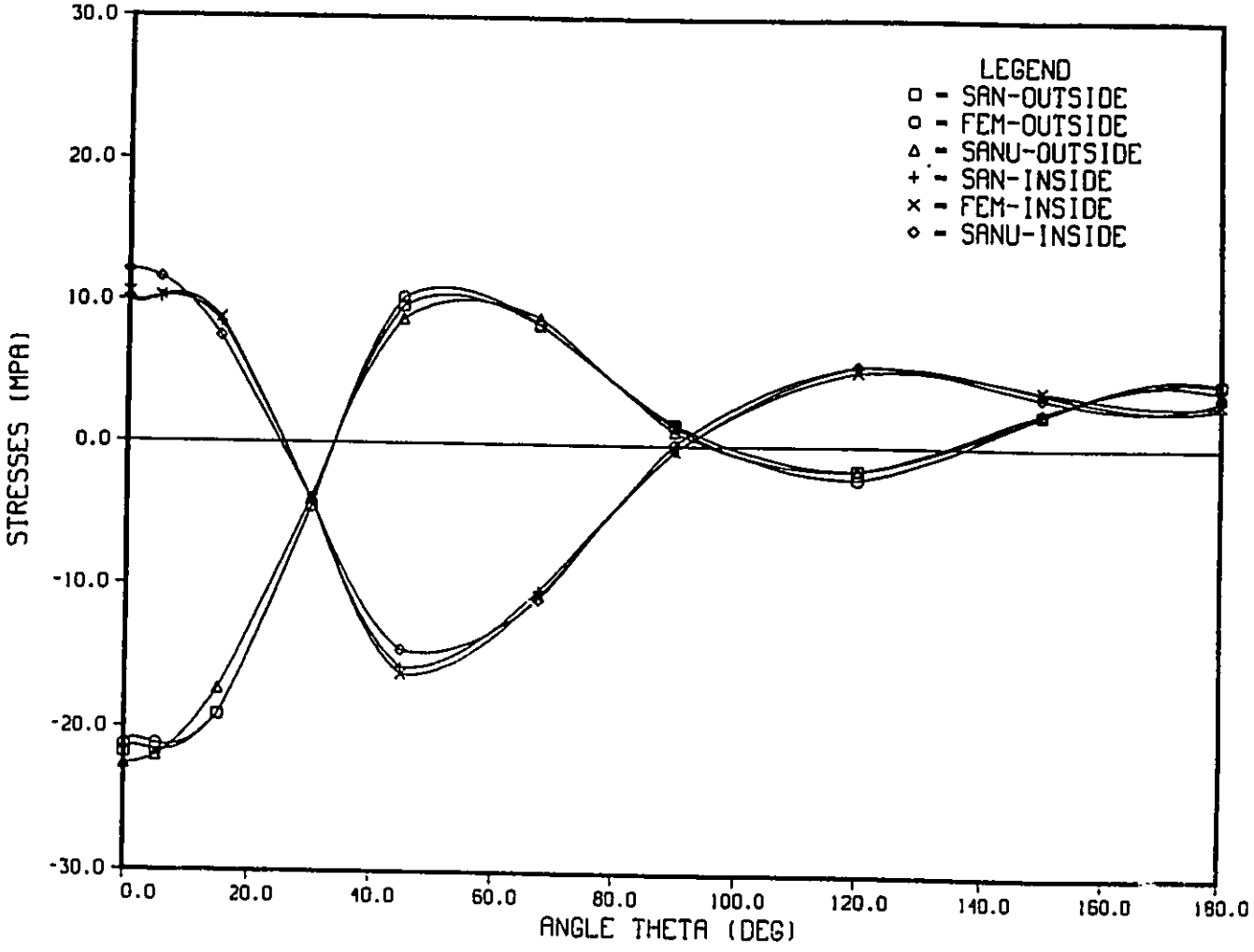

Figure 4.6: Comparison of results for circumferential stress σ_θ on plane $\phi = 45°$.

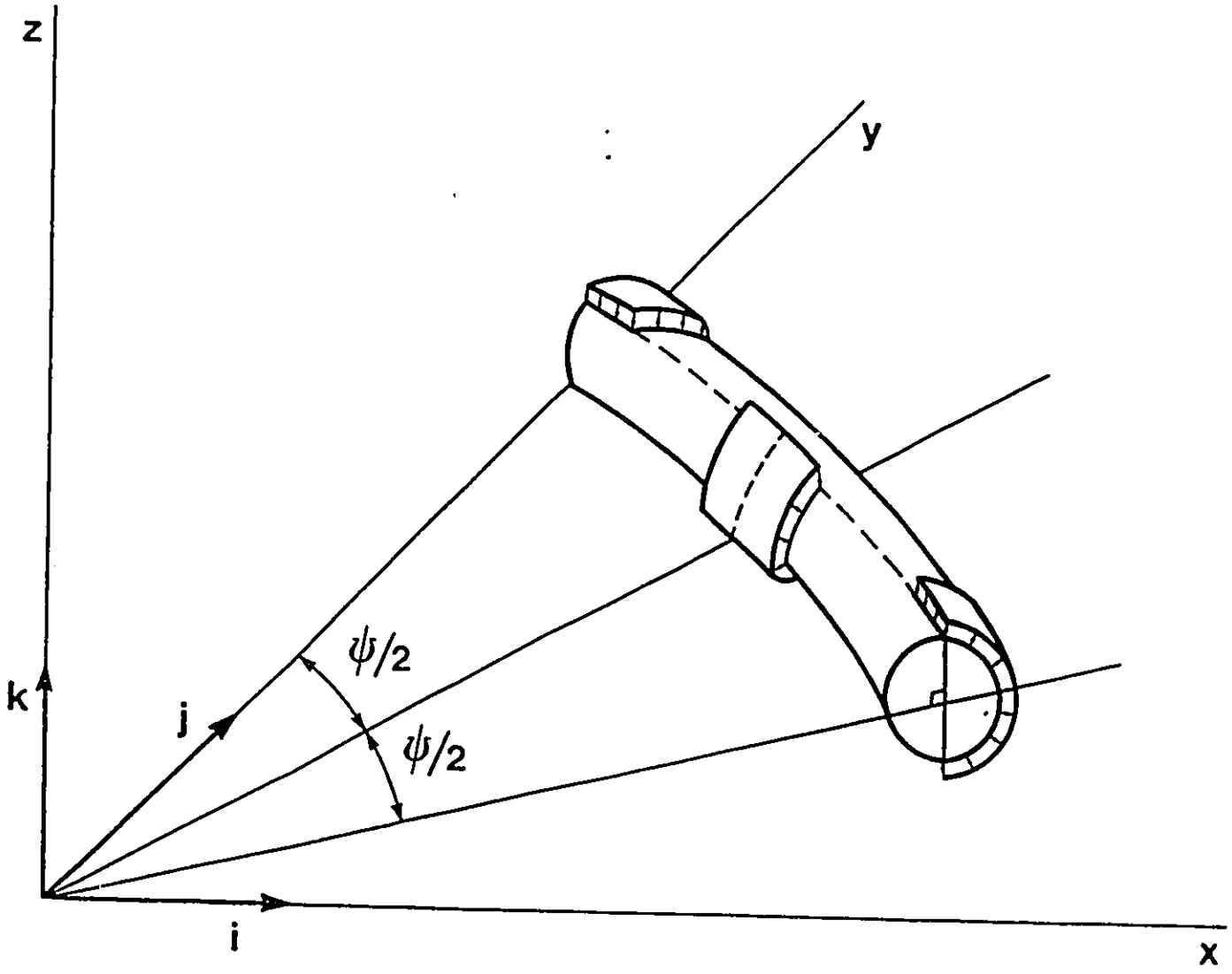

Figure 4.7: Ram bending of a curved pipe.

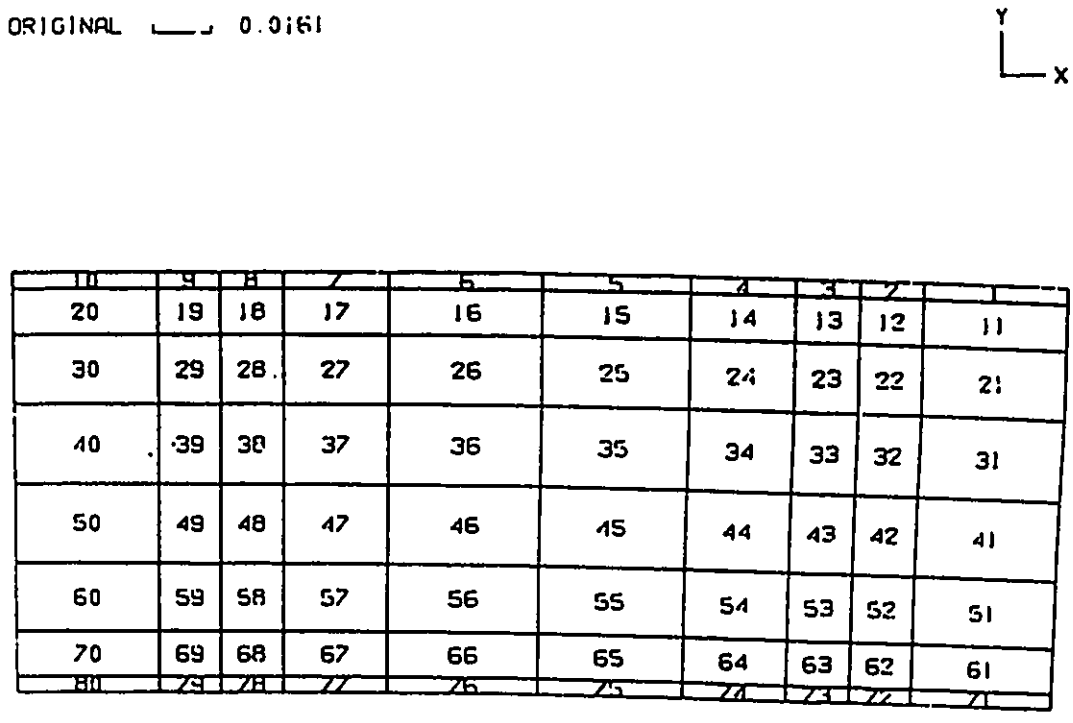

Figure 4.8: FEM mesh for the case of the ram bending.

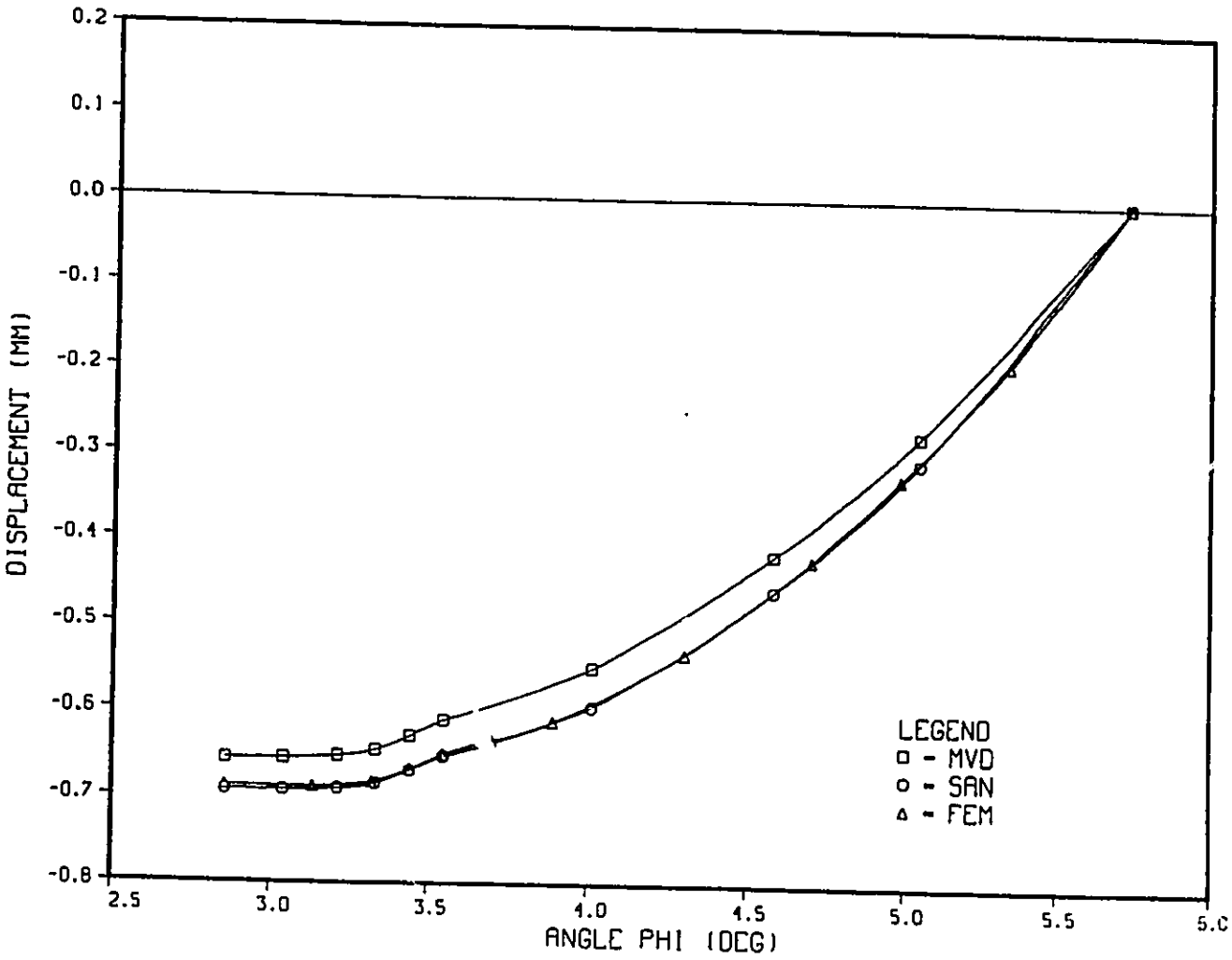

Figure 4.9: Comparison of results for radial displacement w at $\theta = 180°$.

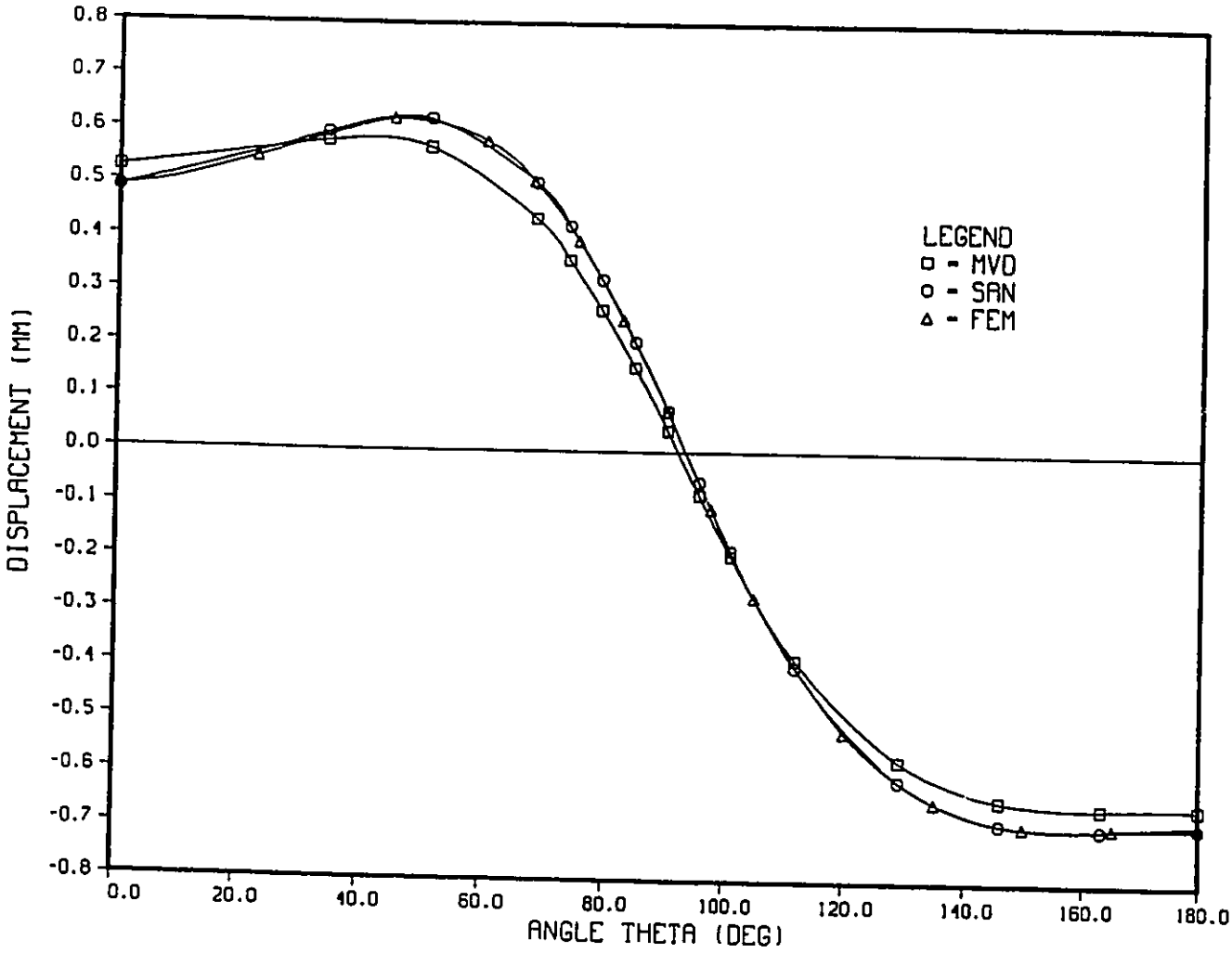

Figure 4.10: Comparison of results for radial displacement w on transverse plane of symmetry.

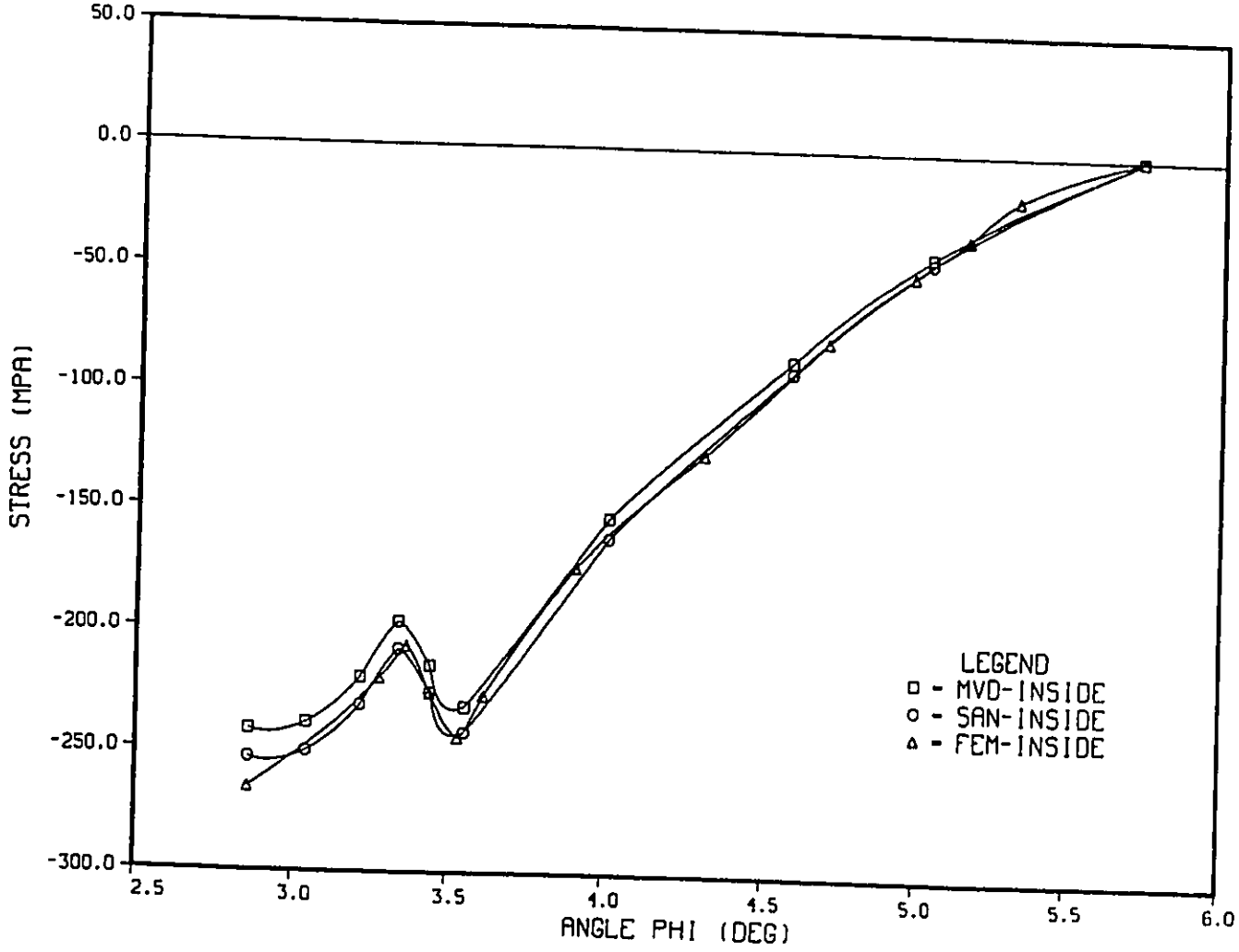

Figure 4.11: Comparison of results for longitudinal stress σ_η at $\theta = 180°$.

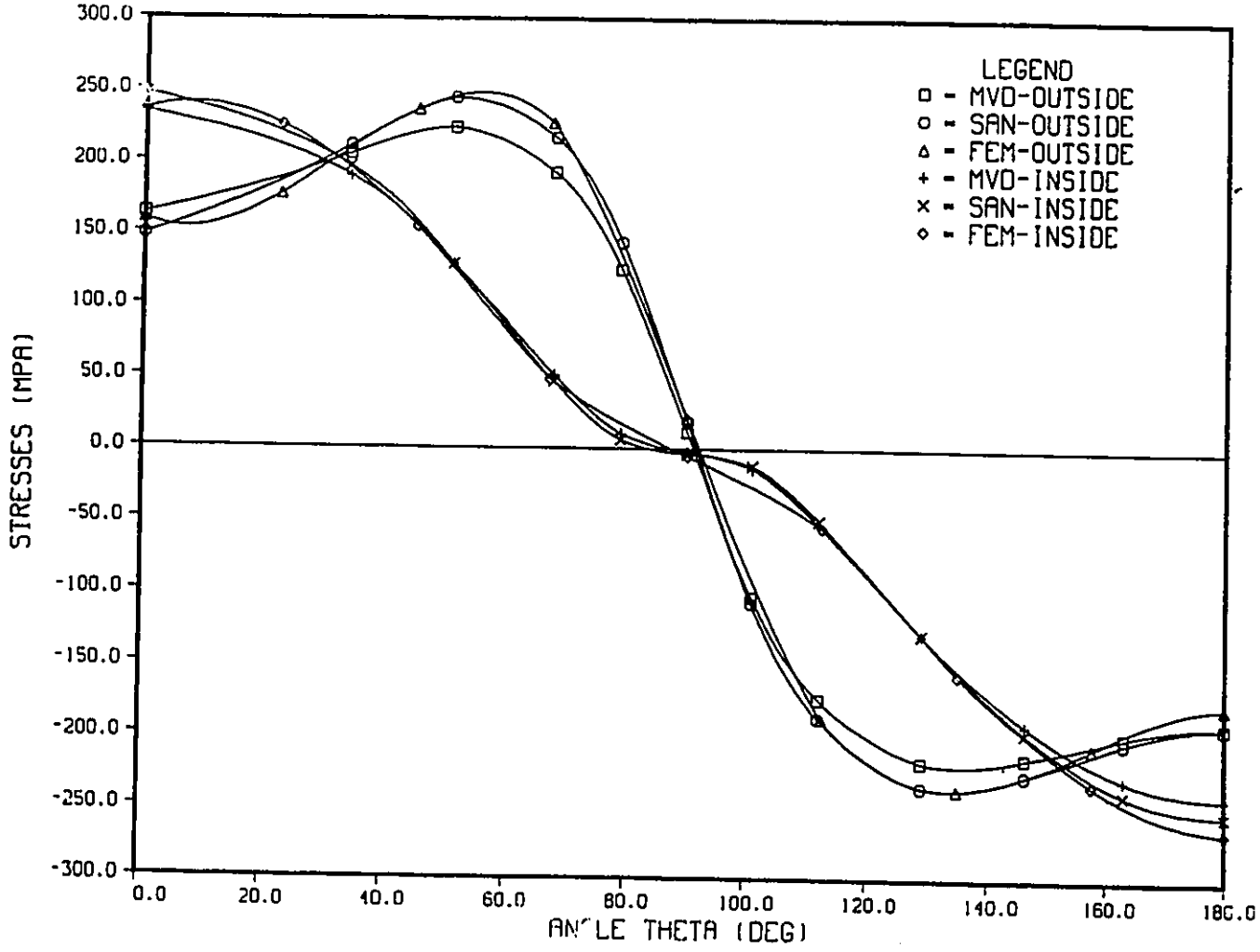

Figure 4.12: Comparison of results for longitudinal stress σ_η on transverse plane of symmetry.

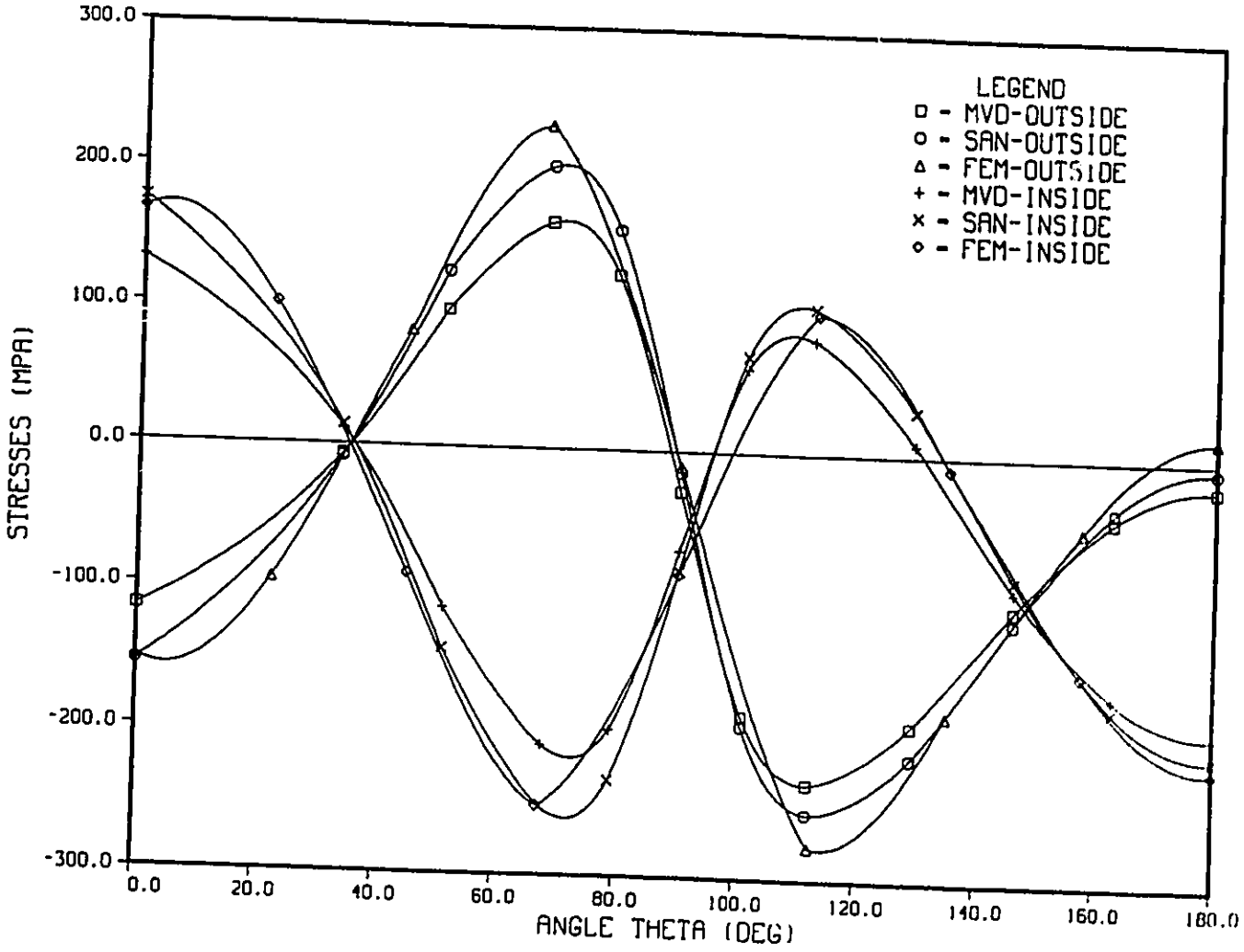

Figure 4.13: Comparison of results for circumferential stress σ_θ on transverse plane of symmetry.

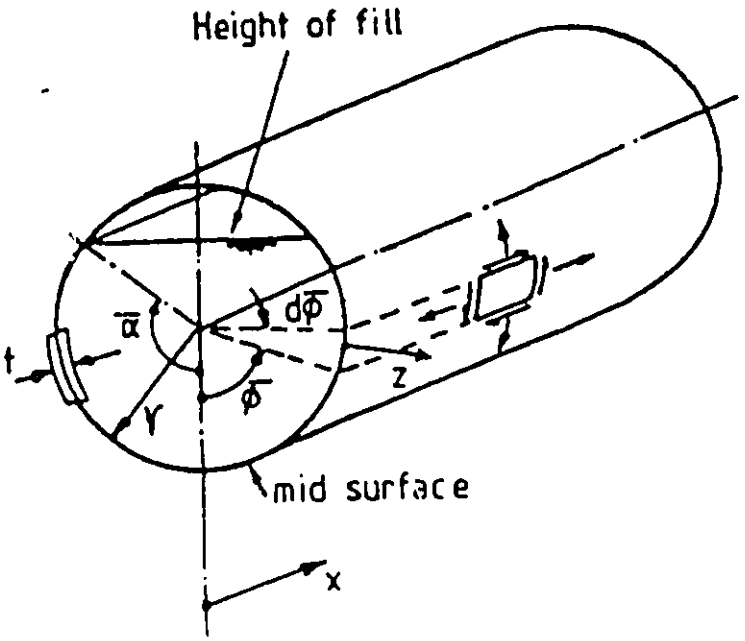

Figure 4.14: Cylindrical vessel.

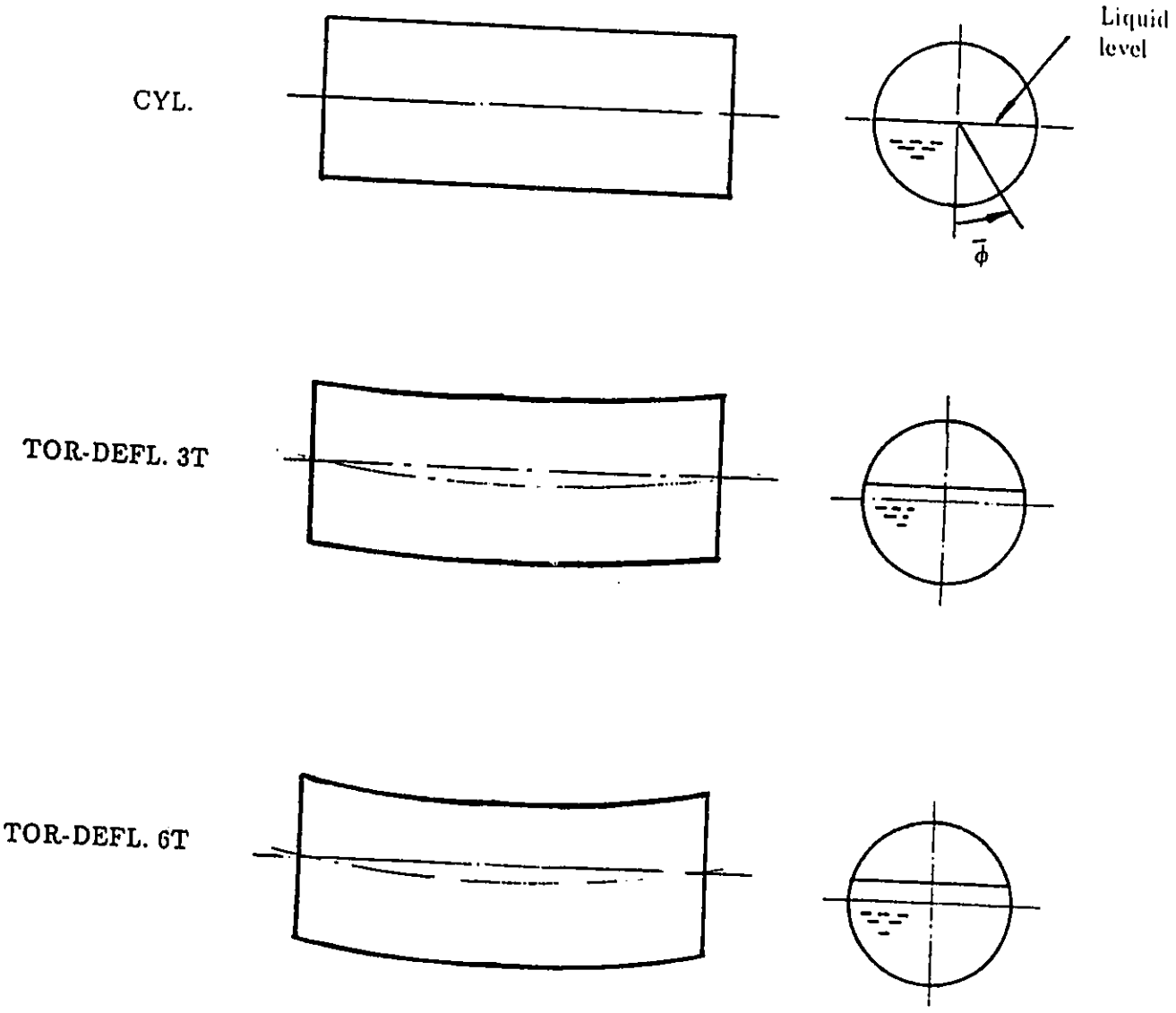

Figure 4.15: Vessels half-filled with fluid.

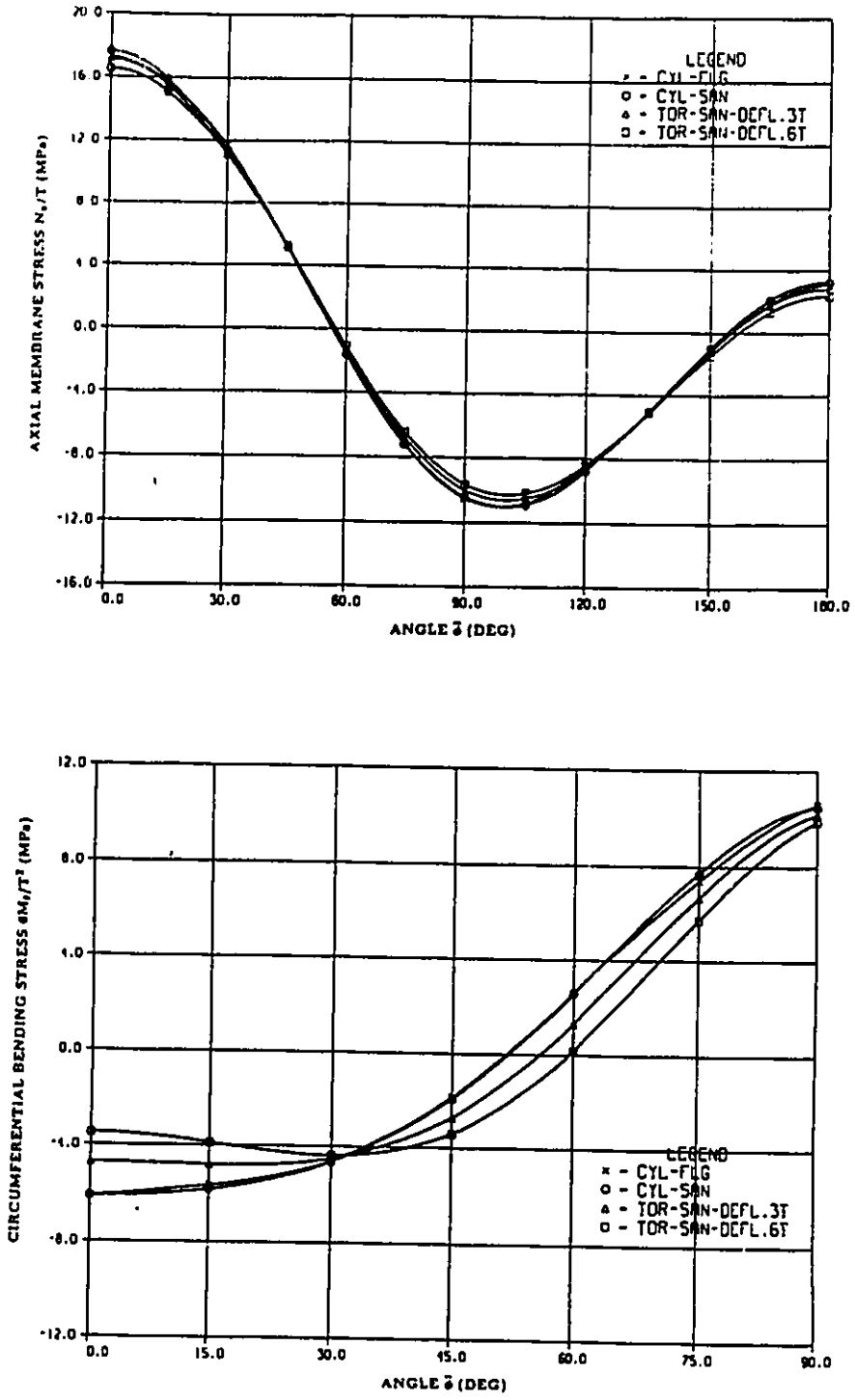

Figure 4.16: Comparison with Flügge solution

Table 4.1: Changes in the diameters for the surface loading problem

	$\Delta Horiz.Diam.(mm)$			$\Delta Vert.Diam.(mm)$		
$\phi°$	*SAN*	*FEM*	*SANU*	*SAN*	*FEM*	*SANU*
0.00	0.0	0.0	0.0	0.0	0.0	0.0
11.25	-0.0049	-0.0052	-0.0049	0.0056	0.0055	0.0056
22.50	-0.0119	-0.0121	-0.0118	0.0123	0.0124	0.0122
30.00	-0.0216	-0.0219	-0.0216	0.0169	0.0171	0.0169
37.50	-0.0303	-0.0307	-0.0309	0.0206	0.0208	0.0204
45.00	-0.0323	-0.0327	-0.0324	0.0219	0.0221	0.0217
52.50	-0.0303	-0.0307	-0.0309	0.0206	0.0208	0.0204
60.00	-0.0216	-0.0219	-0.0216	0.0169	0.0171	0.0169
67.50	-0.0119	-0.0121	-0.0118	0.0123	0.0124	0.0122
78.75	-0.0049	-0.0052	-0.0049	0.0056	0.0055	0.0056
90.00	0.0	0.0	0.0	0.0	0.0	0.0

Table 4.2: Changes in the diameters for the ram bending problem

	$\Delta Horiz.Diam.$			$\Delta Vert.Diam.$		
$\phi°$	MVD	SAN	FEM	MVD	SAN	FEM
2.86	-0.1312	-0.2038	-0.1909	0.0793	0.1525	0.1372
3.04	-0.1313	-0.2036	-0.1887	0.0785	0.1514	0.1340
3.21	-0.1307	-0.2021	-0.1832	0.0768	0.1489	0.1334
3.44	-0.1142	-0.1837	-0.1656	0.0882	0.1581	0.1426
3.66	-0.0964	-0.1630	-0.1446	0.0982	0.1650	0.1489
4.01	-0.0885	-0.1486	-0.1322	0.0880	0.1480	0.1316
4.58	-0.0667	-0.1113	-0.0985	0.0652	0.1094	0.0922
5.04	-0.0452	-0.0735	-0.0657	0.0393	0.0671	0.0496
5.33	-0.0529	-0.0696	-0.0603	-0.0023	0.0141	0.0096
5.73	0.0	0.0	0.0	0.0	0.0	0.0

Chapter 5

Local Loads on a Toroidal Shell

5.1 Introduction

In this chapter, the solution of the Sanders shell theory is applied to the problem of local loads on a sectorial toroidal shell. The solution corresponds to the case of a shell simply supported at the two ends. The effect of pads of uniform normal pressure on the surface at three positions of a 90° piping elbow is considered. These loads are centered at the crown circles, the extrados, and the intrados (Fig. 5.1). Displacement results, as well as stress results, are presented. All results assume linear elastic small-displacement behavior. The results are compared with a similarly loaded cylindrical shell of equal radius, thickness and center-line length. The locations of maximum displacement and stress are identified. Finally three tables are given summarizing characteristic displacements and stresses for a number of shells, covering a wide range of geometric parameters.

5.2 Results for Typical Piping Elbow

Detailed numerical results are presented in this section for a 90° piping elbow having the following values for the geometric and material parameters

$$r = 84.2\,mm;\ R = 252\,mm;\ t = 7.1\,mm \qquad (5.1)$$
$$E = 207{,}000\,MPa;\ \nu = 0.3$$
$$\phi l = 45°$$

These dimensions correspond to a typical pipe used in a power or chemical plant [53]. Results are also given for a comparable straight pipe.

To characterize the geometry of pipe bends the factor Γ has been used [56], while for straight pipes the factors Ω and $\overline{\mathbf{K}}$ are often used [56,57]. These factors are defined as

$$\Gamma = \frac{r^2}{Rt};\ \Omega = \frac{lt^{1/2}}{r^{3/2}};\ \overline{\mathbf{K}} = \Omega^{1/2} \qquad (5.2)$$

where l is the straight pipe center-line length. The values for these three factors for the shell of eqn. (5.1) are $\Gamma = 3.96$, $\Omega = 1.36$, and $\overline{\mathbf{K}} = 1.16$, with l taken as $396mm$.

Results are presented for three cases of local loads (Fig. 5.1). For the first case, corresponding to a 'pinched' shell, the load positions are described by

$$\beta = 90°;\ \lambda = 15°;\ \alpha = 7.5°;\ \delta = 7.5°$$

where the parameters are those of eqn. 3.22.

For convenience this is referred to as the '$p_1 = 1MPa$' case. There are two patches of loadings on the crown circles centered circumferentially at $\theta = 90°$ and 270°. Each load extends 30° circumferentially and from 30° to 60° longitudinally (Fig. 3.2).

For the second case, corresponding to a load at the extrados, the load position is

given by

$$\beta = 15°;\ \lambda = 15°;\ \alpha = 7.5°;\ \delta = 7.5°$$

It is referred to as the '$p_2 = 1MPa$' case. The load extends from $-30°$ to $30°$ circumferentially, and from $30°$ to $60°$ longitudinally.

For the third case, corresponding to a load at the intrados, the load position is described by

$$\beta = 165°;\ \lambda = 15°;\ \alpha = 7.5°;\ \delta = 7.5°$$

It is referred to as the '$p_3 = 1MPa$' case. The load extends from $150°$ to $210°$ circumferentially, and from $30°$ to $60°$ longitudinally.

The convergence of the toroidal shell series solution is further examined in Fig. 5.2 with regard to a $p_2 = 1MPa$ loading case. The longitudinal stress σ_η on the inside shell surface is plotted in the figure versus the longitudinal angle ϕ. Results are given for a 'short', 'medium-length', and 'long' series solution. It is seen that the convergence is rapid. For the 'medium-length' series for which the truncation integers are $M = 51, N = 25$, the results agree very closely with those for the 'long' series. Accordingly the 'medium-length' series was used throughout this study to determine the numerical results.

Results for the three loading cases (Fig. 5.1) are given in Figs. 5.3-5.11. For each load three figures are presented, giving respectively the normal displacement w, the circumferential and longitudinal normal stresses σ_θ, σ_η on the transverse plane of symmetry $\phi = 45°$. For the stresses σ_θ and σ_η, results are given for the inside and outside surfaces. Plotted in each figure are results for the toroidal shell as well as results for a comparable cylindrical shell having the same radius, thickness and center-line length. In each case the boundary conditions at the shell ends are the same, and the total applied

force for the cylindrical shell is equal to that for the toroidal shell. The length of the load pad in the cylindrical shell equals in each case the curved length of the load pad of the toroidal shell.

The toroidal shell results were obtained using the FORTRAN program TORSAN, which is based on the theory presented in Chapter 3. The cylindrical shell results were obtained using the program CYLPAD [19], using the Sanders theory option, with a set of truncation integers of $M = 51, N = 25$. Comparison with FEM results were made for the TORSAN results in Chapter 4, and for the CYLPAD results in ref. [19]. For both programs close agreement was observed in the displacement and stress results from the two methods for local load cases.

Results for the radial displacement w for the 'pinched' shell case ($p_1 = 1MPa$) are given in Fig. 5.3. The maximum displacement under the load for the toroidal shell is very close to that of the cylindrical shell. The displacement pattern for the toroidal shell indicates an inward rigid-body translation of the cross-section resulting in an overall small outward displacement at the extrados and an overall large outward displacement at the intrados.

The results for the stresses σ_θ and σ_η for the 'pinched' shell (Fig. 5.4 and 5.5) indicate maximum values which are nearly equal for the toroidal and cylindrical shells. The stresses in the toroidal shell near the extrados are smaller than those in the cylindrical shell at 90° from the load center, while stresses σ_η on the outside surface and σ_θ at the intrados are greater. Overall for the 'pinched' shell case the cylindrical shell results give a close indication of the results in the toroidal shell.

The results for the case of loading at the extrados ($p_2 = 1MPa$) are presented in Figs. 5.6, 5.7 and 5.8. For the radial displacement w the maximum value for the toroidal shell is less than one-half that for the cylindrical shell. The load is situated at

a positive Gaussian curvature portion of the toroidal shell and thus superior results are to be expected with respect to the cylindrical shell. It is noted that the deflection in the cylindrical shell at a position of 180° from the load center is inward. A finite element method analysis was carried out which served to confirm this particular result.

The results for σ_η on the outside surface and σ_θ in Fig. 5.8 and 5.7 indicate that much greater stresses arise in the cylindrical shell than in the toroidal shell. The stresses are rather localized and decay rapidly away from the loading area. Overall the results indicate that for a local load at the extrados a toroidal shell experiences much smaller deflections and stresses than a comparable cylindrical shell.

The results for the case of loading at the intrados ($p_3 = 1\ MPa$) are presented in Figs. 5.9, 5.10 and 5.11. In this case the maximum value for the radial deflection w for the toroidal shell significantly exceeds that for the cylindrical shell. The quantitative results for the displacements indicate clearly that the intrados of a toroidal shell is most vulnerable to deformation under local loading. Stress results for the third loading case are given in Fig. 5.10 and 5.11. The stress patterns in the toroidal and cylindrical shells are remarkably similar. The maximum values σ_η on the inside surface and σ_θ in the toroidal shell exceed those in the cylindrical shell.

5.3 Parametric Study

The results discussed in the preceding section are for the particular shell described in eqns. (5.1). Ten additional shell cases are described in Tables 5.1-5.3. The geometric parameters are given in Table 5.1. Cases 1 to 3 are relatively thin shells whereas cases 9 and 10 are thick shells, not strictly within the validity of thin shell theory. The last two cases are considered to include cylindrical shells with $\Omega \geq 3$ ($\overline{\mathrm{K}} \geq 1.7$), for which

Calladine [56] predicts mainly 'beam'-type behavior.

Presented in Tables 5.2 and 5.3 are the results for toroidal shells loaded at the extrados and intrados, and the results for comparable cylindrical shells. The four shells analyzed under each case were subjected to the same total load. For the toroidal shells the loads extended through a 30° longitudinal arc, giving longer load pad lengths at the extrados than at the intrados. The load intensity for the extrados loading thus was smaller than that for the intrados loading. Two cylindrical shells were analyzed for each case, with load pad lengths equal to the two corresponding toroidal shell load pad lengths, and load intensities to suit. In Tables 5.2 and 5.3 results are given for the radial displacement w, and the membrane and bending parts of the longitudinal (σ_η) and circumferential (σ_θ) normal stresses at the center of the load pad. Values at this position are at or near the maximum and are referred to in the following as the characteristic values. The membrane stress in each table appears above the bending stress. The results of Table 5.2 represent the case of the loading at the extrados while those of Table 5.3 the case of the loading at the intrados.

The characteristic radial displacement values for toroidal shells in general are smaller than the values for the corresponding cylindrical shell, if the load is at the extrados, and greater if the load is at the intrados. The differences tend to decrease as the $\overline{\mathrm{K}}$ ratio increases. For $\overline{\mathrm{K}} > 1.7$ exceptions arise for the toroidal shell loaded at the extrados.

For the cylindrical shells the characteristic longitudinal membrane stresses are greater than the bending stresses, while the characteristic circumferential membrane stresses are smaller than the bending stresses, for all $\overline{\mathrm{K}}$. For the toroidal shell loaded at the extrados the characteristic longitudinal membrane stresses are greater than the bending stresses for all $\overline{\mathrm{K}}$, while the characteristic circumferential membrane stresses are greater than the bending stresses for $\overline{\mathrm{K}} < 1$. For the toroidal shell loaded at the intrados the characteristic longitudinal and circumferential membrane stresses are smaller than the

bending stresses, for all $\overline{K}$. For loads at the intrados the theory predicts positive (tensile) characteristic longitudinal membrane stresses at the intrados for $\overline{K} < 1.3$. Relatively large outward longitudinal deflections v at the intrados are predicted for these cases at the shell ends. Such displacements are permissible with the boundary conditions defined.

For $\overline{K} < 1.7$ the characteristic membrane and bending stresses in the toroidal shells loaded at the extrados are generally smaller than those for the cylindrical shell. Also for $\overline{K} < 1.7$ the membrane stresses for the toroidal shell loaded at the intrados are generally smaller than those for the cylindrical shell, while the bending stresses are greater. For $\overline{K} > 1.7$ the membrane stresses in the toroidal shell loaded at either the extrados or intrados are similar in magnitude to the membrane stresses in the comparable cylindrical shells. Also for $\overline{K} > 1.7$, the characteristic bending stresses in the toroidal shells loaded at the extrados are smaller than the bending stresses in the comparable cylindrical shell, while the characteristic bending stresses in the toroidal shell loaded at the intrados are greater.

In summary, for $\overline{K} < 1.7$ a local load generally induces smaller characteristic bending stresses in a toroidal shell than in a cylindrical shell if the load is at the extrados, and greater stresses if the load is at the intrados. The results indicate that when shell action predominates a toroidal shell shows superior structural qualities compared to a cylindrical shell if the load is at the extrados, and inferior qualities if the load is at the intrados.

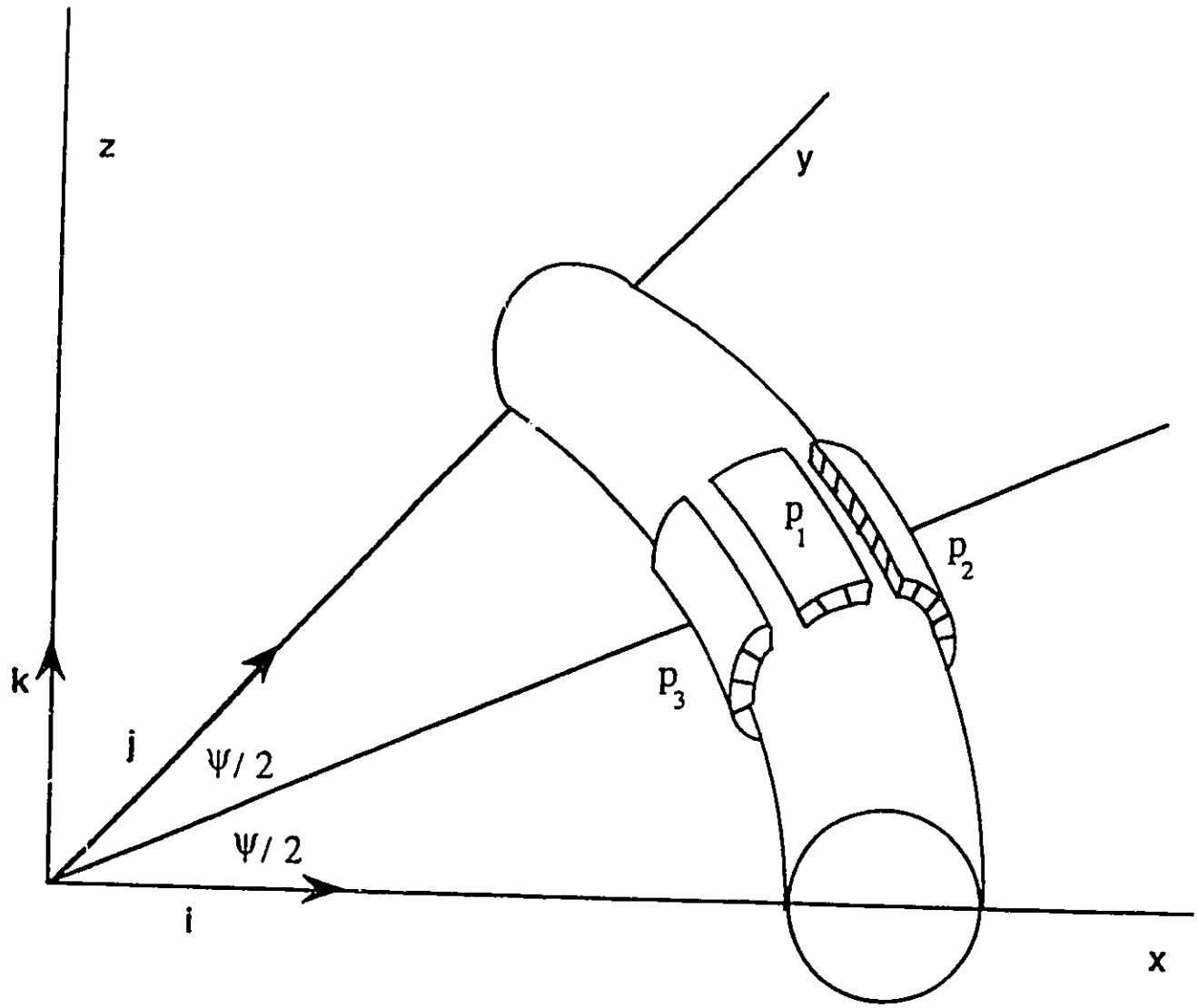

Figure 5.1: Loading cases considered.

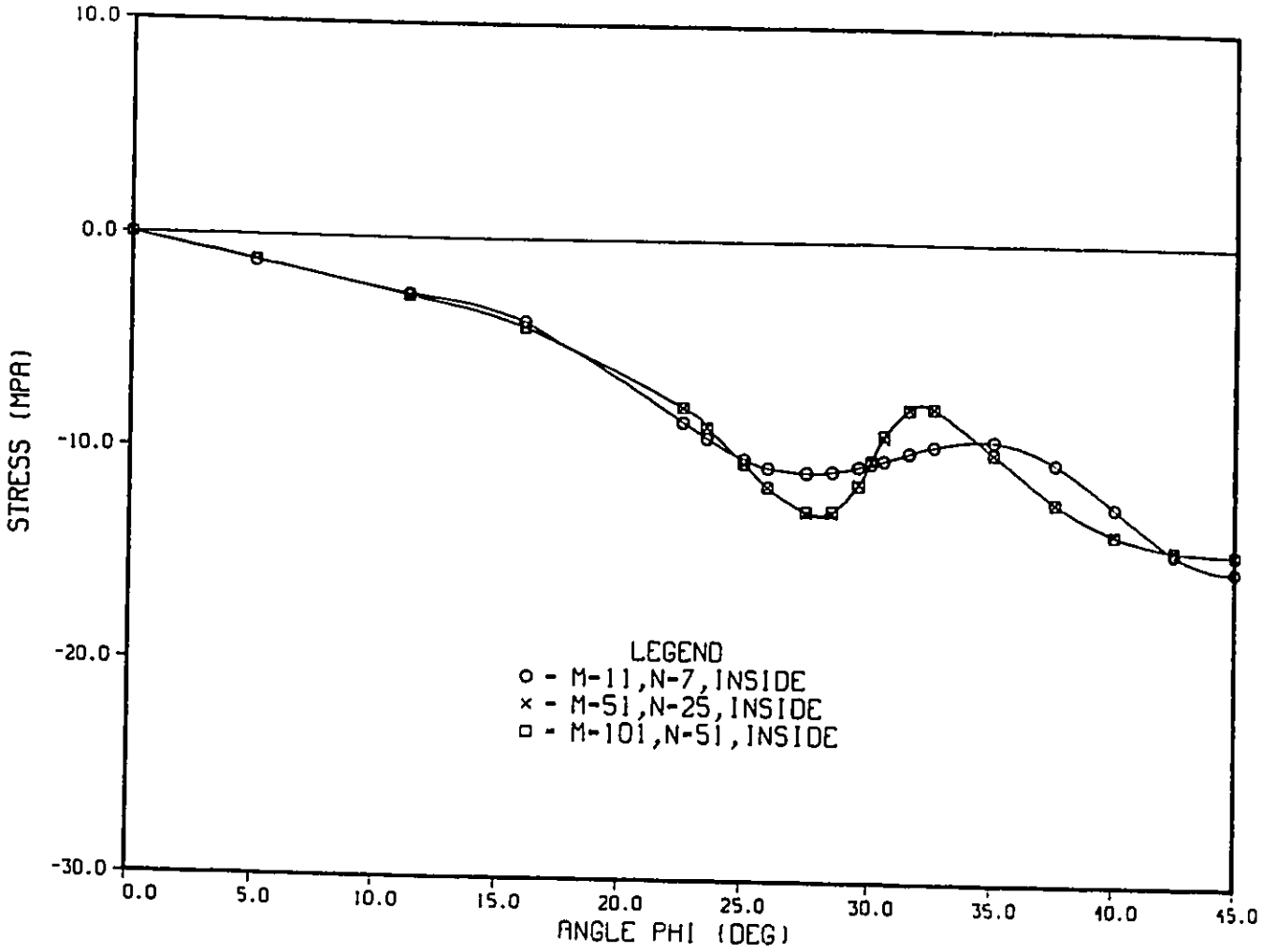

Figure 5.2: Convergence of the Fourier series for the stress σ_η.

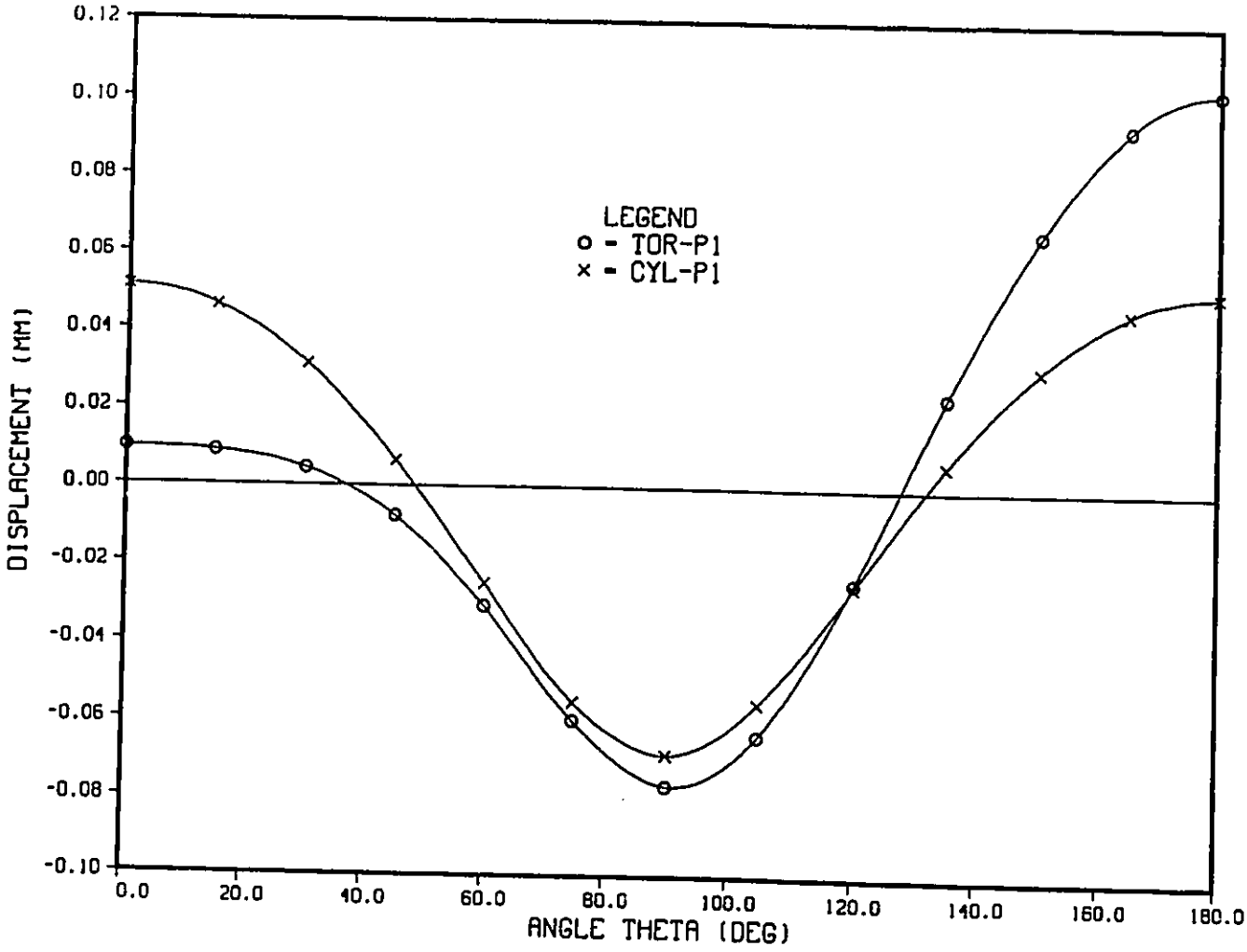

Figure 5.3: Radial displacement w at $\phi = 45°$ for a 'pinched' shell ($p_1 = 1$).

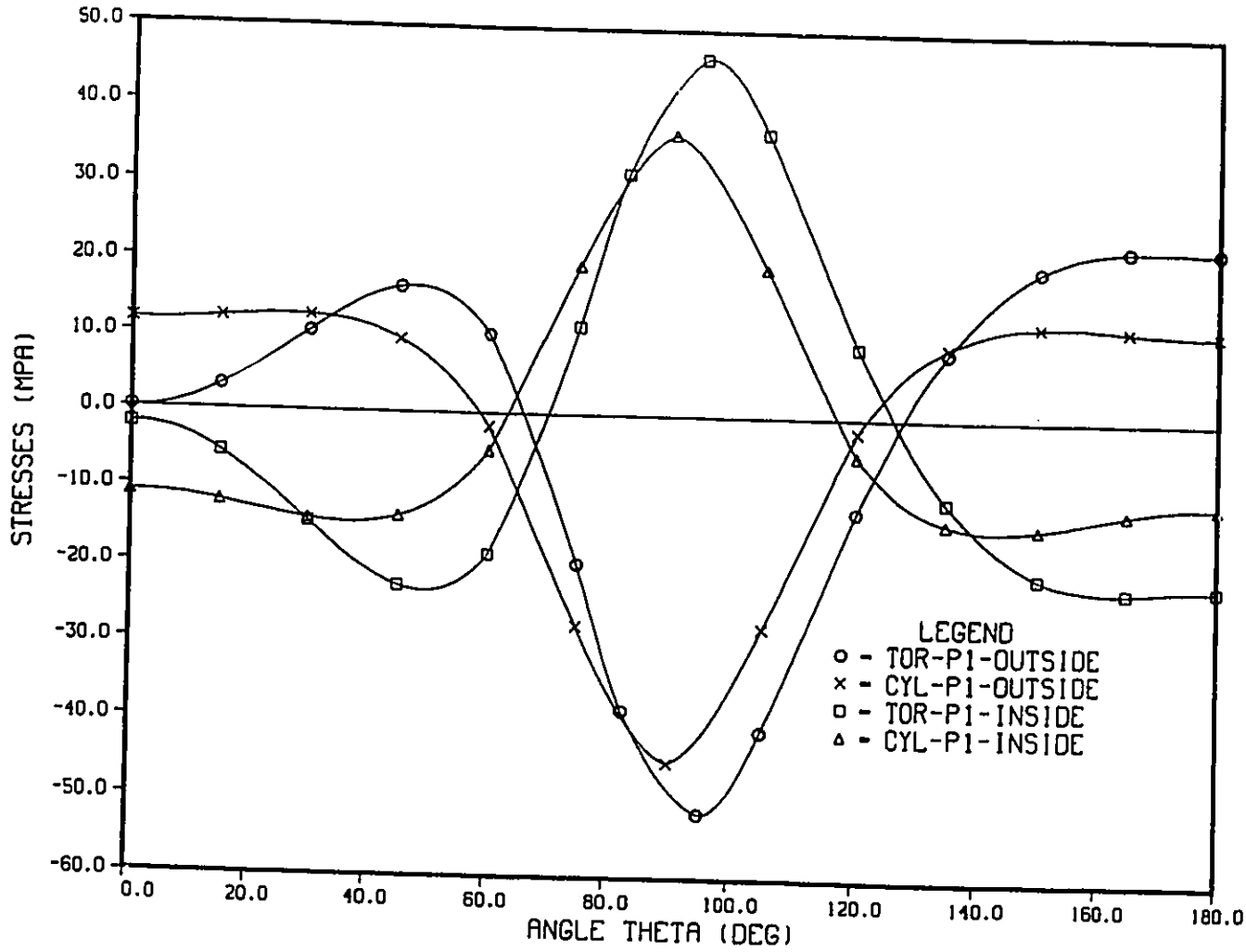

Figure 5.4: Stress σ_θ at $\phi = 45°$ for a 'pinched' shell ($p_1 = 1$).

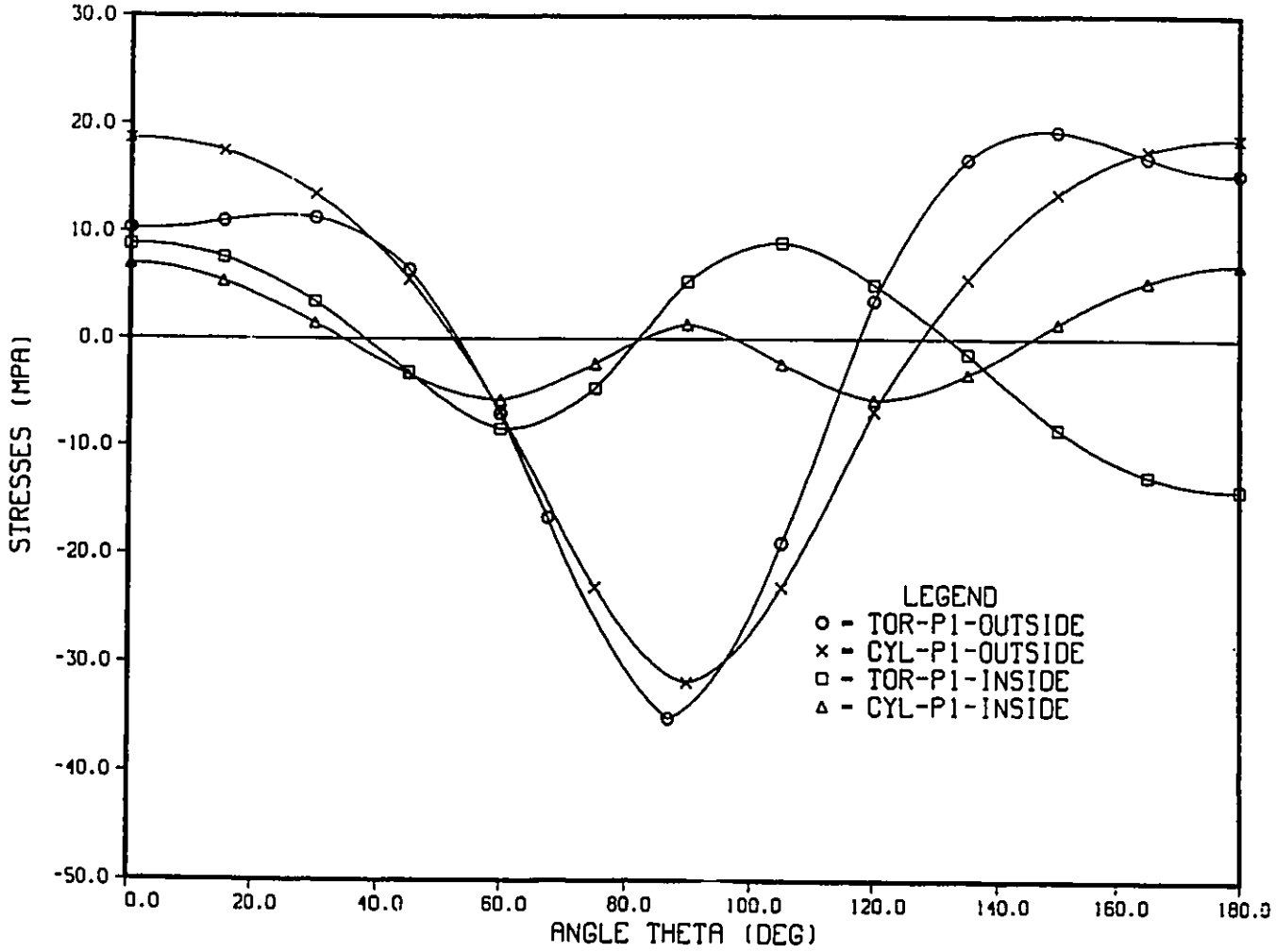

Figure 5.5: Stress σ_η at $\phi = 45°$ for a 'pinched' shell ($p_1 = 1$).

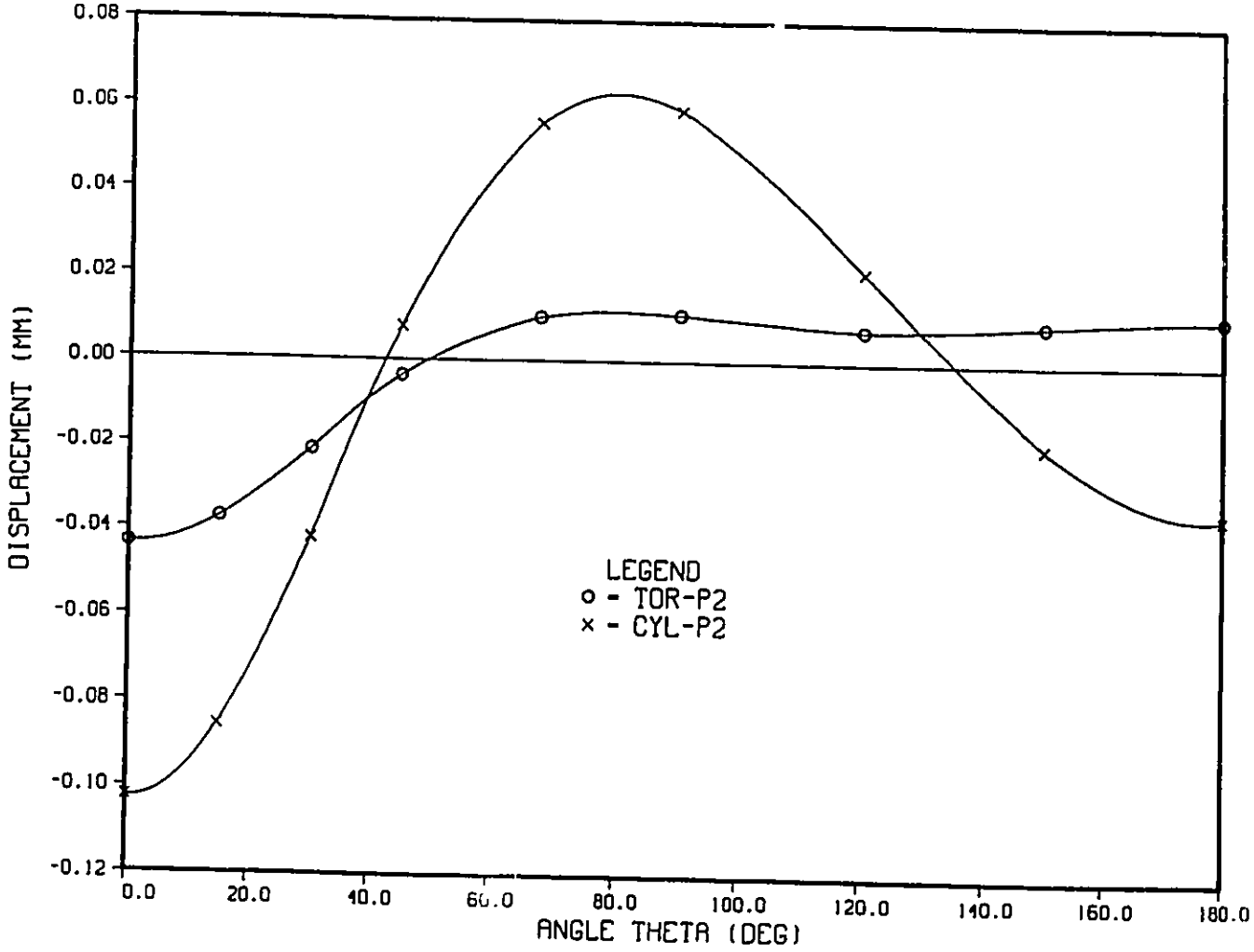

Figure 5.6: Radial displacement w at $\phi = 45°$ for shell loaded at extrados ($p_2 = 1$).

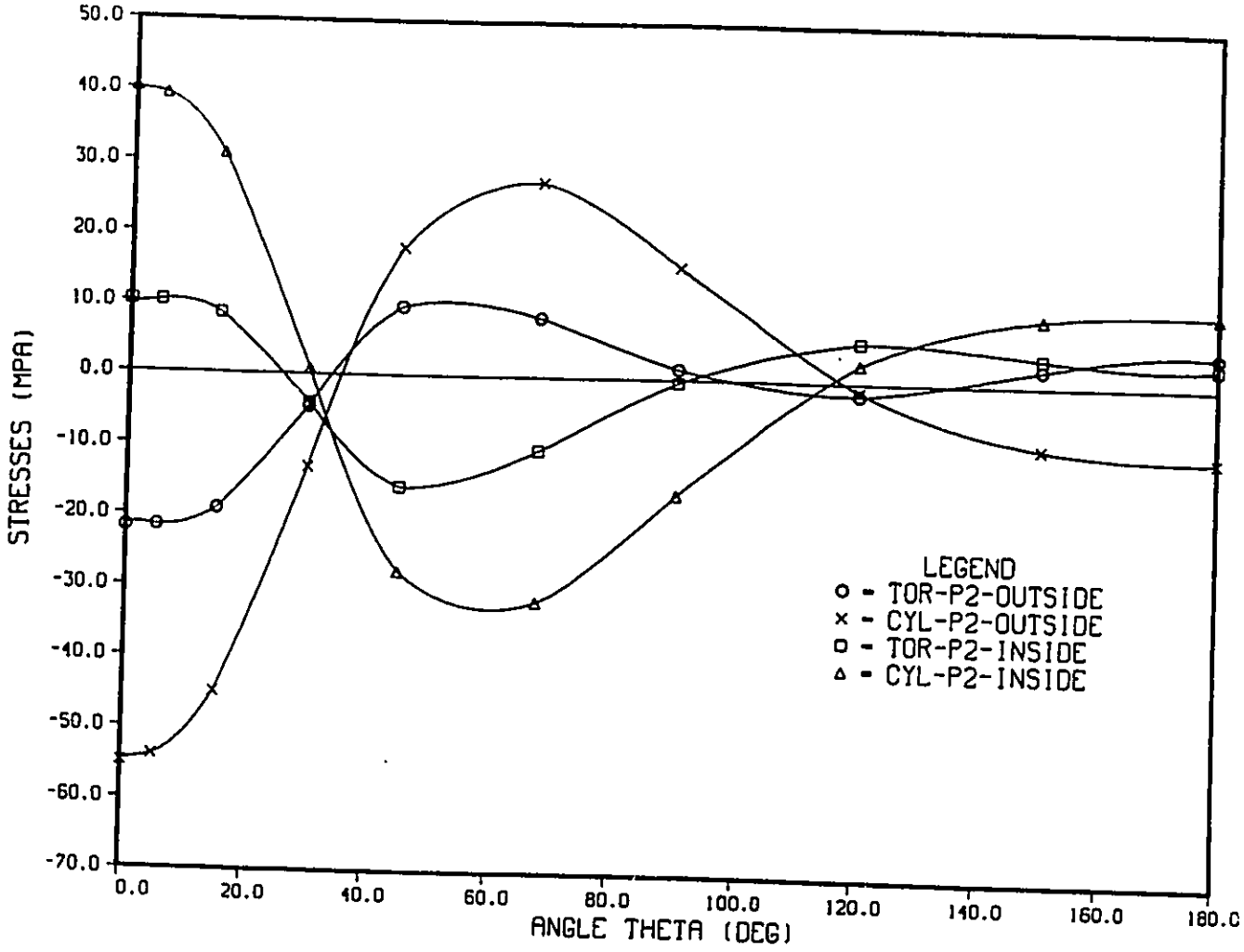

Figure 5.7: Stress σ_θ at $\phi = 45°$ for shell loaded at extrados ($p_2 = 1$).

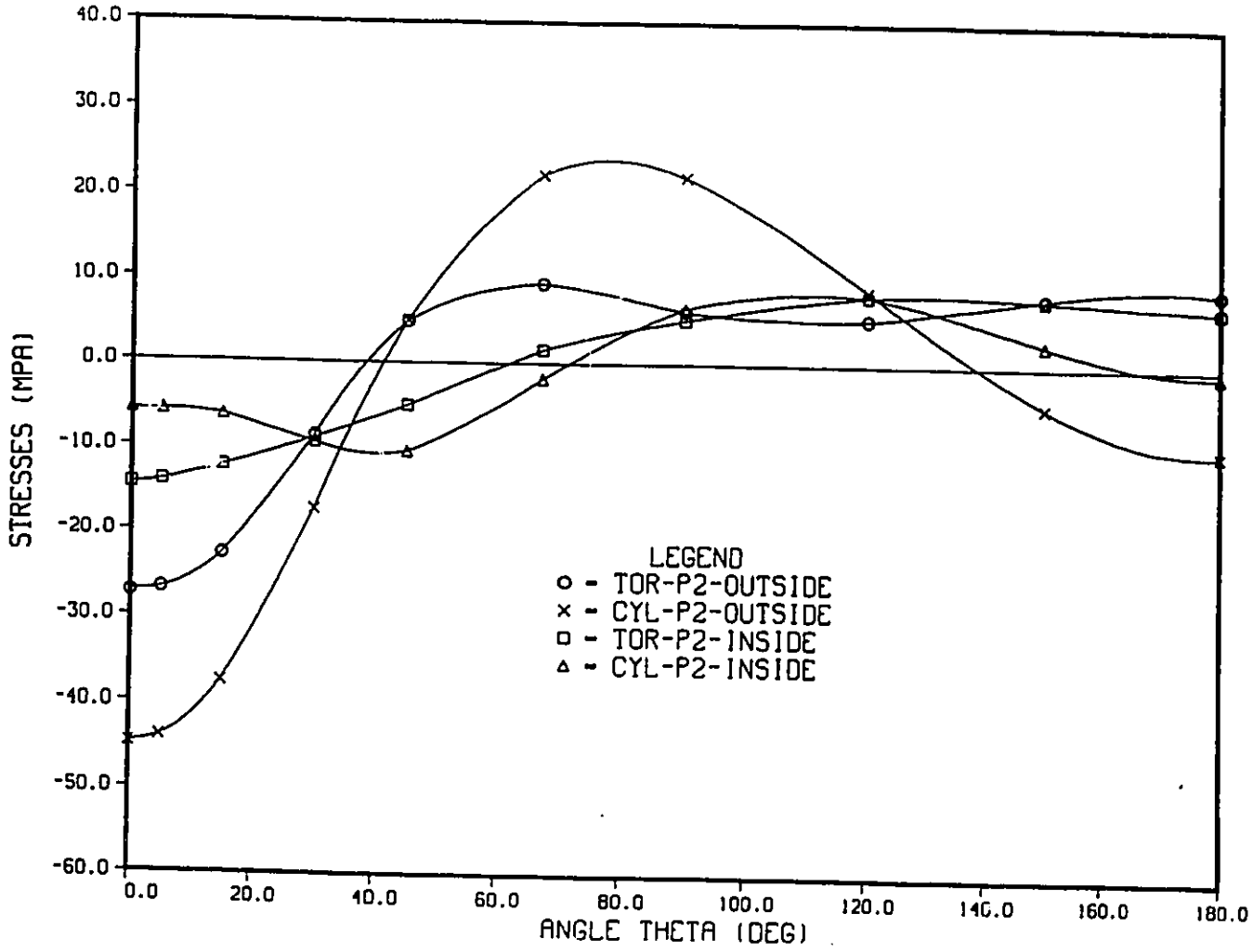

Figure 5.8: Stress σ_η at $\phi = 45°$ for shell loaded at extrados ($p_2 = 1$).

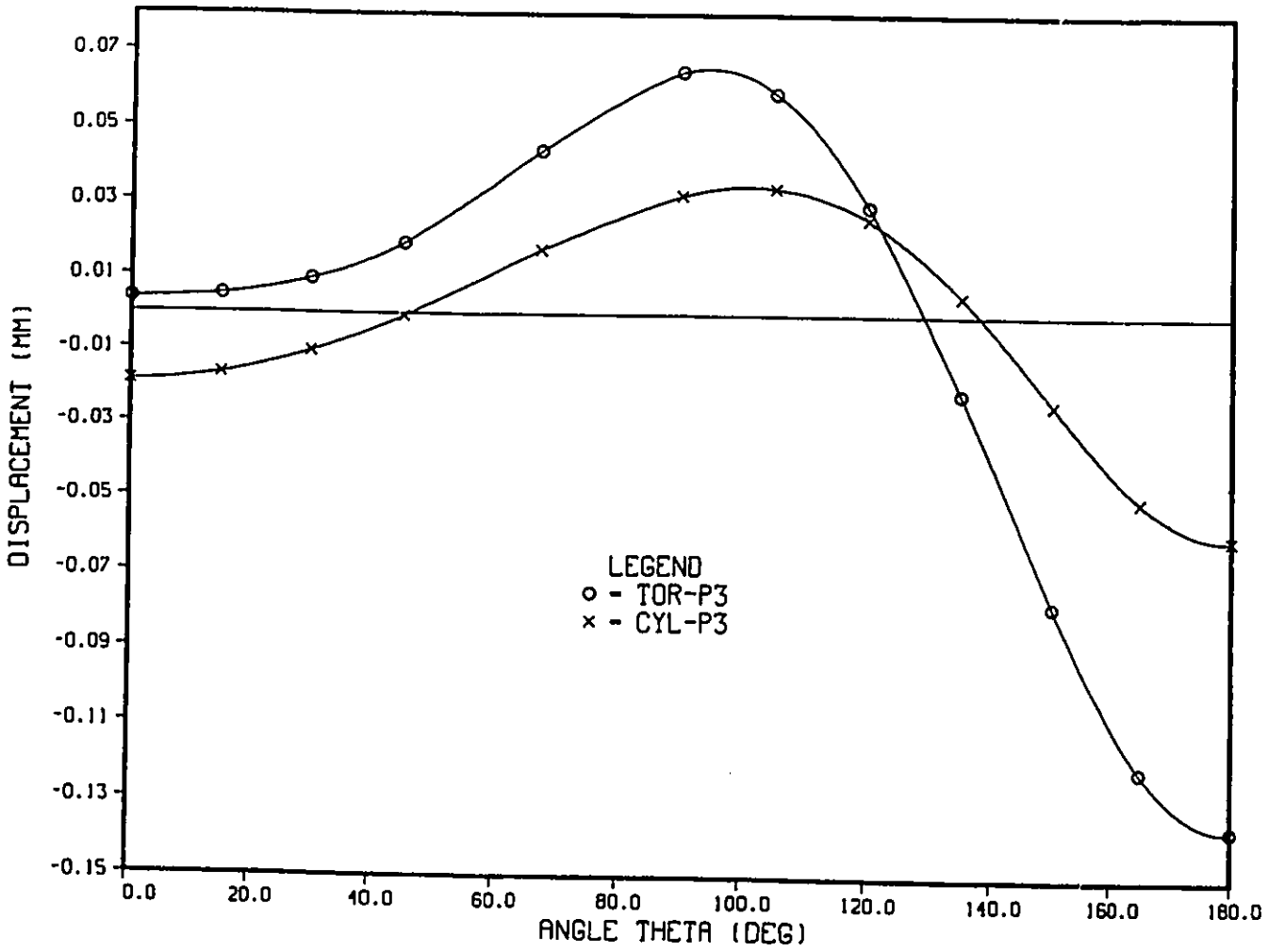

Figure 5.9: Radial displacement w at $\phi = 45°$ for shell loaded at intrados ($p_3 = 1$).

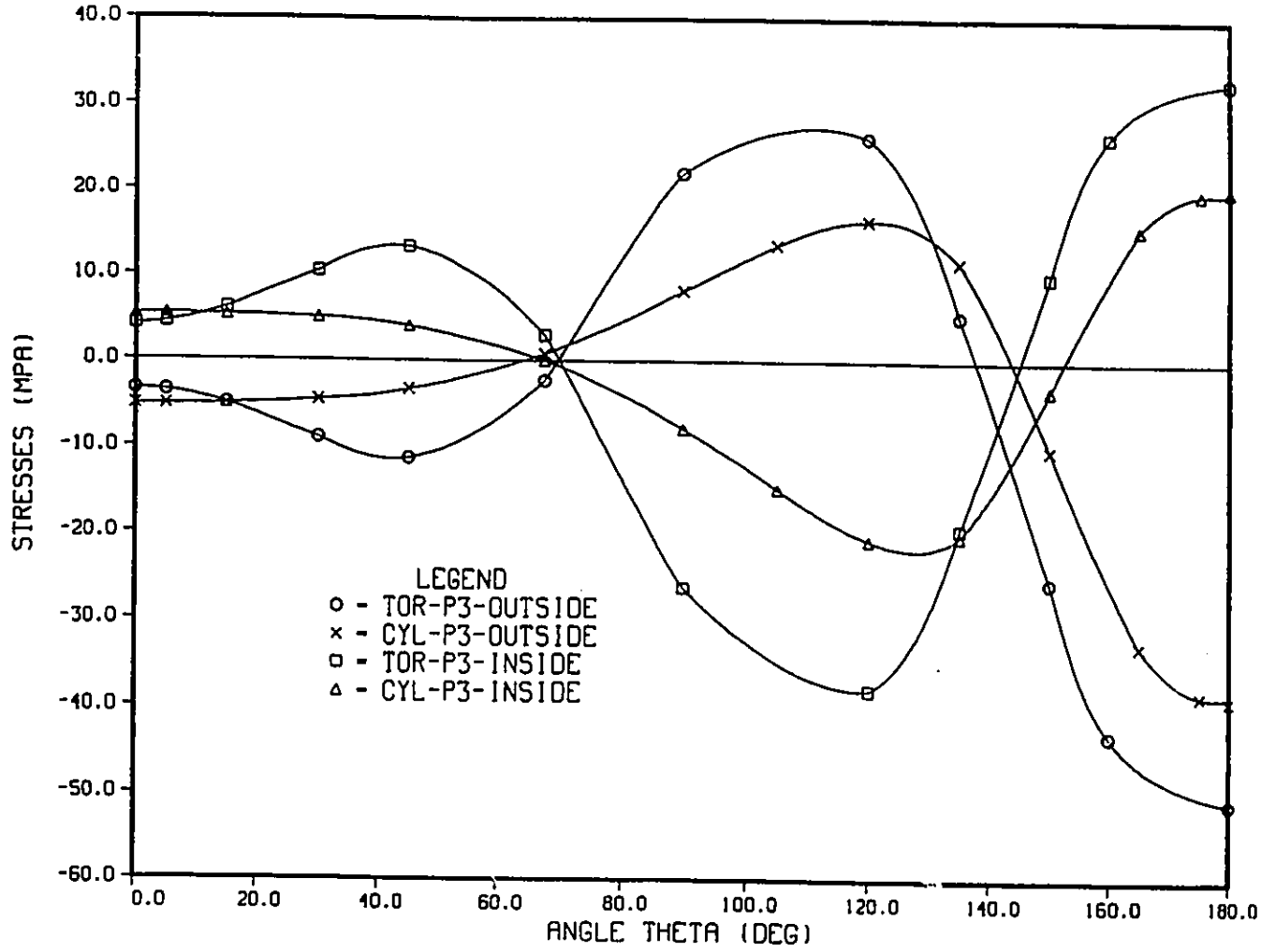

Figure 5.10: Stress σ_θ at $\phi = 45°$ for shell loaded at intrados ($p_3 = 1$).

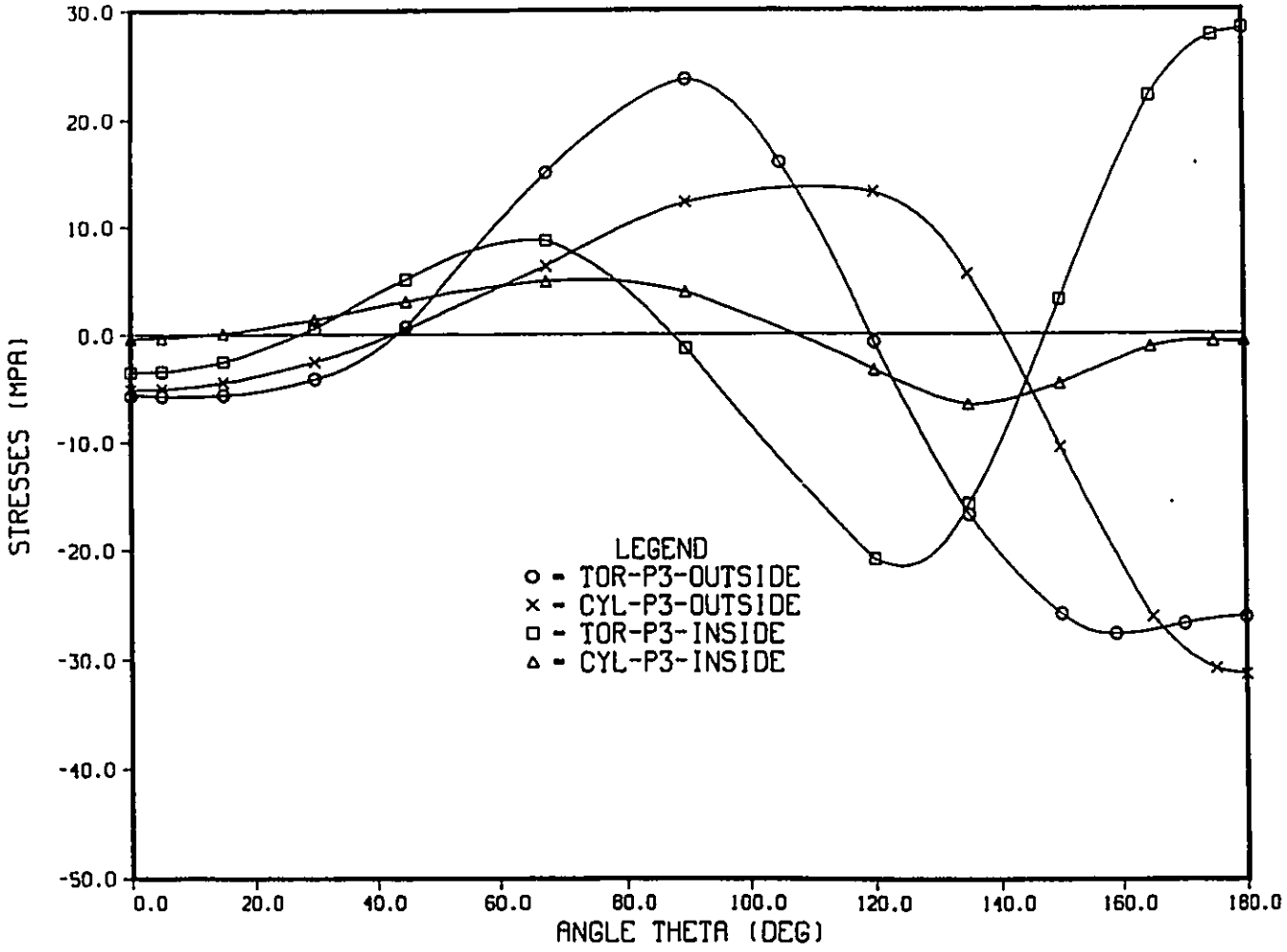

Figure 5.11: Stress σ_η at $\phi = 45°$ for shell loaded at intrados ($p_3 = 1$).

Table 5.1: Geometry of Additional Load Cases

(distances are in mm)

Case	r	R	t	l	Γ	Ω	$\overline{\mathrm{K}}$
1	100	300	.19	471	175.4	.203	.45
2	100	300	.33	471	101.0	.270	.52
3	100	300	.48	471	69.4	.325	.57
4	100	300	1.14	471	29.2	.504	.71
5	100	300	1.8	471	18.5	.640	.8
6	100	300	4.5	471	7.4	1.0	1.0
7	100	400	6.2	628	4.0	1.563	1.25
8	100	400	10.0	628	2.5	1.988	1.41
9	100	600	10.6	943	1.6	3.063	1.75
10	100	600	18.0	943	.9	4.0	2.0

Table 5.2: Characteristic Displacements and Stresses - Load at Extrados

(deflection is in mm, pressure and stresses are in MPa)

Case	*Pres.*	*Cyld. Shell*			*Tor. Shell*		
	p	w	σ_x	σ_θ	w	σ_η	σ_θ
1	.005	-.268	-27.67	-2.95	-.020	-4.89	-1.35
			2.52	8.85		.10	.44
2	.005	-.167	-15.12	-1.67	-.010	-2.82	-.79
			-.86	-2.11		.05	.26
3	.005	-.102	-9.47	-1.12	-.006	-1.95	-.54
			-1.36	-3.77		.05	.25
4	.05	-.252	-28.62	-4.24	-.024	-9.19	-2.30
			-9.27	-25.94		.26	1.37
5	.05	-.112	-14.44	-2.48	-.015	-6.22	-1.46
			-6.06	-16.67		-.10	.13
6	.5	-.200	-34.75	-8.19	-.056	-23.68	-5.65
			-21.03	-54.24		-4.11	-10.02
7	.6	-.222	-31.39	-5.77	-.084	-22.23	-4.50
			-22.32	-59.98		-5.59	-14.15
8	.6	-.078	-13.58	-3.07	-.044	-11.53	-2.68
			-11.30	-29.26		-3.69	-8.81
9	.71	-.156	-20.75	-2.91	-.170	-19.22	-2.81
			-14.10	-38.42		-2.83	-3.38
10	.71	-.064	-10.30	-1.56	-.088	-10.92	-1.56
			-6.06	-14.58		-2.11	-2.08

Table 5.3: Characteristic Displacements and Stresses - Load at Intrados

(deflection is in mm, pressure and stresses are in MPa)

Case	*Pres.*	*Cyld. Shell*			*Tor. Shell*		
	p	w	σ_x	σ_θ	w	σ_η	σ_θ
1	.01	-.27	-28.02	-5.48	-3.5	3.16	-3.97
			3.79	11.98		-12.43	-17.16
2	.01	-.17	-15.88	-3.22	-1.2	.64	-2.63
			-.005	-.04		-7.16	-9.81
3	.01	-.11	-10.29	-2.23	-.54	.19	-1.87
			-.84	-2.49		-4.87	-6.65
4	.1	-.27	-33.65	-9.13	-.95	.90	-7.63
			-8.98	-24.47		-19.34	-25.85
5	.1	-.12	-17.58	-5.54	-.38	1.29	-4.62
			-6.54	-17.13		-11.79	-15.67
6	1.0	-.23	-44.06	-20.12	-.61	10.53	-17.74
			-27.65	-63.27		-49.06	-71.98
7	1.0	-.24	-38.49	-11.67	-.67	6.49	-11.33
			-27.66	-69.58		-47.53	-95.37
8	1.0	-.09	-16.77	-6.56	-.23	-3.11	-6.87
			-14.94	-34.95		-26.84	-53.87
9	1.0	-.17	-24.41	-4.75	-.54	-15.11	-5.42
			-17.32	-45.00		-34.09	-82.71
10	1.0	-.07	-11.85	-2.55	-.17	-12.27	-2.96
			-7.73	-17.67		-14.73	-32.87

Chapter 6

Conclusions

From the present study, the following conclusions can be drawn.

- A solution scheme based on the Sanders shell theory has been developed for the linear elastostatic behavior of a toroidal shell subjected to surface loading.

- The results based on the Sanders shell theory for sample problems agree very closely with results from the FEM, MVD and Flügge shell theories. The accuracy of FEM (ADINA package) for toroidal shell was verified by experimentation in ref. [58]. Indications are that the results of the Sanders theory are superior to those of the MVD theory, and are thus suitable for making ovalization and other predictions for the ram bending process.

  In the present study, Sanders shell theory solutions are limited to a sectorial toroidal shell of range $0° \leq \phi \leq 90°$ with simply supported conditions. In future studies it is suggested that additional end boundary conditions be considered.

- In general when shell action predominates toroidal shells are structurally superior in resisting local loads, compared to cylindrical shells, if the loads are at the extrados and inferior if the loads are at the intrados.

- As a guide to computer time requirements, the CPU time of the Sanders theory is compared with the CPU time of the FEM. The results show that the time for the Sanders theory (40.8 sec.) is significantly less than the time for the FEM (225.8 sec.).

Bibliography

[1] J. L. Sanders Jr., An Improved First-Approximation Theory for Thin Shells, Langley Research Center, TR R-24, 1-11, 1959.

[2] C. L. Dym, Theory of Shells, Pergamon, Oxford, 1974.

[3] A. E. H. Love, A Treatise on the Mathematical Theory of Elasticity, Fourth ed. Dover Publications, 173-174, 1944.

[4] D. Redekop, Ram Bending of a Curved Pipe in the Elastic Range, Int. J Pres. Ves. and Piping, 44, 191-206, 1990.

[5] ADINA - A Finite Element Program for Automatic Dynamic Incremental Nonlinear Analysis, ADINA R&D, Inc., Watertown, MA, 1984.

[6] H. J. Thailer and D. H. Cheng, In-plane Bending of a U-shaped Circular Tube with End Constraints, J.Eng. for Ind., 92, 792-796, 1970.

[7] J. F. Whatham and J. J. Thompson, The Bending and Pressurizing of Pipe Bends with Flanged Tangents. Nuclear Engineering and Design, 54, 17-28, 1979.

[8] G. E. Findlay and J. Spence, Flexibility of Smooth Circular Curved Tubes with Flanged End Constraints; Stress Analysis of Smooth Curved Tubes with Flanged End Constraints. Int. J. Pres. Ves. & Piping, 7, 13-29; 83-103, 1979.

[9] G. Thomson and J. Spence, The Influence of End Constraints on Smooth Pipe Bends. International Conference on Structural Mechanics in Reactor Technology, 6th, Paris, 1981. Edited by J. Rastoin and B. A. Boley. Amsterdam, North-Holland Pub. Co., 1981, F2/7.

[10] G. Thomson and J. Spence, The Influence of Flanged End Constraints on Smooth Curved Tubes Under In-plane Bending. Int. J. Pres. Ves. & Piping, 13, 65-83, 1983.

[11] V. V. Novozhilov, The Theory of Thin Shells, Noordhoff, Groningen, 1959.

[12] J. F. Whatham, Thin Shell Equations of Circular Pipe Bends, Nucl. Eng. Des., 65, 77-89, 1981.

[13] J. F. Whatham, Thin Shell Analysis of Flanged Pipe Bends, Inst. of Eng. CE25, 1-12, 1983.

[14] J. F. Whatham, Pipe Bend Analysis by Thin Shell Theory, J. of Appl. Mech., 53, 173-180, 1986.

[15] M. E. Karabin, E. C. Rodabough and J. F. Whatham, Stress Component Induces for Elbow-straight Pipe Junctions Subjected to In-plane Bending, J. Pres. Ves. Tech., 108, 86-91, 1986.

[16] P. P. Bijlaard, Additional Data on Stresses in Cylindrical Shells Under Local Loading, Welding Research Council Bulletin, 50, 10-50, 1959.

[17] G. Duthie and A. S. Tooth, Local Loads on Cylindrical Vessels: A Fourier Series Solution, in J. Rhodes and J. Spence, (Eds.), Behaviour of Thin-Walled Structures, 1984, (Elsevier, London).

[18] L. S. Ong, A Computer Program for the Analysis of Cylindrical Shells, Int. J. Pres. Ves. Piping, 27, 131-149, 1987.

[19] D. Redekop and P. Azar, Ram Bending of a Cylindrical Pipe in the Elastic Range, Int. J. Pres. Ves. and Piping, 37, 307-320, 1989.

[20] E. L. Axelrad and F. A. Emmerling, Elastic Tubes, Applied Mechanics Reviews, 37, 891-897, 1984.

[21] D. Redekop, A. Colle and V. B. Nguyen, Stress and Deformation of Curved Tubes, IASTED, Proc. of AIMS'87 Conference, New Orleans, 14-17, 1987.

[22] J. F. Whatham, Thin Shell Analysis of Circular Pipe Bends, Inst. of Eng. Aust., CE23, 234-246, 1981.

[23] G. Thompson and J. Spence, The Influence of Flanged End Constraints on Smooth Curved Tubes Under In-plane Bending, Int. J. Pres. Ves. and Piping, 13, 65-83, 1983.

[24] X. Z. Hui and Z. Wei, The General Solution for Thin-walled Curved Tubes with Arbitrary Loadings and Various Boundary Conditions, Int. J. Pres. Ves. and Piping, 26, 129-144, 1986.

[25] R. H. Gallagher, The Development and Evaluation of Matrix Methods for Thin Shell Structural Analysis, Ph.D. thesis, State University of New York at Buffalo, NY 1966.

[26] J. J. Connor and C. A. Brebbia, A Stiffness Matrix for a Shallow Rectangular Shell Element, J. Engng Mech. Div., ASCE 93(5), 43-65, 1967.

[27] C. A. Brebbia and J. M. Deb Nath, A Comparison of Recent Shallow Shell Finite Element Analysis, Int. J. Mech. Sci., 12, 849-857, 1970.

[28] T. Y. Yang, High Order Rectangular Shallow Shell Finite Element, J. Engng Mech. Div., ASCE 99(1), 157-181, 1973.

[29] T. Y. Yang and R. K. Kapania, Shell Elements for Cooling Tower Analysis, J. Engng Mech. Div., ASCE 109(5), 1270-1289, 1983.

[30] C. J. Moore, T. Y. Yang and D. C. Anderson, A New 48 D.O.F. Quadrilateral Shell Element with Variable Order Polynomial and Rational B-spline Geometries with Rigid Body Modes, Int. J. Numer. Mech. Engng, 20, 2121-2142, 1984.

[31] J. S. Hansen and G. R. Heppler, A Mindlin Shell Element which Satisfies Rigid Body Requirements, AIAA Jnl, 22, 288-295, 1985.

[32] G. R. Heppler, I. Sharf and J. S. Jansen, Basis Functions for Axisymmetric Shell Elements which Satisfy Rigid-body Requirememts, AIAA Jnl, 24, 2014-2021, 1986.

[33] K. J. Bathe and E. N. Dvorkin, A Formulation of General Shell elements–The Use of Mixed Interpolation of Tensorial Components, Int. J. Numer. Mech. Engng, 22, 697-722, 1986.

[34] J. Jang and P. M. Pinsky, An Assumed Covariant Strain Based 9-node Shell Element, Int. J. Numer. Mech. Engng, 24, 2389-2411, 1987.

[35] S. S. Murth and R. H. Gallagher, Anisotropic Cylindrical Shell Element Based on Discrete Kirchhoff Theory, Int. J. Numer. Mech. Engng, 19, 1805-1823, 1983.

[36] B. M. Irons and K. J. Draper, Inadequacy of Nodal Connections in a Stiffness Solution for Plate Bending. AIAA Jnl, 3, 961, 1965.

[37] S. Ahmad, B. M. Irons and O. C. Zienkiewicz, Analysis of Thick and Thin Shell Structures by Curved Finite Elements, Int. J. Numer. Mech. Engng, 2, 419-451, 1970.

[38] K. J. Bathe, Finite Element Procedures in Engineering Analysis, Prentice Hall, Englewood Cliffs, NJ, 251-259, 1982.

[39] M. Crisfield, Finite Elements on Solution Procedures for Structural Analysis, Vol. 1–Linear Analysis. Pineridge Press, Swansea, U.K. 1986.

[40] T. J. R. Hughes, The Finite Element Method, Prentice-Hall, Englewood Cliffs, NJ 1987.

[41] O. P. Jacquotte and J. T. Oden, Analysis and Treatment of Hourglass Instablilties in Underintegrated Finite Element Methods, Proc. Int. Con. on Innovative Methods for Nonlinear Analysis, Pineridge Press, Swansea, U.K. 1984.

[42] A. Razzaque, Finite Element Analysis of Plates and Shells. Ph.D. thesis, University of Swansea, U.K. 1972.

[43] A. Razzaque, Program for Triangular Bending Elements with Derivative Smoothing. Int. J. Numer. Meth. Engng, 6, 333-345, 1973.

[44] J. T. Baldwin, A. Razzaque and B. M. Irons, Shape Function Subroutine for an Isoparametric Thin Plate Element, Int. J. Numer. Mech. Engng, 7, 431-440, 1973.

[45] B. M. Irons, The SemiLoof Shell Element, Finite Elements for Thin Shells and Curved Members, John Wiley, New York, 197-222, 1976.

[46] M. A. Crisfield, The Application of Shear-constraint to the Generation of Plate-elements. In Finite Element Methods for Plate and Shell Structures, Pineridge Press, Swansea, U.K., 1, 153-174, 1986.

[47] E. N. Dvorkin and K. J. Bathe, A Continuum Mechanics Based Four-node Shell Element for General Nonlinear Analysis. Engng Comput., 1, 77-88, 1984.

[48] K. C. Park and C. M. Stanley, A Curved C^o Shell Element Based on Assumed Natural-coordinate Strains. J. appl. Mech., ASME 53, 278-290, 1986.

[49] H. C. Huang and E. Hinton, Lagrangian and Serendipity Plate and Shell Elements Through Thick and Thin. Finite Element Methods for Plate and shell Structures, Pineridge Press, Swansea, U.K., 1, 46-61, 1986.

[50] H. C. Huang and E. Hinton, A New Nine Node Degerated Shell Element with Enhanced Membrane and Shear Interpolation, Int. J. Numer. Mech. Engng, 22, 73-92, 1986.

[51] H. Stolarski and T. Belytschko, Shear and Membrane Locking in Curved C^o Elements. Comput. Meth. appl. Mech. Engng, 41, 279-296, 1983.

[52] H. Stolarski and T. Belytschko, Membrane Locking and Reduced Integration for Curved Elements. J. appl. Mech., ASME 49, 172-176, 1982.

[53] G. D. Lewis and Y. J. Chao, Flexibility of Trunnion Piping Elbows, J. Pres. Ves. Tech., 112, 184-187, 1990.

[54] K. J. Bathe and S. Bolourchi, A Geometric and Material Nonlinear Plate and Shell Element, Comput. Structures, 11, 23-48, 1980.

[55] B. W. Char, K. O. Geddes, G. H. Gonnet, and S. M. Watt, MAPLE User's Guide, WATCOM Publications, Waterloo, Ontario, 1985.

[56] C. R. Calladine, Theory of Shell Structures, 1983, (Cambridge University Press, Cambrige).

[57] F. Lu and A. N. Sherbourne, Bending Stresses in Cylindrical Shells Containing Fluid or Granular Material, Trans. CSME, 14, 125-136, 1990.

[58] K. J. Bathe and C. A. Almeida, A Simple and Effective Pipe Elbow Element – Some Nonlinear Capabilities, Comput. Structures, 17, 659-667, 1983.

Appendix A

Coefficients for the Equilibrium Equations of The Sanders Theory

$$\nu_1 = \zeta^4(12r^2 + t^2)/12$$

$$\nu_2 = r^2\zeta^2(1-\nu)/2 + t^2(4\zeta + 4\zeta^2 + 1)(1-\nu)/96$$

$$\nu_3 = -r^2\zeta^3\gamma sin\theta - t^2\zeta^3\gamma sin\theta/12$$

$$\nu_4 = -\zeta^2\gamma^2 sin^2\theta(12r^2 + t^2)/12 - \nu\zeta^3\gamma cos\theta(12r^2 + t^2)/12$$

$$\nu_5 = r^2\zeta^3(1+\nu)/2 + t^2\zeta(2\zeta + 1)(\gamma cos\theta - \frac{1}{2})(1-\nu)/48 + t^2\zeta^2\nu\gamma cos\theta/12$$

$$\nu_6 = [r^2\zeta^2(3-\nu)/2 - t^2\zeta^2\nu/12 + t^2(1-\nu)(1-4\zeta^2)/96]\gamma sin\theta + t^2(4\zeta + 1 - \nu)\gamma^2 sin2\theta/48$$

$$\nu_7 = -t^2\zeta^4/12$$

$$\nu_8 = t^2\zeta(\nu - 2\zeta - 1)/24$$

$$\nu_9 = t^2\zeta^3\gamma sin\theta/12$$

$$\nu_{10} = (\nu - 1 - 4\zeta)t^2\gamma sin\theta/24$$

$$\nu_{11} = (r^2\zeta^4 + t^2\zeta^2\gamma^2 sin^2\theta/12) + \zeta^3\nu\gamma cos\theta(r^2 + t^2/12)$$

$$\nu_{12} = r^2\zeta^2\gamma^2 sin\theta cos\theta - r^2\zeta^3\gamma sin\theta$$

$$\begin{aligned}\nu_{13} = {} & (-\nu\zeta/4 + \zeta^2/2 + \nu\zeta^2/2 + \zeta/4)\gamma cos\theta + 12\nu r^2\zeta^3/t^2 \\ & +6r^2\zeta^3(1-\nu)/t^2 + (\nu - 1)(2\zeta^2 + \zeta)/8\end{aligned}$$

$$\nu_{14} = 6(\nu - 3)\gamma sin\theta r^2\zeta^2/t^2 + \zeta(\nu - 3)\gamma^2 sin2\theta/4 - (3 + 4\zeta)(1 - \nu)\gamma sin\theta/8$$

$$\nu_{15} = 6(1 - \nu)r^2\zeta^4/t^2 + (\nu - 1)\zeta^2\gamma cos\theta/2 + (1 - \nu)\zeta^2\gamma^2 cos^2\theta/2 + (1 - \nu)\zeta^2/8$$

$$\nu_{16} = 12r^2\zeta^2/t^2 + \gamma^2 cos^2\theta$$

$$\begin{aligned}\nu_{17} = {} & 6(\nu - 1)r^2\zeta^3\gamma sin\theta/t^2 + (1 - \nu)\zeta\gamma^3 sin2\theta cos\theta/2 + 3(\nu - 1)\zeta\gamma^2 sin2\theta/8 \\ & +(\nu - 1)\zeta(\gamma cos\theta - \frac{1}{2})(2\gamma^2 sin2\theta + \gamma sin\theta)/4 + (1 - \nu)\zeta\gamma^3 sin\theta cos^2\theta/2 \\ & +(1 - \nu)\zeta^2\gamma sin\theta/2 + (\nu - 1)\zeta^2\gamma^2 sin2\theta/2\end{aligned}$$

$$\begin{aligned}\nu_{18} = {} & 6(1 - \nu)r^2\zeta^3\gamma cos\theta/t^2 - 6(1 - \nu)r^2\zeta^2\gamma^2 sin^2\theta/t^2 + (1 - \nu)\zeta\gamma^3 cos2\theta cos\theta \\ & +(1 - \nu)\zeta\gamma^2 cos^2\theta/4 + (\nu - 1)\gamma^3 sin2\theta sin\theta/2 + (\nu - 1)\zeta^2\gamma^2 cos^2\theta/2 \\ & +(\nu - 1)\zeta\gamma^2 cos2\theta/2 + (1 - \nu)\zeta(2\zeta - 1)\gamma cos\theta/8 + (1 - \nu)\gamma^4 sin^2 2\theta/2 \\ & +(\nu - 1)\gamma^2 sin2\theta(2\gamma^2 sin2\theta + \gamma sin\theta)/4 \\ & +(\nu - 1)(2\gamma^2 sin2\theta + \gamma sin\theta)(1 - 2\zeta)\gamma sin\theta/8 \\ & +\gamma^3 sin^2\theta cos\theta(1 - \nu)(1 - \zeta)/2 + (1 - \nu)(\zeta - 1)\gamma^2 sin^2\theta/4\end{aligned}$$

$$\nu_{19} = -\gamma cos\theta$$

$$\nu_{20} = -\zeta^2\gamma cos\theta + (1-\nu)\zeta^2/2$$

$$\nu_{21} = \zeta\gamma^2 sin2\theta/2 + 3(1-\nu)\zeta\gamma sin\theta/2$$

$$\begin{aligned}\nu_{22} = {} & 12r^2\zeta^2\gamma cos\theta/t^2 + 12\nu\zeta^3 r^2/t^2 + 2(\nu-1)\gamma^3 sin^2\theta cos\theta \\ & +(\nu-1)\zeta\gamma^2 cos^2\theta + (1-\nu)\gamma sin\theta(2\gamma^2 sin2\theta + \gamma sin\theta)/2 \\ & +(1-\nu)\gamma^2 sin^2\theta + (1-\nu)\zeta\gamma cos\theta/2\end{aligned}$$

$$\nu_{23} = -\zeta^4$$

$$\nu_{24} = -\zeta(1-\nu)/2 - \zeta^2$$

$$\nu_{25} = [\zeta - (1-\nu)/2]\gamma sin\theta$$

$$\nu_{26} = 2\gamma sin\theta\zeta^3$$

$$\nu_{27} = 12r^2\zeta^4/t^2 + (12\nu r^2/t^2 + 1 + \nu)\gamma cos\theta\zeta^3 + \gamma^2 sin^2\theta\zeta^2$$

$$\nu_{28} = (1 - 6r^2/t^2)\gamma^2 sin2\theta\zeta^2 - (12r^2/t^2 + 1)\nu\gamma sin\theta\zeta^3 + \gamma^3 sin^3\theta\zeta$$

$$\nu_{29} = -\gamma cos\theta$$

$$\nu_{30} = [-\gamma cos\theta + (1-\nu)/2]\zeta^2$$

$$\nu_{31} = -3\zeta\gamma^2 sin2\theta/2 + [2\zeta^2 - \zeta(1-\nu)/2]\gamma sin\theta$$

$$\begin{aligned}\nu_{32} = {} & [(12r^2/t^2 + 1)\zeta^2 - \zeta(1-\nu)/2]\gamma cos\theta - 2\zeta(1-\nu)\gamma^2 cos2\theta \\ & -\zeta(1+\nu)\gamma^2 cos^2\theta + [\zeta(1+2\nu) - (1-\nu)/2]\gamma^2 sin^2\theta \\ & -2(1-2\nu)\gamma^3 sin^2\theta cos\theta - (1+2\nu)\gamma^3 sin\theta sin2\theta + 12\nu r^2\zeta^3/t^2\end{aligned}$$

$$\nu_{33} = \zeta^4$$

$$\nu_{34} = 1$$

$$\nu_{35} = 2\zeta^2$$

$$\nu_{36} = -2\gamma sin\theta\zeta^3$$

$$\nu_{37} = 2\gamma sin\theta\zeta$$

$$\nu_{38} = 4\gamma^2 sin^2\theta + (3-\nu)\gamma cos\theta\zeta$$

$$\nu_{39} = -\gamma^2 sin^2\theta\zeta^2 - (1+\nu)\gamma cos\theta\zeta^3$$

$$\nu_{40} = -\gamma^3 sin^3\theta\zeta - \gamma^2 sin2\theta\zeta^2 + \nu\gamma sin\theta\zeta^3$$

$$\nu_{41} = 12r^2(\zeta^4 + \gamma^2 cos^2\theta\zeta^2 + 2\nu\gamma cos\theta\zeta^3)/t^2$$

Appendix B

Computer Program TORSAN

```
C     LAST MODIFICATION - JUNE, 1991                                          TOR00010
C     NEED FILES 'TORSAN EXEC' 'TORSAN DATA' 'TORSAN FORTRAN'                 TOR00020
C     RESULTS IN 'TORSAN RESULT'                                              TOR00030
C     PAD LOADING ON TOROIDAL SHELL - ELASTIC SHELL THEORY SOLUTION           TOR00040
C     SANDERS THEORY IN DISPLACEMENT FORM IS USED                             TOR00050
C     BI-SYMMETRIC RADIAL UNIFORM PAD LOADING IS ASSUMED                      TOR00060
C     READIN AND WRITEOUT ALL ANGLES IN DEGREES                               TOR00070
C     D. REDEKOP   U. OF OTTAWA   MARCH 1989                                  TOR00080
C     F. ZHANG     U. OF OTTAWA   JUNE 1991                                   TOR00090
C     NOTE - COORD 'FI' VALUES ARE IO WHILE 'ETA' VALUES ARE CALCULATED       TOR00100
      CALL START                                                              TOR00110
      CALL SOLVE                                                              TOR00120
      CALL RESULT                                                             TOR00130
      STOP                                                                    TOR00140
      END                                                                     TOR00150
C-----------------------------------------------------------------            TOR00160
      SUBROUTINE START                                                        TOR00170
C     INPUT DATA FIX GLOBAL CONSTANTS AND INITIALIZE                          TOR00180
      IMPLICIT DOUBLE PRECISION (A-H,O-Z)                                     TOR00190
      DOUBLE PRECISION M,M2,M3,M4                                             TOR00200
      CHARACTER*20 NAME*60                                                    TOR00210
      COMMON/AAA/R,RR,PSI,T,E,POI,MHI,NHI,NFI,NT,NLOAD                        TOR00220
      COMMON/BBB/RES(40,20,10),GFI(40),GETA(40),GT(20),DATLOD(10,7)           TOR00230
      COMMON/CCC/PI5,PI2,PI,SOP2,RAD,OMP,OMP2,TP,AK,STIF,ROS,R2,R3,CZ,        TOR00240
     1           ZD,PSIR                                                      TOR00250
      COMMON/FFF/P,ZK,ZC,ZX,ZY,G,G2,G3,G4,G5,M,M2,M3,M4,F,Q,A,S,              TOR00260
     1           UMP,DMP,TMP,UPP,DPP,TPP,BB(9),STC(20),STS(20),STZ(20),       TOR00270
     1           B2,B1,VMP,SMP,EKD,EKB,EKC,EKE,EL,EL1,H,EKA                   TOR00280
      PI=3.14159265358979300                                                  TOR00290
      RAD=PI/180.D0                                                           TOR00300
      READ(5,16) NAME                                                         TOR00310
   16 FORMAT(A60)                                                             TOR00320
C     MHI,NHI INDICATES MAX TERMS IN SERIES                                   TOR00330
C     NFI,NT INDICATES SIZE OF GRID          NLOAD=NUMBER OF LOADS            TOR00340
      READ(5,*) MHI,NHI,NFI,NT,NLOAD                                          TOR00350
C     ENTER DISTANCES IN MM ANGLES IN DEGREES                                 TOR00360
C     R=X-SECT RADIUS   RR=TOROIDAL RADIUS   PSI=TOTAL ANGULAR LENGTH         TOR00370
C     T=SHELL THICK     E=YOUNG'S MODULUS    POI=POISSON RATIO                TOR00380
      READ(5,*) R,RR,PSI,T,E,POI                                              TOR00390
C     ENTER COORDS OF RESULT GRID POINTS (DEGREES)                            TOR00400
      READ(5,*) (GFI(I),I=1,NFI)                                              TOR00410
      READ(5,*) (GT(I),I=1,NT)                                                TOR00420
      DO 10 I=1,NLOAD                                                         TOR00430
10    READ(5,*) (DATLOD(I,J),J=1,5)                                           TOR00440
C     LOAD CARD=MAGN-ALPHA-DELTA-BETA-ZETA+PI*ALPHA/PSIR+PI*DELTA/PSIR        TOR00450
      WRITE(8,116) MHI,NHI                                                    TOR00460
116   FORMAT(/1X,'MHI=',I4/1X,'NHI=',I4)                                      TOR00470
      WRITE(8,117)                                                            TOR00480
117   FORMAT(/' SHELL THEORY IS THAT OF SANDERS ')                            TOR00490
      WRITE(8,126) R,RR,PSI,T,E,POI                                           TOR00500
126   FORMAT(/' TOROIDAL SHELL'/                                              TOR00510
     1  1X,' X-SECT.  RAD.    =',E12.5,2X,'MM'/                              TOR00520
     2  1X,' TOROIDAL RAD.    =',E12.5,2X,'MM'/                              TOR00530
     2  1X,' ANGULAR LENGTH   =',E12.5,2X,'DEG'/                             TOR00540
     3  1X,' THICKNESS        =',E12.5,2X,'MM'/                              TOR00550
```

```
     4  1X,' YOUNG  MODULUS  =',E12.5,2X,'MPA'/                          TOR00560
     5  1X,' POISSON RATIO   =',E12.5  /)                                TOR00570
      WRITE(8,136)                                                       TOR00580
136   FORMAT(' LOAD DATA'/                                               TOR00590
     1 ' LOAD  PRESS.(MPA)',3X,'ALPHA(DEG)',3X,'DELTA(DEG)',            TOR00600
     2  4X,'BETA(DEG)',  4X,'ZETA(DEG)')                                TOR00610
      PSIR=PSI*RAD                                                       TOR00620
      DO 110 I=1,NLOAD                                                   TOR00630
      WRITE(8,146)I,(DATLOD(I,J),J=1,5)                                  TOR00640
146   FORMAT(1X,I4,5E13.5)                                               TOR00650
      DO 111 J=2,5                                                       TOR00660
111   DATLOD(I,J)=DATLOD(I,J)*RAD                                        TOR00670
      DATLOD(I,6)=PI*DATLOD(I,2)/PSIR                                    TOR00680
110   DATLOD(I,7)=PI*DATLOD(I,3)/PSIR                                    TOR00690
C     GLOBAL CONSTANTS                                                   TOR00700
      PI2=PI*PI                                                          TOR00710
      PI5=.5D0*PI                                                        TOR00720
      SOP2=16.D0/PI2                                                     TOR00730
      OMP=1.D0-POI                                                       TOR00740
      OMP2=1.D0-POI*POI                                                  TOR00750
      TP=2.D0+POI                                                        TOR00760
      STIF=E*T/OMP2                                                      TOR00770
      ROS=R*R/STIF                                                       TOR00780
      R2=R*R                                                             TOR00790
      R3=R2*R                                                            TOR00800
      R4=R3*R                                                            TOR00810
      B2=1-R                                                             TOR00820
      B1=1+R                                                             TOR00830
      CZ=6.D0/(T*T)                                                      TOR00840
      P=POI                                                              TOR00850
      ZK=(T/R)*(T/R)/12.D0                                               TOR00860
      ZC=E*T/(1.D0-POI*POI)                                              TOR00870
      AK=ZC                                                              TOR00880
      ZX=E*(T*T*T)/(12.D0*OMP2)                                          TOR00890
      ZD=ZX                                                              TOR00900
      F=.5D0                                                             TOR00910
      ZY=-F*R4/ZD                                                        TOR00920
      G=R/RR                                                             TOR00930
      G2=G*G                                                             TOR00940
      G3=G2*G                                                            TOR00950
      G4=G2*G2                                                           TOR00960
      G5=G4*G                                                            TOR00970
      H=T                                                                TOR00980
      H2=H*H                                                             TOR00990
      EL=H2/12.D0                                                        TOR01000
      EL1=12.D0/H2                                                       TOR01010
      EKA=R2/H2                                                          TOR01020
      Q=.25D0                                                            TOR01030
      A=.125D0                                                           TOR01040
      S=.0625D0                                                          TOR01050
      UMP=1.D0-P                                                         TOR01060
      DMP=2.D0-P                                                         TOR01070
      TMP=3.D0-P                                                         TOR01080
      VMP=4.D0-P                                                         TOR01090
      SMP=5.D0-P                                                         TOR01100
```

```
      UPP=1.D0+P                                                        TOR01110
      DPP=2.D0+P                                                        TOR01120
      TPP=3.D0+P                                                        TOR01130
      EKD=1.D0+3.D0*P                                                   TOR01140
      EKB=1.D0+2.D0*P                                                   TOR01150
      EKC=1.D0-3.D0*P                                                   TOR01160
      EKE=1.D0-2.D0*P                                                   TOR01170
      BB(1)=ZY*A*G4                                                     TOR01180
      BB(2)=ZY*G3                                                       TOR01190
      BB(3)=ZY*(3.D0*G2+F*G4)                                           TOR01200
      BB(4)=ZY*(4.D0*G+3.D0*G3)                                         TOR01210
      BB(5)=ZY*(1.D0+3.D0*G2+.375*G4)*2.D0                              TOR01220
      BB(6)=BB(4)                                                       TOR01230
      BB(7)=BB(3)                                                       TOR01240
      BB(8)=BB(2)                                                       TOR01250
      BB(9)=BB(1)                                                       TOR01260
C     INITIALIZE                                                        TOR01270
      DO 200 I=1,NFI                                                    TOR01280
      DO 210 J=1,NT                                                     TOR01290
      RES(I,J,1)=GFI(I)                                                 TOR01300
      RES(I,J,2)=GT(J)                                                  TOR01310
C     INITIALLY RES CONTAINS  FI(DEG) THETHA(DEG) U V W E1 E2 K1 K2 P   TOR01320
C     RESULTS TO BE GIVEN IN SETS OF CIRCULAR ARCS AROUND X-SECTION     TOR01330
      DO 220 K=3,10                                                     TOR01340
220   RES(I,J,K)=.0D0                                                   TOR01350
210   CONTINUE                                                          TOR01360
200   CONTINUE                                                          TOR01370
      DO 225 J=1,NFI                                                    TOR01380
225   GETA(J)=GFI(J)*RAD/G                                              TOR01390
      DO 230 J=1,NT                                                     TOR01400
230   GT(J)=GT(J)*RAD                                                   TOR01410
C     STORE TRIG FUNCTIONS OF THETA                                     TOR01420
      DO 300 J=1,NT                                                     TOR01430
      STC(J)=COS(GT(J))                                                 TOR01440
      STS(J)=SIN(GT(J))                                                 TOR01450
 300  STZ(J)=1.+G*STC(J)                                                TOR01460
      RETURN                                                            TOR01470
      END                                                               TOR01480
C-------------------------------------------------------------------    TOR01490
      SUBROUTINE SOLVE                                                  TOR01500
C     MAIN CONTROL ROUTINE TO FIND DISPLACEMENT COEFFTS AND ADD TO      TOR01510
C       BASIC UNKNOWNS (U,V,W,E1,E2,K1,K2,P) AT EACH OF GRID POINTS     TOR01520
      IMPLICIT DOUBLE PRECISION (A-H,O-Z)                               TOR01530
      DOUBLE PRECISION M,M2,M3,M4                                       TOR01540
      COMMON/AAA/R,RR,PSI,T,E,POI,MHI,NHI,NFI,NT,NLOAD                  TOR01550
      COMMON/BBB/ RES(40,20,10),GFI(40),GETA(40),GT(20),DATLOD(10,7)    TOR01560
      COMMON/CCC/PI5,PI2,PI,SOP2,RAD,OMP,OMP2,TP,AK,STIF,ROS,R2,R3,CZ,  TOR01570
     1           ZD,PSIR                                                TOR01580
      COMMON/EEE/AA(200,200),B(200),X(200),PX(200),                     TOR01590
     1           AN(200,200),BN(200,1),XN(200),WK(200)                  TOR01600
      COMMON/FFF/P,ZK,ZC,ZX,ZY,G,G2,G3,G4,G5,M,M2,M3,M4,F,Q,A,S,        TOR01610
     1           UMP,DMP,TMP,UPP,DPP,TPP,BB(9),STC(20),STS(20),STZ(20), TOR01620
     1           B2,B1,VMP,SMP,EKD,EKB,EKC,EKE,EL,EL1,H,EKA             TOR01630
      NHIDUP=NHI+3                                                      TOR01640
      WRITE(6,*) '  CALCULATIONS IN PROGRESS FOR M = '                  TOR01650
```

```
C     CALCULATE CONTRIBUTIONS TERM BY TERM                                    TOR01660
      DO 1000 MS=1,MHI,2                                                      TOR01670
      EM=REAL(MS)                                                             TOR01680
      M=EM*PI*G/PSIR                                                          TOR01690
      M2=M*M                                                                  TOR01700
      M3=M2*M                                                                 TOR01710
      M4=M2*M2                                                                TOR01720
      WRITE(6,*) MS                                                           TOR01730
C     SET UP EQUIL EQNS FOR THIS MS  FOR N=0,1,...NHI                         TOR01740
C     CALCULATE RHS COEFFTS     PX(200),B(200)                                TOR01750
      CALL LOAD(MS,NHIDUP)                                                    TOR01760
C     CALCULATE LHS COEFFTS     AA(200,200)                                   TOR01770
      CALL COEFFD(MS,NHIDUP)                                                  TOR01780
C     SOLVE THE EQNS SET USING CUSTOMIZED BAND SOLVER     X(200)              TOR01790
      CALL BANSOL(NHIDUP)                                                     TOR01800
C     ADD TO BASIC UNKNOWNS CONTRIBUTIONS FROM N=0                            TOR01810
      N=0                                                                     TOR01820
      U=.0                                                                    TOR01830
      V=X(1)                                                                  TOR01840
      W=X(2)                                                                  TOR01850
      PR=PX(1)                                                                TOR01860
      CALL ADVAL(MS,N,U,V,W,PR)                                               TOR01870
C     ADD TO BASIC UNKNOWNS CONTRIBUTIONS FROM N=1,2,...,NHI                  TOR01880
      DO 1100 N=1,NHI                                                         TOR01890
      IX=(N-1)*3+2                                                            TOR01900
      U=X(IX+1)                                                               TOR01910
      V=X(IX+2)                                                               TOR01920
      W=X(IX+3)                                                               TOR01930
      PR=PX(N+1)                                                              TOR01940
      CALL ADVAL(MS,N,U,V,W,PR)                                               TOR01950
1100  CONTINUE                                                                TOR01960
1000  CONTINUE                                                                TOR01970
      RETURN                                                                  TOR01980
      END                                                                     TOR01990
C-----------------------------------------------------------------------      TOR02000
      SUBROUTINE LOAD(MS,NHI)                                                 TOR02010
C     DEFINE PX AND B VECTORS FOR THIS MS                                     TOR02020
C     PX CONTAINS COEFTS OF FOURIER SERIES FOR LOAD                           TOR02030
C     B IS RIGHT HAND SIDE OF EQUILIBRIUM EQN SET                             TOR02040
      IMPLICIT DOUBLE PRECISION (A-H,O-Z)                                     TOR02050
      DOUBLE PRECISION M,M2,M3,M4                                             TOR02060
      COMMON/AAA/R,RR,PSI,T,E,POI,MHI,NHIDUM,NFI,NT,NLOAD                     TOR02070
      COMMON/BBB/RES(40,20,10),GFI(40),GETA(40),GT(20),DATLOD(10,7)           TOR02080
      COMMON/CCC/PI5,PI2,PI,SOP2,RAD,OMP,OMP2,TP,AK,STIF,ROS,R2,R3,CZ,        TOR02090
     1           ZD,PSIR                                                      TOR02100
      COMMON/EEE/AA(200,200),B(200),X(200),PX(200),                           TOR02110
     1           AN(200,200),BN(200,1),XN(200),WK(200)                        TOR02120
      COMMON/FFF/P,ZK,ZC,ZX,ZY,G,G2,G3,G4,G5,M,M2,M3,M4,F,Q,A,S,               TOR02130
     1           UMP,DMP,TMP,UPP,DPP,TPP,BB(9),STC(20),STS(20),STZ(20),       TOR02140
     1           B2,B1,VMP,SMP,EKD,EKB,EKC,EKE,EL,EL1,H,EKA                   TOR02150
      DIMENSION PROD(10)                                                      TOR02160
      EM=REAL(MS)                                                             TOR02170
C     FIND LOAD COEFFICIENT FOR N=0 CASE                                      TOR02180
1000  PR=.0D0                                                                 TOR02190
      DO 10 I=1,NLOAD                                                         TOR02200
```

```
      BLM=DATLOD(I,6)*EM                                                TOR02210
      CLM=DATLOD(I,7)*EM                                                TOR02220
      PROD(I)=SIN(EM*PI5)*COS(BLM)*SIN(CLM)                             TOR02230
10    PR=PR+(SOP2*DATLOD(I,1)*DATLOD(I,5)/EM)*FROD(I)                   TOR02240
      PX(1)=PR                                                          TOR02250
C     FIND LOAD COEFFICIENT FOR N GT 0 CASE                             TOR02260
 2000 DO 2100 N=1,NHI                                                   TOR02270
      EN=REAL(N)                                                        TOR02280
      N1=N+1                                                            TOR02290
      PR=.0D0                                                           TOR02300
      DO 2010 I=1,NLOAD                                                 TOR02310
      BET=EN*DATLOD(I,4)                                                TOR02320
      ZET=EN*DATLOD(I,5)                                                TOR02330
 2010 PR=PR+(2.*SOP2*DATLOD(I,1)/(EM*EN))*COS(BET)*SIN(ZET)*PROD(I)     TOR02340
 2100 PX(N1)=PR                                                         TOR02350
C     NOW FORM 'B' VECTOR                                               TOR02360
 3000 NEQ=3*NHI+2                                                       TOR02370
      DO 3010 I=1,NEQ                                                   TOR02380
 3010 B(I)=.0                                                           TOR02390
      NHIP1=NHI+1                                                       TOR02400
      DO 3100 I=1,NHIP1                                                 TOR02410
      NN=I-1                                                            TOR02420
      NNBLO=NN-5                                                        TOR02430
      ICBLO=2+NNBLO*3                                                   TOR02440
      PR=PX(I)                                                          TOR02450
C     EACH PR MAKES SEVEN CONTRIBUTIONS TO 'B' VECTOR                   TOR02460
      DO 3200 J=1,9                                                     TOR02470
      ICB=ICBLO+J*3                                                     TOR02480
      IF(ICB.GT.1) GO TO 3210                                           TOR02490
      IF(ICB.EQ.-10) ICB=ICB+24                                         TOR02500
      IF(ICB.EQ. -7) ICB=ICB+18                                         TOR02510
      IF(ICB.EQ. -4) ICB=ICB+12                                         TOR02520
      IF(ICB.EQ. -1) ICB=ICB+ 6                                         TOR02530
 3210 IF(ICB.GT.NEQ) GO TO 3200                                         TOR02540
      B(ICB)=B(ICB)+BB(J)*PR                                            TOR02550
 3200 CONTINUE                                                          TOR02560
 3100 CONTINUE                                                          TOR02570
      RETURN                                                            TOR02580
      END                                                               TOR02590
C-----------------------------------------------------------------------TOR02600
      SUBROUTINE COEFFD(MS,NHI)                                         TOR02610
C     DEFINE LHS OF EQUIL EQNS FOR THIS MS                              TOR02620
C     G=GAMMA  P=POISSON   ZK=(T/R)*(T/R)/12                            TOR02630
C     IHI=NUMBER OF SETS OF 3(OR 2) EQNS TO BE WRITTEN                  TOR02640
C     NEQ=TOTAL NUMBER OF EQNS   NEQ=NHI*3+2                            TOR02650
C     IQ=NUMBER OF EQUATION BEING WRITTEN IN MATRIX AA                  TOR02660
C     NN=ORDER OF EQN SET BEING WRITTEN                                 TOR02670
C     N=ORDER OF TERM WHOSE COEFT IS TO BE INSERTED IN THE EQN          TOR02680
C     IC=COLUMN OF FIRST NON-ZERO ENTRY                                 TOR02690
      IMPLICIT DOUBLE PRECISION (A-H,O-Z)                               TOR02700
      DOUBLE PRECISION M,M2,M3,M4                                       TOR02710
      COMMON/AAA/R,RR,PSI,T,E,POI,MHI,NHIDUP,NFI,NT,NLOAD               TOR02720
      COMMON/BBB/RES(40,20,10),GFI(40),GETA(40),GT(20),DATLOD(10,7)     TOR02730
      COMMON/CCC/PI5,PI2,PI,SOP2,RAD,OMP,OMP2,TP,AK,STIF,ROS,R2,R3,CZ,  TOR02740
     1           ZD,PSIR                                                TOR02750
```

```
      COMMON/FFF/P,ZK,ZC,ZX,ZY,G,G2,G3,G4,G5,M,M2,M3,M4,F,Q,A,S,        TOR02760
     1           UMP,DMP,TMP,UPP,DPP,TPP,BB(9),STC(20),STS(20),STZ(20), TOR02770
     1           B2,B1,VMP,SMP,EKD,EKB,EKC,EKE,EL,EL1,H,EKA             TOR02780
      COMMON/EEE/AA(200,200) ,B(200),X(200),PX(200),                    TOR02790
     1           AN(200,200),BN(200,1),XN(200),WK(200)                  TOR02800
      EM=REAL(MS)                                                       TOR02810
      NEQ=3*NHI+2                                                       TOR02820
      DO 1 I=1,NEQ                                                      TOR02830
      DO 2 J=1,27                                                       TOR02840
    2 AA(I,J)=.0                                                        TOR02850
    1 CONTINUE                                                          TOR02860
 1000 IQ=0                                                              TOR02870
      IHI=NHI+1                                                         TOR02880
C     SET UP EQUATION SET FOR THIS MS  DEFINE AA MATRIX AND BB VECTOR   TOR02890
      R4=R3*R                                                           TOR02900
      H2=H*H                                                            TOR02910
      EKA=R2/H2                                                         TOR02920
      DO 900 I=1,IHI                                                    TOR02930
      NN=I-1                                                            TOR02940
      IF(NN.EQ.0) GO TO 210                                             TOR02950
C     FIRST OF THREE EQUATIONS  'U' EQN  MISSING IF NN=0                TOR02960
      IQ=IQ+1                                                           TOR02970
      IC=1                                                              TOR02980
  110 N=NN-4                                                            TOR02990
      N2=N*N                                                            TOR03000
      N3=N2*N                                                           TOR03010
      AA(IQ,IC  )=                                                      TOR03020
     1 (-.0625*N2*(R2+.08333333333*H2)                                  TOR03030
     1 -.0625*N*(R2+.08333333333*H2)                                    TOR03040
     1 -.0625*P*(R2+.08333333333*H2)+.0625*R2+.005208333333*H2)*G4      TOR03050
      AA(IQ,IC+1)=.0                                                    TOR03060
      AA(IQ,IC+2)=                                                      TOR03070
     1 (-.005208333335*N3*H2-.005208333335*N2*H2                        TOR03080
     1 -.5*N*(.125*R2+.125*P*(R2+.08333333333*H2)-.01041666667*H2))*G4  TOR03090
  120 N=NN-3                                                            TOR03100
      N2=N*N                                                            TOR03110
      N3=N2*N                                                           TOR03120
      AA(IQ,IC+3)=                                                      TOR03130
     1 (-.5*N2*(R2+.08333333333*H2)                                     TOR03140
     1 -.375*N*(R2+.08333333333*H2)                                     TOR03150
     1 -.375*P*(R2+.08333333333*H2)+.25*R2+.02083333333*H2)*G3          TOR03160
      AA(IQ,IC+4)=                                                      TOR03170
     1 (.5*N*M*(.125*R2*(1.+P)+.02083333334*H2*P+.01041666667*H2        TOR03180
     1 *(1.-P))-.5*M                                                    TOR03190
     1 *(.125*(3.-P)*R2-.02083333334*H2*P                               TOR03200
     1 -.01041666667*H2*UMP+.04166666667*H2))*G3                        TOR03210
      AA(IQ,IC+5)=                                                      TOR03220
     1 (-.04166666667*N3*H2-.03125*N2*H2                                TOR03230
     1 -.5*N*(.75*P*(R2+.08333333333*H2)+R2-.04166666668*H2)            TOR03240
     1 -.125*R2)*G3                                                     TOR03250
  130 N=NN-2                                                            TOR03260
      N2=N*N                                                            TOR03270
      N3=N2*N                                                           TOR03280
      AA(IQ,IC+6)=                                                      TOR03290
     1 (-1.5*N2*(R2+.08333333333*H2)                                    TOR03300
```

```
     1 -.75*N*(R2+.08333333333*H2)                                          TOR03310
     1 -.5*M2*(.25*R2*(1.-P)+.02083333334*H2*(1.-P))+.25*R2                 TOR03320
     1 +.02083333333*H2-.75*P*(R2+.08333333333*H2))*G2                      TOR03330
     1 +(-.25*N2*(R2+.08333333333*H2)                                       TOR03340
     1 -.125*N*(R2+.08333333333*H2)                                         TOR03350
     1 -.25*P*(R2+.08333333333*H2))*G4                                      TOR03360
      AA(IQ,IC+7)=                                                          TOR03370
     1 (.5*N*M*(.75*R2*(1.+P)+.08333333335*H2*P+.04166666667*H2             TOR03380
     1 *(1.-P))-.5*M                                                        TOR03390
     1 *(.5*(3.-P)*R2-.08333333335*H2*P                                     TOR03400
     1 -.04166666668*H2*UMP+.02083333333*H2*(5.-P)))*G2                     TOR03410
      AA(IQ,IC+8)=                                                          TOR03420
     1 (-.125*N3*H2-.06250000002*N2*H2                                      TOR03430
     1 -.5*N*(3.*R2-.04166666667*H2+1.5*P*(R2+.08333333333*H2))             TOR03440
     1 +.04166666667*M2*H2-.5*R2-.02083333334*N*M2*H2)*G2                   TOR03450
     1 +(-.02083333334*N3*H2-.01041666667*N2*H2                             TOR03460
     1 -.5*N*(.5*R2+.5*P*(R2+.08333333333*H2)))*G4                          TOR03470
 140 N=NN-1                                                                 TOR03480
     N2=N*N                                                                 TOR03490
     N3=N2*N                                                                TOR03500
     AA(IQ,IC+9)=                                                           TOR03510
    1 (-.5*N*(R2+.08333333333*H2)                                           TOR03520
    1 -.5*M2*(R2*(1.-P)+.125*H2*(1.-P))                                     TOR03530
    1 -2.*N2*(R2+.08333333333*H2)-.5*P*(R2+.08333333333*H2))*G              TOR03540
    1 +(-1.5*N2*(R2+.08333333333*H2)-.25*R2-.02083333333*H2                 TOR03550
    1 -.375*N*(R2+.08333333333*H2)                                          TOR03560
    1 -1.125*P*(R2+.08333333333*H2))*G3                                     TOR03570
     AA(IQ,IC+10)=                                                          TOR03580
    1 (.5*N*M*(1.5*R2*(1.+P)+.08333333333*H2*P+.01041666667*H2              TOR03590
    1 *(1.-P))-.5*M                                                         TOR03600
    1 *(.5*(3.-P)*R2-.08333333334*H2*P                                      TOR03610
    1 -.03125000001*H2*UMP))*G                                              TOR03620
    1 +(.5*N*M*(.375*R2*(1.+P)+.0625*H2*P+.03125000001*H2                   TOR03630
    1 *(1.-P))-.5*M                                                         TOR03640
    1 *(.125*(3.-P)*R2-.02083333334*H2*P                                    TOR03650
    1 -.01041666667*H2*UMP+.04166666667*H2))*G3                             TOR03660
     AA(IQ,IC+11)=                                                          TOR03670
    1 (-.04166666667*N2*H2-.1666666667*N3*H2-.02083333334*N*M2*H2*SMP       TOR03680
    1 -.02083333334*M2*H2*(P-5.)-.5*N*(P*(R2+.08333333333*H2)+4.*R2)        TOR03690
    1 -.5*R2)*G                                                             TOR03700
    1 +(-.125*N3*H2-.125*R2-.03125*N2*H2                                    TOR03710
    1 -.5*N*(3.*R2+2.25*P*(R2+.08333333333*H2)+.04166666668*H2))*G3         TOR03720
 150 N=NN                                                                   TOR03730
     N2=N*N                                                                 TOR03740
     N3=N2*N                                                                TOR03750
     AA(IQ,IC+12)=                                                          TOR03760
    1 -N2*(R2+.08333333333*H2)                                              TOR03770
    1 -M2*(.5*R2*(1.-P)+.09375000003*H2*(1.-P))                             TOR03780
    1 +(-.5*R2-.04166666667*H2-1.5*P*(R2+.08333333333*H2)                   TOR03790
    1 -3.*N2*(R2+.08333333333*H2)                                           TOR03800
    1 -M2*(.25*R2*(1.-P)+.02083333334*H2*(1.-P)))*G2                        TOR03810
    1 +(-.375*N2*(R2+.08333333333*H2)-.125*R2-.01041666667*H2               TOR03820
    1 -.375*P*(R2+.08333333333*H2))*G4                                      TOR03830
     AA(IQ,IC+13)=                                                          TOR03840
    1 N*M*(.5*R2*(1.+P)-.03125000001*H2*(1.-P))                             TOR03850
```

```
     1 +(N*M*(.75*R2*(1.+P)+.08333333335*H2*P+.04166666668*H2                TOR03860
     1 *(1.-P)))*G2                                                         TOR03870
      AA(IQ,IC+14)=                                                         TOR03880
     1 -N*R2 -.08333333333*N3*H2+.04166666667*N*M2*H2*(P-3.)                 TOR03890
     1 +(-.25*N3*H2-.04166666667*N*M2*H2                                    TOR03900
     1 -N*(1.5*P*(R2+.08333333333*H2)+.04166666667*H2+3.*R2))*G2             TOR03910
     1 +(-.03125*N3*H2                                                      TOR03920
     1 -N*(.375*R2+.375*P*(R2+.08333333333*H2)+.01041666667*H2))*G4         TOR03930
   160 N=NN+1                                                               TOR03940
      N2=N*N                                                                TOR03950
      N3=N2*N                                                               TOR03960
      AA(IQ,IC+15)=                                                         TOR03970
     1 (.5*N*(R2+.08333333333*H2)                                           TOR03980
     1 -.5*M2*(R2*(1.-P)+.125*H2*(1.-P))                                    TOR03990
     1 -2.*N2*(R2+.08333333333*H2)-.5*P*(R2+.08333333333*H2))*G             TOR04000
     1 +(-1.5*N2*(R2+.08333333333*H2)-.25*R2-.02083333333*H2                TOR04010
     1 +.375*N*(R2+.08333333333*H2)                                         TOR04020
     1 -1.125*P*(R2+.08333333333*H2))*G3                                    TOR04030
      AA(IQ,IC+16)=                                                         TOR04040
     1 (.5*N*M*(1.5*R2*(1.+P)+.08333333333*H2*P+.01041666667*H2             TOR04050
     1 *(1.-P))+.5*M                                                        TOR04060
     1 *(.5*(3.-P)*R2-.08333333334*H2*P                                     TOR04070
     1 -.03125000001*H2*UMP))*G                                             TOR04080
     1 +(.5*N*M*(.375*R2*(1.+ P)+.0625*H2*P+.03125000001*H2                 TOR04090
     1 *(1.-P))+.5*M                                                        TOR04100
     1 *(.125*(3.-P)*R2-.02083333334*H2*P                                   TOR04110
     1 -.01041666667*H2*UMP+.04166666667*H2))*G3                            TOR04120
      AA(IQ,IC+17)=                                                         TOR04130
     1 (.04166666667*N2*H2-.1666666667*N3*H2-.02083333334*N*M2*H2*SMP       TOR04140
     1 +.02083333334*M2*H2*(P-5.)-.5*N*(P*(R2+.08333333333*H2)+4.*R2)       TOR04150
     1 +.5*R2)*G                                                            TOR04160
     1 +(-.125*N3*H2+.125*R2+.03125*N2*H2                                   TOR04170
     1 -.5*N*(3.*R2+2.25*P*(R2+.08333333333*H2)+.04166666668*H2))*G3        TOR04180
   170 N=NN+2                                                               TOR04190
      N2=N*N                                                                TOR04200
      N3=N2*N                                                               TOR04210
      AA(IQ,IC+18)=                                                         TOR04220
     1 (-1.5*N2*(R2+.08333333333*H2)                                        TOR04230
     1 +.75*N*(R2+.08333333333*H2)                                          TOR04240
     1 -.5*M2*(.25*R2*(1.-P)+.02083333334*H2*(1.-P))+.25*R2                 TOR04250
     1 +.02083333333*H2-.75*P*(R2+.08333333333*H2))*G2                      TOR04260
     1 +(-.25*N2*(R2+.08333333333*H2)                                       TOR04270
     1 +.125*N*(R2+.08333333333*H2)                                         TOR04280
     1 -.25*P*(R2+.08333333333*H2))*G4                                      TOR04290
      AA(IQ,IC+19)=                                                         TOR04300
     1 (.5*N*M*(.75*R2*(1. + P) + .08333333335*H2*P + .04166666667*H2       TOR04310
     1 *(1.-P))+.5*M                                                        TOR04320
     1 *(.5*(3.-P)*R2-.08333333335*H2*P                                     TOR04330
     1 -.04166666668*H2*UMP+.02083333333*H2*(5.-P)))*G2                     TOR04340
      AA(IQ,IC+20)=                                                         TOR04350
     1 (-.125*N3*H2+.06250000002*N2*H2                                      TOR04360
     1 - .5*N*(3.*R2-.04166666667*H2+1.5*P*(R2+.08333333333*H2))            TOR04370
     1 -.04166666667*M2*H2+.50*R2-.02083333334*N*M2*H2)*G2                  TOR04380
     1 +(-.02083333334*N3*H2+.01041666667*N2*H2                             TOR04390
     1 -.5*N*(.5*R2+.5*P*(R2+.08333333333*H2)))*G4                          TOR04400
```

```
  180 N=NN+3                                                                TOR04410
      N2=N*N                                                                TOR04420
      N3=N2*N                                                               TOR04430
      AA(IQ,IC+21)=                                                         TOR04440
     1 (-.5*N2*(R2+.08333333333*H2)                                         TOR04450
     1 +.375*N*(R2+.08333333333*H2)                                         TOR04460
     1 -.375*P*(R2+.08333333333*H2)+.25*R2+.02083333333*H2)*G3              TOR04470
      AA(IQ,IC+22)=                                                         TOR04480
     1 (.5*N*M*(.125*R2*(1.+P)+.02083333334*H2*P+.01041666667*H2            TOR04490
     1 *(1.-P))+.5*M                                                        TOR04500
     1 *(.125*(3.-P)*R2-.02083333334*H2*P                                   TOR04510
     1 -.01041666667*H2*UMP+.04166666667*H2))*G3                            TOR04520
      AA(IQ,IC+23)=                                                         TOR04530
     1 (-.04166666667*N3*H2+.03125000000*N2*H2                              TOR04540
     1 -.5*N*(.75*P*(R2+.08333333333*H2)+R2-.04166666668*H2)                TOR04550
     1 +.125*R2)*G3                                                         TOR04560
  190 N=NN+4                                                                TOR04570
      N2=N*N                                                                TOR04580
      N3=N2*N                                                               TOR04590
      AA(IQ,IC+24)=                                                         TOR04600
     1 (-.0625*N2*(R2+.08333333333*H2)                                      TOR04610
     1 +.0625*N*(R2 +.08333333333*H2)                                       TOR04620
     1 -.0625*P*(R2+.08333333333*H2)+.0625*R2+.005208333333*H2)*G4          TOR04630
      AA(IQ,IC+25)=.0                                                       TOR04640
      AA(IQ,IC+26)=                                                         TOR04650
     1 (-.005208333335*N3*H2+.005208333335*N2*H2                            TOR04660
     1 -.5*N*(.125*R2 +.125*P*(R2+.08333333333*H2)-.01041666667*H2))*G4     TOR04670
C     SECOND EQUATION  'V' EQN                                              TOR04680
  210 IQ=IQ+1                                                               TOR04690
      IC=1                                                                  TOR04700
  310 N=NN-4                                                                TOR04710
      N2=N*N                                                                TOR04720
      AA(IQ,IC  )=.0                                                        TOR04730
      AA(IQ,IC+1)=                                                          TOR04740
     1 (-.5*N2*(.75*UMP*EKA+.0625-.0625*P)                                  TOR04750
     1 +.5*N*(-.75*EKA*UMP-.0625+.0625*P)+.0625-.0625*P+.75*UMP*EKA)*G4     TOR04760
      AA(IQ,IC+2)=.0                                                        TOR04770
  320 N=NN-3                                                                TOR04780
      N2=N*N                                                                TOR04790
      AA(IQ,IC+3)=                                                          TOR04800
     1 (.5*N*M*(.125+.125*P+3.*P*EKA+1.5*UMP*EKA)                           TOR04810
     1 -.5*M*(.25*(6.*P-18.)*EKA-.375+.125*P))*G3                           TOR04820
      AA(IQ,IC+4)=                                                          TOR04830
     1 (-.5*N2*(6.*UMP*EKA+.125-.125*P)+.5*N*(-4.5*UMP*EKA-.375+.375*P)     TOR04840
     1 +3.75*UMP*EKA+.09375-.09375*P)*G3                                    TOR04850
      AA(IQ,IC+5)=                                                          TOR04860
     1 (.125*N2*M+.125*N*M+.5*M*(6.*EKA*F*UPP-.25+.25*P))*G3                TOR04870
  330 N=NN-2                                                                TOR04880
      N2=N*N                                                                TOR04890
      AA(IQ,IC+6)=                                                          TOR04900
     1 (.5*N*M*(.5+.5*P+18.*P*EKA+9.*UMP*EKA)                               TOR04910
     1 -.5*M*((6.*P-18.)*EKA-1.+.5*P))*G2                                   TOR04920
      AA(IQ,IC+7)=                                                          TOR04930
     1 (-.5*N2*(18.*(1.-P)*EKA-.1875+.1875*P)+6.*(1.-P)*EKA                 TOR04940
     1+.5*N*(-.1875+.1875*P-9.*UMP*EKA)-.25+.25*P-.5*M2*(6.*EKA+.5))*G2     TOR04950
```

```
     1 +(-.5*N2*(3.*UMP*EKA+.25-.25*P)+.125-.125*P                      TOR04960
     1 +.5*N*(-.125+.125*P-1.5*UMP*EKA)+1.5*UMP*EKA)*G4                 TOR04970
      AA(IQ,IC+8)=                                                      TOR04980
     1 (-.5*N2*M*(-.75-.25*P)+.5*N*M*(1.25-.75*P)                       TOR04990
     1 +.5*M*(6.*EKA*(2.+3.*P)-1.+P))*G2                                TOR05000
 340 N=NN-1                                                             TOR05010
      N2=N*N                                                            TOR05020
      AA(IQ,IC+9)=                                                      TOR05030
     1 (.5*N*M*(.125+.875*P+36.*P*EKA+18.*UMP*EKA)                      TOR05040
     1 -.5*M*((6.*P-18.)*EKA-.875+.875*P))*G                            TOR05050
     1 +(.5*N*M*(9.*P*EKA+.625*P+.375+4.5*UMP*EKA)                      TOR05060
     1 - .5*M*(.25*(6.*P-18.)*EKA-.375+.125*P))*G3                      TOR05070
      AA(IQ,IC+10)=                                                     TOR05080
     1 (-.5*N2*(24.*(1.-P)*EKA-.25+.25*P)+3.*UMP*EKA                    TOR05090
     1 +.5*N*(.625-.625*P-6.*UMP*EKA)+.0625-.0625*P                     TOR05100
     1 -12.*M2*EKA)*G                                                   TOR05110
     1 +(-.5*N2*(18.*(1.-P)*EKA+.375-.375*P)-.25+.25*P                  TOR05120
     1 +.5*N*(-4.5*UMP*EKA-.375+.375*P)+5.25*UMP*EKA)*G3                TOR05130
      AA(IQ,IC+11)=                                                     TOR05140
     1 (.5*M3+.50*N2*M*P+.5*N*M*(1.5-1.5*P)                             TOR05150
     1 +.5*M*(6.*EKA*(2.+6.*P)+.5-.5*P))*G                              TOR05160
     1 +(.375*N2*M+.125*N*M+.5*M*(6.*EKA*1.5*UPP-.75+.75*P))*G3         TOR05170
 350 N=NN                                                               TOR05180
      N2=N*N                                                            TOR05190
      AA(IQ,IC+12)=                                                     TOR05200
     1 N*M*(12.*P*EKA-.375+.375*P+6.*UMP*EKA)                           TOR05210
     1 +N*M*(.5+.5*P+18.*P*EKA+9.*UMP*EKA)*G2                           TOR05220
      AA(IQ,IC+13)=                                                     TOR05230
     1 -N2*(6.*(1.-P)*EKA+.125-.125*P)-12.*M2*EKA                       TOR05240
     1 +(6.*(1.-P)*EKA-N2*(18.*(1.-P)*EKA-.1875+.1875*P)                TOR05250
     1 +.125-.125*P-M2*(6.*R2/H2+.5))*G2                                TOR05260
     1 +(-N2*(2.25*(1.-P)*EKA+.1875-.1875*P)                            TOR05270
     1 +.125-.125*P+1.5*(1.-P)*EKA)*G4                                  TOR05280
      AA(IQ,IC+14)=                                                     TOR05290
     1 -N2*M*(.5-.5*P)+12.*EKA*M*P                                      TOR05300
     1 +(-N2*M*(-.75-.25*P)+M*(6.*EKA*(2.+3.*P)+.5-.5*P))*G2            TOR05310
 360 N=NN+1                                                             TOR05320
      N2=N*N                                                            TOR05330
      AA(IQ,IC+15)=                                                     TOR05340
     1 (.5*N*M*(.875*P+.125+36.*P*EKA+18.*UMP*EKA)                      TOR05350
     1 +.5*M*((6.*P-18.)*EKA-.875+.875*P))*G                            TOR05360
     1 +(.5*N*M*(9.*P*R2/H2+.625*P+.375+4.5*UMP*EKA)                    TOR05370
     1 +.5*M*(.25*(6.*P-18.)*R2/H2-.375+.125*P))*G3                     TOR05380
      AA(IQ,IC+16)=                                                     TOR05390
     1 (-.5*N2*(24.*(1.-P)*R2/H2-.25+.25*P)                             TOR05400
     1 -.5*N*(.625-.625*P-6.*UMP*EKA)+3.*(1.-P)*R2/H2                   TOR05410
     1 + .0625-.0625*P-12.*M2*R2/H2)*G                                  TOR05420
     1 +(-.5*N2*(18.*(1.-P)*R2/H2+.375-.375*P)-.25+.25*P                TOR05430
     1 -.5*N*(-4.5*UMP*EKA-.375+.375*P)+5.25*UMP*EKA)*G3                TOR05440
      AA(IQ,IC+17)=                                                     TOR05450
     1 (.5*M3+.5*N2*M*P-.5*N*M*(1.5-1.5*P)                              TOR05460
     1 +.5*M*(6.*EKA*(2.+6.*P)+.5-.5*P))*G                              TOR05470
     1 +(.375*N2*M-.125*N*M+.5*M*(6.*EKA*1.5*UPP-.75+.75*P))*G3         TOR05480
 370 N=NN+2                                                             TOR05490
      N2=N*N                                                            TOR05500
```

```
      AA(IQ,IC+18)=                                                     TOR05510
     1 (.5*N*M*(.5+.5*P+18.*P*R2/H2+9.*UMP*EKA)                         TOR05520
     1 +.5*M*((6.*P-18.)*R2/H2+.5*P-1.))*G2                             TOR05530
      AA(IQ,IC+19)=                                                     TOR05540
     1 (-.5*N2*(18.*(1.-P)*R2/H2-.1875+.1875*P)+6.*(1.-P)*R2/H2         TOR05550
     1-.5*N*(-.1875+.1875*P-9.*UMP*EKA)-.5*M2*(6.*EKA+.5)-.25+.25*P)*G2 TOR05560
     1 +(-.5*N2*(3.*(1.-P)*R2/H2+.25-.25*P)+.125-.125*P                 TOR05570
     1 -.5*N*(-.125+.125*P-1.5*UMP*EKA)+1.5*(1.-P)*R2/H2)*G4            TOR05580
      AA(IQ,IC+20)=                                                     TOR05590
     1 (-.5*N2*M*(-.75-.25*P)-.5*N*M*(1.25-.75*P)                       TOR05600
     1 +.5*M*(6.*EKA*(2.+3.*P)-1.+P))*G2                                TOR05610
  380 N=NN+3                                                            TOR05620
      N2=N*N                                                            TOR05630
      AA(IQ,IC+21)=                                                     TOR05640
     1 (.5*N*M*(.125*P+.125+3.*P*R2/H2+1.5*UMP*EKA)                     TOR05650
     1 +.5*M*(.25*(6.*P-18.)*R2/H2-.375+.125*P))*G3                     TOR05660
      AA(IQ,IC+22)=                                                     TOR05670
     1 (-.5*N2*(3.*(1.-P)*R2/H2+.125-.125*P)-.5*N*(-4.5*UMP*EKA         TOR05680
     1 -.375+.375*P)+3.75*UMP*EKA+.09375-.09375*P)*G3                   TOR05690
      AA(IQ,IC+23)=                                                     TOR05700
     1 (.125*N2*M-.125*N*M+.5*M*(6.*EKA*F*UPP-.25+.25*P))*G3            TOR05710
  390 N=NN+4                                                            TOR05720
      N2=N*N                                                            TOR05730
      AA(IQ,IC+24)=.0                                                   TOR05740
      AA(IQ,IC+25)=                                                     TOR05750
     1 (-.5*N2*(.75*(1.-P)*R2/H2+.0625-.0625*P)-.5*N*                   TOR05760
     1 (-.75*UMP*EKA-.0625+.0625*P)+.0625-.0625*P+.75*UMP*EKA)*G4       TOR05770
      AA(IQ,IC+26)=.0                                                   TOR05780
C     EQUATION3   'W' EQUATION                                          TOR05790
  410 IQ=IQ+1                                                           TOR05800
      IC=1                                                              TOR05810
  510 N=NN-4                                                            TOR05820
      N2=N*N                                                            TOR05830
      N3=N2*N                                                           TOR05840
      N4=N3*N                                                           TOR05850
      AA(IQ,IC  )=                                                      TOR05860
     1 (.0625*N3+.5*N*(1.5*EKA+1.5*P*EKA+.125*P)+.125*N2-.0625          TOR05870
     1 +.75*EKA+.0625*(12.*EKA+1.)*P)*G4                                TOR05880
      AA(IQ,IC+1)=.0                                                    TOR05890
      AA(IQ,IC+2)=                                                      TOR05900
     1 (.0625*N4+.0625*N3*P+6.*EKA*.25*UPP+.125*N3                      TOR05910
     1 +.5*N*(-.125+.125*P))*G4                                         TOR05920
  520 N=NN-3                                                            TOR05930
      N2=N*N                                                            TOR05940
      N3=N2*N                                                           TOR05950
      N4=N3*N                                                           TOR05960
      AA(IQ,IC+3)=                                                      TOR05970
     1 (.5*N3+.5*N*(12.*EKA+9.*P*EKA+.25+.75*P)+.75*N2-.375             TOR05980
     1 +3.*EKA+.375*(12.*EKA+1.)*P)*G3                                  TOR05990
      AA(IQ,IC+4)=                                                      TOR06000
     1 (-.5*M*(3.*EKA -.25+.25*P+3.*P*EKA)-.125*N2*M+.125*N*M)*G3       TOR06010
      AA(IQ,IC+5)=                                                      TOR06020
     1 (.5*N4-.5*N2*(-.25-.75*P)+6.*EKA*1.5*UPP+.75*N3                  TOR06030
     1 +.5*N*(-.75+.75*P))*G3                                           TOR06040
  530 N=NN-2                                                            TOR06050
```

```
      N2=N*N                                                            TOR06060
      N3=N2*N                                                           TOR06070
      N4=N3*N                                                           TOR06080
      AA(IQ,IC+6)=                                                      TOR06090
     1 (.5*N*(36.*EKA+18.*P*EKA+1.+1.5*P)+1.5*N3+.25*M2-.5              TOR06100
     1 +3.*EKA+1.5*N2+.75*(12.*EKA+1.)*P+.25*N*M2)*G2                   TOR06110
     1 +(.25*N3+.25*N2+.5*N*(6.*EKA+6.*P*EKA+.5+.5*P)-.375              TOR06120
     1 +1.5*EKA+.125*(12.*EKA+1.)*P)*G4                                 TOR06130
      AA(IQ,IC+7)=                                                      TOR06140
     1 (-.5*M*(12.*EKA-2.+.5*P+18.*P*EKA)+.5*N2*M*(-.75-.25*P)          TOR06150
     1 -.5*N*M*(.25+.25*P))*G2                                          TOR06160
      AA(IQ,IC+8)=                                                      TOR06170
     1 (1.5*N4-.5*N2*(-1.-1.5*P)-.5*M2*(-.5-.5*P)                       TOR06180
     1 +6.*EKA*(3.5+3.*P)+.5*M2*N2+1.5*N3+.5*N*(-1.+1.5*P)              TOR06190
     1 -.5*N*M2)*G2                                                     TOR06200
     1 +(.25*N4-.5*N2*(-.5-.5*P)+.25*N3+6.*EKA*UPP                      TOR06210
     1 +.5*N*(-.75+.25*P))*G4                                           TOR06220
  540 N=NN-1                                                            TOR06230
      N2=N*N                                                            TOR06240
      N3=N2*N                                                           TOR06250
      N4=N3*N                                                           TOR06260
      AA(IQ,IC+9)=                                                      TOR06270
     1 (N2+.5*N*(48.*EKA+12.*P*EKA+1.+P)                                TOR06280
     1 -.5*N*M2*(-2.5+.5*P)+2.*N3+.5*(12.*EKA+1.)*P                     TOR06290
     1 +.25*M2*(1.+P))*G                                                TOR06300
     1 +(1.5*N3+.75*N2+.5*N*(36.*EKA+ 27.*P*EKA+2.75+2.25*P)-.875       TOR06310
     1 + 3.*EKA+.375*(12.*EKA+1.)*P)*G3                                 TOR06320
      AA(IQ,IC+10)=                                                     TOR06330
     1 (-.5*M3-.5*M*(12.*EKA+.5+.5*P+36.*P*EKA)-.5*N2*M*P               TOR06340
     1 -.5*N*M*(1.5+.5*P))*G                                            TOR06350
     1 +(-.5*M*(9.*EKA-1.75+.75*P+9.*P*EKA)-.375*N2*M+.125*N*M)*G3      TOR06360
      AA(IQ,IC+11)=                                                     TOR06370
     1 (2.*N4-.5*N2*(-1.-P)-.5*M2*(3.-P)+6.*EKA*2.*DPP                  TOR06380
     1 +2.*M2*N2+N3+.5*N*P-N*M2)*G                                      TOR06390
     1 +(1.5*N4-.5*N2*(-2.75-2.25*P)+.75*N3+6.*EKA*4.5*UPP              TOR06400
     1 +.5*N*(-1.75+.75*P))*G3                                          TOR06410
  550 N=NN                                                              TOR06420
      N2=N*N                                                            TOR06430
      N3=N2*N                                                           TOR06440
      N4=N3*N                                                           TOR06450
      AA(IQ,IC+12)=                                                     TOR06460
     1 12.*N*EKA+N3-N*M2*(-1.5+.5*P)                                    TOR06470
     1 +(3.*N3+.5*N*M2+N*(2.+18.*P*EKA+1.5*P+36.*EKA))*G2               TOR06480
     1 +(.375*N3+N*(4.5*EKA+.5+4.5*P*EKA+.375*P))*G4                    TOR06490
      AA(IQ,IC+13)=                                                     TOR06500
     1 -12.*M*P*EKA+N2*M*(.5-.5*P)                                      TOR06510
     1 +(-M*(12.*EKA+.5+P+18.*P*EKA)+N2*M*(-.75-.25*P))*G2              TOR06520
      AA(IQ,IC+14)=                                                     TOR06530
     1 2.*M2*N2+M4+N4+12.*EKA                                           TOR06540
     1 +(M2*N2-N2*(-2.-1.5*P)+3.*N4+12.*EKA*(3.5+3.*P)                  TOR06550
     1 -M2*(3.5-.5*P))*G2                                               TOR06560
     1 +(.375*N4+12.*EKA*.75*UPP-N2*(-.5-.375*P))*G4                    TOR06570
  560 N=NN+1                                                            TOR06580
      N2=N*N                                                            TOR06590
      N3=N2*N                                                           TOR06600
```

```
      N4=N3*N                                                           TOR06610
      AA(IQ,IC+15)=                                                     TOR06620
     1 (-N2+.5*N*(48.*EKA+12.*P*EKA+1.+P)                               TOR06630
     1 -.5*N*M2*(-2.5+.5*P)+2.*N3-.5*(12.*EKA+1.)*P                     TOR06640
     1 -.25*M2*(1.+P))*G                                                TOR06650
     1 +(1.5*N3-.75*N2+.5*N*(36.*EKA+27.*P*EKA+2.75+2.25*P)+.875        TOR06660
     1 - 3.*EKA-.375*(12.*EKA+1.)*P)*G3                                 TOR06670
      AA(IQ,IC+16)=                                                     TOR06680
     1 (-.5*M3-.5*M*(12.*EKA+.5+.5*P+36.*P*EKA)-.5*N2*M*P               TOR06690
     1 +.5*N*M*(1.5+.5*P))*G                                            TOR06700
     1 +(-.5*M*(9.*EKA-1.75+.75*P+9.*P*EKA)-.375*N2*M-.125*N*M)*G3      TOR06710
      AA(IQ,IC+17)=                                                     TOR06720
     1 (2.*N4-.5*N2*(-1.-P)-.5*M2*(3.-P)+6.*EKA*2.*DPP                  TOR06730
     1 +2.*M2*N2-N3-.5*N*P+N*M2)*G                                      TOR06740
     1 +(1.5*N4-.5*N2*(-2.75-2.25*P)-.75*N3+6.*EKA*4.5*UPP              TOR06750
     1 -.5*N*(-1.75+.75*P))*G3                                          TOR06760
  570 N=NN+2                                                            TOR06770
      N2=N*N                                                            TOR06780
      N3=N2*N                                                           TOR06790
      N4=N3*N                                                           TOR06800
      AA(IQ,IC+18)=                                                     TOR06810
     1 (.5*N*(36.*EKA+18.*P*EKA+1.+1.5*P)+1.5*N3-.25*M2+.5              TOR06820
     1 - 3.*EKA-1.5*N2-.75*(12.*EKA+1.)*P+.25*N*M2)*G2                  TOR06830
     1 +(.25*N3-.25*N2+.5*N*(6.*EKA+6.*P*EKA+.5+.5*P)+.375              TOR06840
     1 - 1.5*EKA-.125*(12.*EKA+1.)*P)*G4                                TOR06850
      AA(IQ,IC+19)=                                                     TOR06860
     1 (-.5*M*(12.*EKA-2.+.5*P+18.*P*EKA)+.5*N2*M*(-.75-.25*P)          TOR06870
     1 +.5*N*M*(.25+.25*P))*G2                                          TOR06880
      AA(IQ,IC+20)=                                                     TOR06890
     1 (1.5*N4-.5*N2*(-1.-1.5*P)-.5*M2*(-.5-.5*P)                       TOR06900
     1 +6.*EKA*(3.5+3.*P)+.5*M2*N2-1.5*N3-.5*N*(-1.+1.5*P)              TOR06910
     1 +.5*N*M2)*G2                                                     TOR06920
     1 +(.25*N4-.5*N2*(-.5-.5*P)-.25*N3+6.*EKA*UPP                      TOR06930
     1 -.5*N*(-.75+.25*P))*G4                                           TOR06940
  580 N=NN+3                                                            TOR06950
      N2=N*N                                                            TOR06960
      N3=N2*N                                                           TOR06970
      N4=N3*N                                                           TOR06980
      AA(IQ,IC+21)=                                                     TOR06990
     1 (.5*N3+.5*N*(12.*EKA+9.*P*EKA+.25+.75*P)-.75*N2+.375             TOR07000
     1 - 3.*EKA-.375*(12.*EKA+1.)*P)*G3                                 TOR07010
      AA(IQ,IC+22)=                                                     TOR07020
     1 (-.5*M*(3.*EKA-.25+.25*P+3.*P*EKA)-.125*N2*M-.125*N*M)*G3        TOR07030
      AA(IQ,IC+23)=                                                     TOR07040
     1 (.5*N4-.5*N2*(-.25-.75*P)+6.*EKA*1.5*UPP-.75*N3                  TOR07050
     1 -.5*N*(-.75+.75*P))*G3                                           TOR07060
  590 N=NN+4                                                            TOR07070
      N2=N*N                                                            TOR07080
      N3=N2*N                                                           TOR07090
      N4=N3*N                                                           TOR07100
      AA(IQ,IC+24)=                                                     TOR07110
     1 (.0625*N3+.5*N*(1.5*EKA+1.5*P*EKA+.125*P)-.125*N2+.0625          TOR07120
     1 -.75*EKA-.0625*(12.*EKA+1.)*P)*G4                                TOR07130
      AA(IQ,IC+25)=.0                                                   TOR07140
      AA(IQ,IC+26)=                                                     TOR07150
```

```
     1 (.0625*N4+.0625*N2*P+6.*EKA*.25*UPP-.125*N3                      TOR07160
     1 -.5*N*(-.125+.125*P))*G4                                         TOR07170
  900 CONTINUE                                                          TOR07180
C     FIX UP 'U' EQUATIONS                                             TOR07190
 2100 JHI=10                                                            TOR07200
      JEQ=3                                                             TOR07210
      DO 2110 I=1,4                                                     TOR07220
      DO 2120 J=1,JHI                                                   TOR07230
 2120 AA(JEQ,J)=.0                                                      TOR07240
      JHI=JHI-3                                                         TOR07250
 2110 JEQ=JEQ+3                                                         TOR07260
      AA(3,11)=AA(3,11)                                                 TOR07270
     1 -((.5*.0*M*(1.5*R2*(1.+P)+.08333333333*H2*P+.01041666667*H2      TOR07280
     1 *(1.-P))+.5*M                                                    TOR07290
     1 *(.5*(3.-P)*R2-.08333333334*H2*P                                 TOR07300
     1 -.03125000001*H2*UMP))*G                                         TOR07310
     1 +(.5*.0*M*(.375*R2*(1.+ P)+.0625*H2*P+.03125000001*H2            TOR07320
     1 *(1.-P))+.5*M                                                    TOR07330
     1 *(.125*(3.-P)*R2-.02083333334*H2*P                               TOR07340
     1 -.01041666667*H2*UMP+.04166666667*H2))*G3)                       TOR07350
      AA(3,12)=AA(3,12)                                                 TOR07360
     1 -((.04166666667*0.*H2-.1666666667*0.*H2-.02083333334*0.*M2*H2*SMPTOR07370
     1 +.02083333334*M2*H2*(P-5.)-.5*0.*(P*(R2+.08333333333*H2)+4.*R2)  TOR07380
     1 +.5*R2)*G                                                        TOR07390
     1 +(-.125*0.*H2+.125*R2+.03125*0.*H2                               TOR07400
     1 -.5*0.*(3.*R2+2.25*P*(R2+.08333333333*H2)+.04166666668*H2))*G3)  TOR07410
      AA(3,13)=AA(3,13)                                                 TOR07420
     1 -((-1.5*(R2+.08333333333*H2)                                     TOR07430
     1 +.75*(R2+.08333333333*H2)                                        TOR07440
     1 -.5*M2*(.25*R2*(1.-P)+.02083333334*H2*(1.-P))+.25*R2             TOR07450
     1 +.02083333333*H2-.75*P*(R2+.08333333333*H2))*G2                  TOR07460
     1 +(-.25*(R2+.08333333333*H2)                                      TOR07470
     1 +.125*(R2+.08333333333*H2)                                       TOR07480
     1 -.25*P*(R2+.08333333333*H2))*G4)                                 TOR07490
      AA(3,14)=AA(3,14)                                                 TOR07500
     1 -((.5*M*(.75*R2*(1. + P) + .08333333335*H2*P + .04166666667*H2   TOR07510
     1 *(1.-P))+.5*M                                                    TOR07520
     1 *(.5*(3.-P)*R2-.08333333335*H2*P                                 TOR07530
     1 -.04166666668*H2*UMP+.02083333333*H2*(5.-P)))*G2)                TOR07540
      AA(3,15)=AA(3,15)                                                 TOR07550
     1 -((-.125*H2+.06250000002*H2                                      TOR07560
     1 - .5*(3.*R2-.04166666667*H2+1.5*P*(R2+.08333333333*H2))          TOR07570
     1 -.04166666667*M2*H2+.50*R2-.02083333334*M2*H2)*G2                TOR07580
     1 +(-.02083333334*H2+.01041666667*H2                               TOR07590
     1 -.5*(.5*R2+.5*P*(R2+.08333333333*H2)))*G4)                       TOR07600
      AA(3,16)=AA(3,16)                                                 TOR07610
     1 -((-.5*4.*(R2+.08333333333*H2)                                   TOR07620
     1 +.375*2.*(R2+.08333333333*H2)                                    TOR07630
     1 -.375*P*(R2+.08333333333*H2)+.25*R2+.02083333333*H2)*G3)         TOR07640
      AA(3,17)=AA(3,17)                                                 TOR07650
     1 -((.5*2.*M*(.125*R2*(1.+P)+.02083333334*H2*P+.01041666667*H2     TOR07660
     1 *(1.-P))+.5*M                                                    TOR07670
     1 *(.125*(3.-P)*R2-.02083333334*H2*P                               TOR07680
     1 -.01041666667*H2*UMP+.04166666667*H2))*G3)                       TOR07690
      AA(3,18)=AA(3,18)                                                 TOR07700
```

```
     1 -((-.04166666667*8.*H2+.03125000000*4.*H2                                    TOR07710
     1 -.5*2.*(.75*P*(R2+.08333333333*H2)+R2-.04166666668*H2)                       TOR07720
     1 +.125*R2)*G3)                                                                TOR07730
      AA(3,19)=AA(3,19)                                                             TOR07740
     1 -((-.0625*9.*(R2+.08333333333*H2)                                            TOR07750
     1 +.0625*3.*(R2 +.08333333333*H2)                                              TOR07760
     1 -.0625*P*(R2+.08333333333*H2)+.0625*R2+.005208333333*H2)*G4)                 TOR07770
      AA(3,21)=AA(3,21)                                                             TOR07780
     1 -((-.005208333335*27.*H2+.005208333335*9.*H2                                 TOR07790
     1 -.5*3.*(.125*R2+.125*P*(R2+.08333333333*H2)-.01041666667*H2))*G4)            TOR07800
      AA(6,8)=AA(6,8)                                                               TOR07810
     1 -((.5*0.*M*(.75*R2*(1. + P) + .08333333335*H2*P + .04166666667*H2            TOR07820
     1 *(1.-P))+.5*M                                                                TOR07830
     1 *(.5*(3.-P)*R2-.08333333335*H2*P                                             TOR07840
     1 -.04166666668*H2*UMP+.02083333333*H2*(5.-P)))*G2)                            TOR07850
      AA(6,9)=AA(6,9)                                                               TOR07860
     1 -((-.125*0.*H2+.06250000002*0.*H2                                            TOR07870
     1 - .5*0.*(3.*R2-.04166666667*H2+1.5*P*(R2+.08333333333*H2))                   TOR07880
     1 -.04166666667*M2*H2+.50*R2-.02083333334*0.*M2*H2)*G2                         TOR07890
     1 +(-.02083333334*0.*H2+.01041666667*0.*H2                                     TOR07900
     1 -.5*0.*(.5*R2+.5*P*(R2+.08333333333*H2)))*G4)                                TOR07910
      AA(6,10)=AA(6,10)                                                             TOR07920
     1 -((-.5*(R2+.08333333333*H2)                                                  TOR07930
     1 +.375*(R2+.08333333333*H2)                                                   TOR07940
     1 -.375*P*(R2+.08333333333*H2)+.25*R2+.02083333333*H2)*G3)                     TOR07950
      AA(6,11)=AA(6,11)                                                             TOR07960
     1 -((.5*M*(.125*R2*(1.+P)+.02083333334*H2*P+.01041666667*H2                    TOR07970
     1 *(1.-P))+.5*M                                                                TOR07980
     1 *(.125*(3.-P)*R2-.02083333334*H2*P                                           TOR07990
     1 -.01041666667*H2*UMP+.04166666667*H2))*G3)                                   TOR08000
      AA(6,12)=AA(6,12)                                                             TOR08010
     1 -((-.04166666667*H2+.03125000000*H2                                          TOR08020
     1 -.5*(.75*P*(R2+.08333333333*H2)+R2-.04166666668*H2)                          TOR08030
     1 +.125*R2)*G3)                                                                TOR08040
      AA(6,13)=AA(6,13)                                                             TOR08050
     1 -((-.0625*4.*(R2+.08333333333*H2)                                            TOR08060
     1 +.0625*2.*(R2 +.08333333333*H2)                                              TOR08070
     1 -.0625*P*(R2+.08333333333*H2)+.0625*R2+.005208333333*H2)*G4)                 TOR08080
      AA(6,15)=AA(6,15)                                                             TOR08090
     1 -((-.005208333335*8.*H2+.005208333335*4.*H2                                  TOR08100
     1 -.5*2.*(.125*R2+.125*P*(R2+.08333333333*H2)-.01041666667*H2))*G4)            TOR08110
      AA(9,5)=AA(9,5)                                                               TOR08120
     1 -((.5*0.*M*(.125*R2*(1.+P)+.02083333334*H2*P+.01041666667*H2                 TOR08130
     1 *(1.-P))+.5*M                                                                TOR08140
     1 *(.125*(3.-P)*R2-.02083333334*H2*P                                           TOR08150
     1 -.01041666667*H2*UMP+.04166666667*H2))*G3)                                   TOR08160
      AA(9,6)=AA(9,6)                                                               TOR08170
     1 -((-.04166666667*0.*H2+.03125*0.*H2                                          TOR08180
     1 -.5*0.*(.75*P*(R2+.08333333333*H2)+R2-.04166666668*H2)                       TOR08190
     1 +.125*R2)*G3)                                                                TOR08200
      AA(9,7)=AA(9,7)                                                               TOR08210
     1 -((-.0625*(R2+.08333333333*H2)                                               TOR08220
     1 +.0625*(R2 +.08333333333*H2)                                                 TOR08230
     1 -.0625*P*(R2+.08333333333*H2)+.0625*R2+.005208333333*H2)*G4)                 TOR08240
      AA(9,9)=AA(9,9)                                                               TOR08250
```

```
     1 -((-.005208333335*H2+.005208333335*H2                                TOR08260
     1 -.5*(.125*R2+.125*P*(R2+.08333333333*H2)-.01041666667*H2))*G4)       TOR08270
      AA(12,3)=AA(12,3)                                                     TOR08280
     1 -((-.005208333335*0.*H2+.005208333335*0.*H2                          TOR08290
     1 -.5*0.*(.125*R2+.125*P*(R2+.08333333333*H2)-.01041666667*H2))*G4)    TOR08300
C     FIX UP 'V' EQUATIONS                                                  TOR08310
 2200 JHI=13                                                                TOR08320
      JEQ=1                                                                 TOR08330
      DO 2210 I=1,5                                                         TOR08340
      DO 2220 J=1,JHI                                                       TOR08350
 2220 AA(JEQ,J)=.0                                                          TOR08360
      JHI=JHI-3                                                             TOR08370
 2210 JEQ=JEQ+3                                                             TOR08380
      AA(4,11)=AA(4,11)+                                                    TOR08390
     1 (-.5*0.*(24.*(1.-P)*R2/H2-.25+.25*P)                                 TOR08400
     1 -.5*0.*(.625-.625*P-6.*UMP*EKA)+3.*(1.-P)*R2/H2                      TOR08410
     1 + .0625-.0625*P-12.*M2*R2/H2)*G                                      TOR08420
     1 +(-.5*0.*(18.*(1.-P)*R2/H2+.375-.375*P)-.25+.25*P                    TOR08430
     1 -.5*0.*(-4.5*UMP*EKA-.375+.375*P)+5.25*UMP*EKA)*G3                   TOR08440
      AA(4,12)=AA(4,12)+                                                    TOR08450
     1 (.5*M3+.5*0.*M*P-.5*0.*M*(1.5-1.5*P)                                 TOR08460
     1 +.5*M*(6.*EKA*(2.+6.*P)+.5-.5*P))*G                                  TOR08470
     1 +(.375*0.*M-.125*0.*M+.5*M*(6.*EKA*1.5*UPP-.75+.75*P))*G3            TOR08480
      AA(4,13)=AA(4,13)+                                                    TOR08490
     1 (.5*M*(.5+.5*P+18.*P*R2/H2+9.*UMP*EKA)                               TOR08500
     1 +.5*M*((6.*P-18.)*R2/H2+.5*P-1.))*G2                                 TOR08510
      AA(4,14)=AA(4,14)+                                                    TOR08520
     1 (-.5*(18.*(1.-P)*R2/H2-.1875+.1875*P)+6.*(1.-P)*R2/H2                TOR08530
     1 -.5*(-.1875+.1875*P-9.*UMP*EKA)-.5*M2*(6.*EKA+.5)-.25+.25*P)*G2      TOR08540
     1 +(-.5*(3.*(1.-P)*R2/H2+.25-.25*P)+.125-.125*P                        TOR08550
     1 -.5*(-.125+.125*P-1.5*UMP*EKA)+1.5*(1.-P)*R2/H2)*G4                  TOR08560
      AA(4,15)=AA(4,15)+                                                    TOR08570
     1 (-.5*M*(-.75-.25*P)-.5*M*(1.25-.75*P)                                TOR08580
     1 +.5*M*(6.*EKA*(2.+3.*P)-1.+P))*G2                                    TOR08590
      AA(4,16)=AA(4,16)+                                                    TOR08600
     1 (.5*2.*M*(.125*P+.125+3.*P*R2/H2+1.5*UMP*EKA)                        TOR08610
     1 +.5*M*(.25*(6.*P-18.)*R2/H2-.375+.125*P))*G3                         TOR08620
      AA(4,17)=AA(4,17)+                                                    TOR08630
     1 (-.5*4.*(6.*(1.-P)*R2/H2+.125-.125*P)-.5*2.*(-4.5*EKA*UMP            TOR08640
     1 -.375+.375*P)+3.75*UMP*EKA+.09375-.09375*P)*G3                       TOR08650
      AA(4,18)=AA(4,18)+                                                    TOR08660
     1 (.125*4.*M-.125*2.*M+.5*M*(6.*EKA*F*UPP-.25+.25*P))*G3               TOR08670
      AA(4,20)=AA(4,20)+                                                    TOR08680
     1 (-.5*9.*(.75*(1.-P)*R2/H2+.0625-.0625*P)-.5*3.*                      TOR08690
     1 (-.75*UMP*EKA-.0625+.0625*P)+.75*UMP*EKA+.0625-.0625*P)*G4           TOR08700
      AA(7,8)=AA(7,8)+                                                      TOR08710
     1 (-.5*0.*(18.*(1.-P)*R2/H2-.1875+.1875*P)+6.*(1.-P)*R2/H2             TOR08720
     1 -.5*0.*(-.1875+.1875*P-9.*UMP*EKA)-.25+.25*P-.5*M2*(6.*EKA+.5))      TOR08730
     1 *G2+(-.5*0.*(3.*(1.-P)*R2/H2+.25-.25*P)+.125-.125*P                  TOR08740
     1 -.5*0.*(-.125+.125*P-1.5*UMP*EKA)+1.5*(1.-P)*R2/H2)*G4               TOR08750
      AA(7,9)=AA(7,9)+                                                      TOR08760
     1 (-.5*0.*M*(-.75-.25*P)-.5*0.*M*(1.25-.75*P)                          TOR08770
     1 +.5*M*(6.*EKA*(2.+3.*P)-1.+P))*G2                                    TOR08780
      AA(7,10)=AA(7,10)+                                                    TOR08790
     1 (.5*M*(.125*P+.125+3.*P*R2/H2+1.5*UMP*EKA)                           TOR08800
```

```
     1 +.5*M*(.25*(6.*P-18.)*R2/H2-.375+.125*P))*G3                    TOR08810
      AA(7,11)=AA(7,11)+                                               TOR08820
     1 (-.5*(6.*(1.-P)*R2/H2+.125-.125*P)-.5*(-4.5*(1.-P)*R2/H2        TOR08830
     1 -.375+.375*P)+3.75*UMP*EKA+.09375-.09375*P)*G3                  TOR08840
      AA(7,12)=AA(7,12)+                                               TOR08850
     1 (.125*M-.125*M+.5*M*(6.*EKA*F*UPP-.25+.25*P))*G3                TOR08860
      AA(7,14)=AA(7,14)+                                               TOR08870
     1 (-.5*4.*(.75*(1.-P)*R2/H2+.0625-.0625*P)-.5*2.*                 TOR08880
     1 (-.75*UMP*EKA-.0625+.0625*P)+.75*UMP*EKA+.0625-.0625*P)*G4      TOR08890
      AA(10,5)=AA(10,5)+                                               TOR08900
     1 (-.5*0.*(6.*(1.-P)*R2/H2+.125-.125*P)-.5*0.*(-4.5*(1.-P)*R2/H2  TOR08910
     1 -.375+.375*P)+3.75*UMP*EKA+.09375-.09375*P)*G3                  TOR08920
      AA(10,6)=AA(10,6)+                                               TOR08930
     1 (.125*0.*M-.125*0.*M+.5*M*(6.*EKA*F*UPP-.25+.25*P))*G3          TOR08940
      AA(10,8)=AA(10,8)+                                               TOR08950
     1 (-.5*(.75*(1.-P)*R2/H2+.0625-.0625*P)-.5*                       TOR08960
     1 (-.75*UMP*EKA-.0625+.0625*P)+.75*UMP*EKA+.0625-.0625*P)*G4      TOR08970
      AA(13,2)=AA(13,2)+                                               TOR08980
     1 (-.5*0.*(.75*(1.-P)*R2/H2+.0625-.0625*P)-.5*0.*                 TOR08990
     1 (-.75*UMP*EKA-.0625+.0625*P)+.75*UMP*EKA+.0625-.0625*P)*G4      TOR09000
      AA(13,3)=0.                                                      TOR09010
C     FIX UP 'W' EQUATIONS                                             TOR09020
 2300 JHI=13                                                           TOR09030
      JEQ=2                                                            TOR09040
      DO 2310 I=1,5                                                    TOR09050
      DO 2320 J=1,JHI                                                  TOR09060
 2320 AA(JEQ,J)=.0                                                     TOR09070
      JHI=JHI-3                                                        TOR09080
 2310 JEQ=JEQ+3                                                        TOR09090
      AA(5,11)=AA(5,11)+                                               TOR09100
     1 (-.5*M3-.5*M*(12.*EKA+.5+.5*P+36.*P*EKA)-.5*0.*M*P              TOR09110
     1 +.5*0.*M*(1.5+.5*P))*G                                          TOR09120
     1 +(-.5*M*(9.*EKA-1.75+.75*P+9.*P*EKA)-.375*0.*M-.125*0.*M)*G3    TOR09130
      AA(5,12)=AA(5,12)+                                               TOR09140
     1 (2.*0.-.5*0.*(-1.-P)-.5*M2*(3.-P)+6.*EKA*2.*DPP                 TOR09150
     1 +2.*M2*0.-0.-.5*0.*P+0.*M2)*G                                   TOR09160
     1 +(1.5*0.-.5*0.*(-2.75-2.25*P)-.75*0.+6.*EKA*4.5*UPP             TOR09170
     1 -.5*0.*(-1.75+.75*P))*G3                                        TOR09180
      AA(5,13)=AA(5,13)+                                               TOR09190
     1 (.5*(36.*EKA+18.*P*EKA+1.+1.5*P)+1.5-.25*M2+.5                  TOR09200
     1 - 3.*EKA-1.5-.75*(12.*EKA+1.)*P+.25*M2)*G2                      TOR09210
     1 +(.25-.25+.5*(6.*EKA+6.*P*EKA+.5+.5*P)+.375                     TOR09220
     1 - 1.5*EKA-.125*(12.*EKA+1.)*P)*G4                               TOR09230
      AA(5,14)=AA(5,14)+                                               TOR09240
     1 (-.5*M*(12.*EKA-2.+.5*P+18.*P*EKA)+.5*M*(-.75-.25*P)            TOR09250
     1 +.5*M*(.25+.25*P))*G2                                           TOR09260
      AA(5,15)=AA(5,15)+                                               TOR09270
     1 (1.5-.5*(-1.-1.5*P)-.5*M2*(-.5-.5*P)                            TOR09280
     1 +6.*EKA*(3.5+3.*P)+.5*M2-1.5-.5*(-1.+1.5*P)                     TOR09290
     1 +.5*M2)*G2                                                      TOR09300
     1 +(.25-.5*(-.5-.5*P)-.25+6.*EKA*UPP                              TOR09310
     1 -.5*(-.75+.25*P))*G4                                            TOR09320
      AA(5,16)=AA(5,16)+                                               TOR09330
     1 (.5*8.+.5*2.*(12.*EKA+9.*P*EKA+.25+.75*P)-.75*4.+.375           TOR09340
     1 - 3.*EKA-.375*(12.*EKA+1.)*P)*G3                                TOR09350
```

```
      AA(5,17)=AA(5,17)+                                                TOR09360
     1 (-.5*M*(3.*EKA-.25+.25*P+3.*P*EKA)-.125*4.*M-.125*2.*M)*G3       TOR09370
      AA(5,18)=AA(5,18)+                                                TOR09380
     1 (.5*16.-.5*4.*(-.25-.75*P)+6.*EKA*1.5*UPP-.75*8.                 TOR09390
     1 -.5*2.*(-.75+.75*P))*G3                                          TOR09400
      AA(5,19)=AA(5,19)+                                                TOR09410
     1 (.0625*27.+.5*3.*(1.5*EKA+1.5*P*EKA+.125*P)-.125*9.+.0625        TOR09420
     1 -.75*EKA-.0625*(12.*EKA+1.)*P)*G4                                TOR09430
      AA(5,21)=AA(5,21)+                                                TOR09440
     1 (.0625*81.+.0625*9.*P+6.*EKA*.25*UPP-.125*27.                    TOR09450
     1 -.5*3.*(-.125+.125*P))*G4                                        TOR09460
      AA(8,8)=AA(8,8)+                                                  TOR09470
     1 (-.5*M*(12.*EKA-2.+.5*P+18.*P*EKA)+.5*0.*M*(-.75-.25*P)          TOR09480
     1 +.5*0.*M*(.25+.25*P))*G2                                         TOR09490
      AA(8,9)=AA(8,9)+                                                  TOR09500
     1 (1.5*0.-.5*0.*(-1.-1.5*P)-.5*M2*(-.5-.5*P)                       TOR09510
     1 +6.*EKA*(3.5+3.*P)+.5*M2*0.-1.5*0.-.5*0.*(-1.+1.5*P)             TOR09520
     1 +.5*0.*M2)*G2                                                    TOR09530
     1 +(.25*0.-.5*0.*(-.5-.5*P)-.25*0.+6.*EKA*UPP                      TOR09540
     1 -.5*0.*(-.75+.25*P))*G4                                          TOR09550
      AA(8,10)=AA(8,10)+                                                TOR09560
     1 (.5+.5*(12.*EKA+9.*P*EKA+.25+.75*P)-.75+.375                     TOR09570
     1 - 3.*EKA-.375*(12.*EKA+1.)*P)*G3                                 TOR09580
      AA(8,11)=AA(8,11)+                                                TOR09590
     1 (-.5*M*(3.*EKA-.25+.25*P+3.*P*EKA)-.125*M-.125*M)*G3             TOR09600
      AA(8,12)=AA(8,12)+                                                TOR09610
     1 (.5-.5*(-.25-.75*P)+6.*EKA*1.5*UPP-.75                           TOR09620
     1 -.5*(-.75+.75*P))*G3                                             TOR09630
      AA(8,13)=AA(8,13)+                                                TOR09640
     1 (.0625*8.+.5*2.*(1.5*EKA+1.5*P*EKA+.125*P)-.125*4.+.0625         TOR09650
     1 -.75*EKA-.0625*(12.*EKA+1.)*P)*G4                                TOR09660
      AA(8,15)=AA(8,15)+                                                TOR09670
     1 (.0625*16.+.0625*4.*P+6.*EKA*.25*UPP-.125*8.                     TOR09680
     1 -.5*2.*(-.125+.125*P))*G4                                        TOR09690
      AA(11,5)=AA(11,5)+                                                TOR09700
     1 (-.5*M*(3.*EKA-.25+.25*P+3.*P*EKA)-.125*0.*M-.125*0.*M)*G3       TOR09710
      AA(11,6)=AA(11,6)+                                                TOR09720
     1 (.5*0.-.5*0.*(-.25-.75*P)+6.*EKA*1.5*UPP-.75*0.                  TOR09730
     1 -.5*0.*(-.75+.75*P))*G3                                          TOR09740
      AA(11,7)=AA(11,7)+                                                TOR09750
     1 (.0625+.5*(1.5*EKA+1.5*P*EKA+.125*P)-.125+.0625                  TOR09760
     1 -.75*EKA-.0625*(12.*EKA+1.)*P)*G4                                TOR09770
      AA(11,9)=AA(11,9)+                                                TOR09780
     1 (.0625+.0625*P+6.*EKA*.25*UPP-.125                               TOR09790
     1 -.5*(-.125+.125*P))*G4                                           TOR09800
      AA(14,3)=AA(14,3)+                                                TOR09810
     1 (.0625*0.+.0625*0.*P+6.*EKA*.25*UPP-.125*0.                      TOR09820
     1 -.5*0.*(-.125+.125*P))*G4                                        TOR09830
      RETURN                                                            TOR09840
      END                                                               TOR09850
C-----------------------------------------------------------------------TOR09860
      SUBROUTINE BANSOL(NHI)                                            TOR09870
      IMPLICIT DOUBLE PRECISION (A-H,O-Z)                               TOR09880
C     CUSTOMIZED BAND SOLVER FOR STRIP BANDED MATRIX - TOROIDAL SHELL   TOR09890
      COMMON/EEE/A(200,200),B(200),X(200),PX(200),                      TOR09900
```

```
     1          AN(200,200),BN(200,1),XN(200),WK(200)                    TOR09910
C     THE U'ZERO' EQN IS THE ZERO EQN OF THE SYSTEM                       TOR09920
C     IROW= ROW NO OF EQN BEFORE SET TO BE REDUCED                        TOR09930
C     IO  = ROW NO OF EQN TO BE REDUCED (ORIGIN ROW)                      TOR09940
C     JOS = COL NO OF PIVOT  (16,17 OR 18)  ON DESTINATION ROW            TOR09950
C     ID  = ROW NO OF EQN TO BE MODIFIED (DESTINATION ROW)                TOR09960
C     KLO = COL NO OF 1ST  COF OF ORIGIN ROW TO BE ADDED TO DEST ROW      TOR09970
C     KHI = COL NO OF LAST COF OF ORIGIN ROW TO BE ADDED TO DEST ROW      TOR09980
C     JDS = COL NO OF FACTOR OF DESTINATION ROW                           TOR09990
C     JD  = COL NO OF DESTINATION ROW TO BE MODIFIED                      TOR10000
      NEQ=NHI*3+2                                                         TOR10010
      IHI=NHI+1                                                           TOR10020
      IO=0                                                                TOR10030
C     REDUCE EQNS FOR EACH ORDER OF N                                     TOR10040
      DO 1000 I=1,IHI                                                     TOR10050
C     THREE EQNS REDUCED FOR EACH N (EXCEPT FOR N=0 THEN ONLY TWO)        TOR10060
      DO 1100 IG=1,3                                                      TOR10070
C     IG=1 'U' EQN   IG=2 'V' EQN    IG=3 'W' EQN                         TOR10080
      IF(IO.EQ.0) GO TO 1100                                              TOR10090
      IF(IO.EQ.NEQ) GO TO 1100                                            TOR10100
      JOS=12+IG                                                           TOR10110
      D=1./A(IO,JOS)                                                      TOR10120
      ID=IO                                                               TOR10130
C     A GIVEN PIVOT AFFECTS VERTICALLY 6 GROUPS OF EQNS                   TOR10140
      DO 1200 J=1,5                                                       TOR10150
      JHI=15-JOS                                                          TOR10160
      IF(J.GT.1) JHI=3                                                    TOR10170
      IF(JHI.EQ.0) GO TO 1200                                             TOR10180
C     MUST CONSIDER 1,2 OR 3 EQNS VERTICALLY IN EACH GROUP                TOR10190
      DO 1300 JG=1,JHI                                                    TOR10200
      ID=ID+1                                                             TOR10210
      IF(ID.GT.NEQ) GO TO 1300                                            TOR10220
      JDS=JOS-(J-1)*3                                                     TOR10230
      IF(JDS.LT.1) GO TO 1300                                             TOR10240
      FAC=A(ID,JDS)*D                                                     TOR10250
      IF(ABS(FAC).LT.(1.E-15)) GO TO 1300                                 TOR10260
      KLO=JOS+1                                                           TOR10270
      KHI=27                                                              TOR10280
      JD=JDS                                                              TOR10290
      DO 1400 K=KLO,KHI                                                   TOR10300
      JD=JD+1                                                             TOR10310
      IF(JD.GT.27) GO TO 1400                                             TOR10320
      A(ID,JD)=A(ID,JD)-FAC*A(IO,K)                                       TOR10330
 1400 CONTINUE                                                            TOR10340
      B(ID)=B(ID)-FAC*B(IO)                                               TOR10350
 1300 CONTINUE                                                            TOR10360
 1200 CONTINUE                                                            TOR10370
 1100 IO=IO+1                                                             TOR10380
 1000 CONTINUE                                                            TOR10390
C     BACKSUBSTITUTE   DONT HAVE '1' ON DIAGONALS                         TOR10400
C     BOTTOM SET OF THREE EQUATIONS                                       TOR10410
      X(NEQ)=B(NEQ)/A(NEQ,15)                                             TOR10420
      NEQ1=NEQ-1                                                          TOR10430
      X(NEQ1)=(B(NEQ1)-A(NEQ1,15)*X(NEQ))/A(NEQ1,14)                      TOR10440
      NEQ2=NEQ-2                                                          TOR10450
```

```
      X(NEQ2)=(B(NEQ2)-A(NEQ2,14)*X(NEQ1)-A(NEQ2,15)*X(NEQ))/A(NEQ2,13) TOR10460
C     BACKSUBSTITUTE NHI-1 GROUPS OF THREE EQUATIONS                    TOR10470
      NHIM1=NHI-1                                                       TOR10480
      DO 2000 I=1,NHIM1                                                 TOR10490
C     START WITH 'W' EQN  THEN 'V' EQN   LAST 'U' EQN                   TOR10500
      DO 2100 IG=1,3                                                    TOR10510
      JHI=15+I*3                                                        TOR10520
      IF(JHI.GT.27) JHI=27                                              TOR10530
      IF(I.GT.2.AND.IG.GT.1) JHI=24                                     TOR10540
      JLO=17-IG                                                         TOR10550
      IRA=NEQ+1-(I*3+IG)                                                TOR10560
      IK=0                                                              TOR10570
      SUM=.0                                                            TOR10580
      DO 2200 J=JLO,JHI                                                 TOR10590
      IK=IK+1                                                           TOR10600
      IRB=IRA+IK                                                        TOR10610
 2200 SUM=SUM+A(IRA,J)*X(IRB)                                           TOR10620
      X(IRA)=(B(IRA)-SUM)/A(IRA,JLO-1)                                  TOR10630
 2100 CONTINUE                                                          TOR10640
 2000 CONTINUE                                                          TOR10650
C     TOP SET OF TWO EQUATIONS                                          TOR10660
      IK=0                                                              TOR10670
      SUM=.0                                                            TOR10680
      DO 2310 J=16,27                                                   TOR10690
      IK=IK+1                                                           TOR10700
 2310 SUM=SUM+A(2,J)*X(2+IK)                                            TOR10710
      X(2)=(B(2)-SUM)/A(2,15)                                           TOR10720
      IK=0                                                              TOR10730
      SUM=.0                                                            TOR10740
      DO 2330 J=15,27                                                   TOR10750
      IK=IK+1                                                           TOR10760
 2330 SUM=SUM+A(1,J)*X(1+IK)                                            TOR10770
      X(1)=(B(1)-SUM)/A(1,14)                                           TOR10780
      RETURN                                                            TOR10790
      END                                                               TOR10800
C-------------------------------------------------------------------    TOR10810
      SUBROUTINE ADVAL(MS,N,U,V,W,PR)                                   TOR10820
      IMPLICIT DOUBLE PRECISION (A-H,O-Z)                               TOR10830
      DOUBLE PRECISION MDUM,M2,M3,M4                                    TOR10840
C     ADD CONTRIBUTION FROM ONE TERM TO DISP-STRAIN-CURV                TOR10850
C         AT EACH OF OUTPUT POINTS                                      TOR10860
      COMMON/AAA/R,RR,PSI,T,E,POI,MHI,NHI,NFI,NT,NLOAD                  TOR10870
      COMMON/BBB/ RES(40,20,10),GFI(40),GETA(40),GT(20),DATLOD(10,7)    TOR10880
      COMMON/CCC/PI5,PI2,PI,SOP2,RAD,OMP,OMP2,TP,AK,STIF,ROS,R2,R3,CZ,  TOR10890
     1           ZD,PSIR                                                TOR10900
      COMMON/FFF/P,ZK,ZC,ZX,ZY,G,G2,G3,G4,G5,MDUM,M2,M3,M4,F,Q,A,S,     TOR10910
     1           UMP,DMP,TMP,UPP,DPP,TPP,BB(9),STC(20),STS(20),STZ(20), TOR10920
     1           B2,B1,VMP,SMP,EKD,EKB,EKC,EKE,EL,EL1,H,EKA             TOR10930
      DIMENSION SETA(40),CETA(40),ST(20),CT(20)                         TOR10940
      EM=REAL(MS)                                                       TOR10950
      EN=REAL(N)                                                        TOR10960
      IF(N.GT.0) GO TO 2000                                             TOR10970
C     CASE FOR N=0   REMEMBER 'FI' SIGNIFIES 'ETA'                      TOR10980
      B=EM*PI*G/PSIR                                                    TOR10990
      DO 10 I=1,NFI                                                     TOR11000
```

```
      ARG=B*GETA(I)                                                     TOR11010
      SETA(I)=SIN(ARG)                                                  TOR11020
 10   CETA(I)=COS(ARG)                                                  TOR11030
C     COMPUTING V W E1 E2 K1 K2 PR FOR EACH OF GRID POINTS              TOR11040
      DO 11 I=1,NFI                                                     TOR11050
      DO 11 J=1,NT                                                      TOR11060
      C=STC(J)                                                          TOR11070
      Z=STZ(J)                                                          TOR11080
      ET=W/R                                                            TOR11090
      EFI=(-B*V+G*C*W)/(R*Z)                                            TOR11100
      AKFI=(-B*V*G*C+B*B*W)/(R2*Z*Z)                                    TOR11110
      RES(I,J,4)=RES(I,J,4)+V*CETA(I)                                   TOR11120
      RES(I,J,5)=RES(I,J,5)+W*SETA(I)                                   TOR11130
      RES(I,J,6)=RES(I,J,6)+ET*SETA(I)                                  TOR11140
      RES(I,J,7)=RES(I,J,7)+EFI*SETA(I)                                 TOR11150
      RES(I,J,9)=RES(I,J,9)+AKFI*SETA(I)                                TOR11160
 11   RES(I,J,10)=RES(I,J,10)+PR*SETA(I)                                TOR11170
      RETURN                                                            TOR11180
C     CASE FOR N.GT.0                                                   TOR11190
 2000 DO 20 J=1,NT                                                      TOR11200
      ARG=EN*GT(J)                                                      TOR11210
      ST(J)=SIN(ARG)                                                    TOR11220
 20   CT(J)=COS(ARG)                                                    TOR11230
C     COMPUTING U V W EX EFI KX KFI FOR EACH OF GRID POINTS             TOR11240
      DO 21 I=1,NFI                                                     TOR11250
      DO 21 J=1,NT                                                      TOR11260
      C=STC(J)                                                          TOR11270
      S=STS(J)                                                          TOR11280
      Z=STZ(J)                                                          TOR11290
      CC=CT(J)*CETA(I)                                                  TOR11300
      CS=CT(J)*SETA(I)                                                  TOR11310
      SS=ST(J)*SETA(I)                                                  TOR11320
      SC=ST(J)*CETA(I)                                                  TOR11330
      ET=(N*U+W)/R                                                      TOR11340
      EFIS=(-G*S*U)/(Z*R)                                               TOR11350
      EFIC=(-B*V+G*C*W)/(R*Z)                                           TOR11360
      AKT=(N*U+N*N*W)/R2                                                TOR11370
      AKFIC=(-C*B*V*G+B*B*W)/(R2*Z*Z)                                   TOR11380
      AKFIS=G*S*(-U-N*W)/(R2*Z)                                         TOR11390
      RES(I,J,3)=RES(I,J,3)+U*SS                                        TOR11400
      RES(I,J,4)=RES(I,J,4)+V*CC                                        TOR11410
      RES(I,J,5)=RES(I,J,5)+W*CS                                        TOR11420
      RES(I,J,6)=RES(I,J,6)+ET*CS                                       TOR11430
      RES(I,J,7)=RES(I,J,7)+(EFIC*CS+EFIS*SS)                           TOR11440
      RES(I,J,8)=RES(I,J,8)+AKT*CS                                      TOR11450
      RES(I,J,9)=RES(I,J,9)+(AKFIC*CS+AKFIS*SS)                         TOR11460
 21   RES(I,J,10)=RES(I,J,10)+PR*CS                                     TOR11470
      RETURN                                                            TOR11480
      END                                                               TOR11490
C-----------------------------------------------------------------------TOR11500
      SUBROUTINE RESULT                                                 TOR11510
      IMPLICIT DOUBLE PRECISION (A-H,O-Z)                               TOR11520
C     FINALIZE SOLUTION VALUES AND WRITEOUT                             TOR11530
      COMMON/AAA/R,RR,PSI,T,E,POI,MHI,NHI,NFI,NT,NLOAD                  TOR11540
      COMMON/BBB/ RES(40,20,10),GFI(40),GETA(40),GT(20),DATLOD(10,7)    TOR11550
```

```
      COMMON/CCC/PI5,PI2,PI,SOP2,RAD,OMP,OMP2,TP,AK,STIF,ROS,R2,R3,CZ,  TOR11560
     1           ZD,PSIR                                                TOR11570
C     START WITH   FI T(DEG) U V W ET  EFI KT  KFI  PR                   TOR11580
C     FINALISE TO  FI T(DEG) U V W STT STB SFIT SFIB  PR                 TOR11590
      WRITE(8,16)                                                       TOR11600
 16   FORMAT(/' RESULTS FOR DISPLACEMENTS(MM) AND STRESSES(MPA)'/       TOR11610
     1   7X,'FI',3X,'THETA',9X,'U',14X,'V',14X,'W',11X,                 TOR11620
     2   'STTOP',10X,'STBOT',10X,'SFITOP',9X,'SFIBOT',7X,'PR')          TOR11630
      DO 100 I=1,NFI                                                    TOR11640
      DO 110 J=1,NT                                                     TOR11650
      ENT=AK*(RES(I,J,6)+POI*RES(I,J,7))                                TOR11660
      ENFI=AK*(RES(I,J,7)+POI*RES(I,J,6))                               TOR11670
      EMT=ZD*(RES(I,J,8)+POI*RES(I,J,9))                                TOR11680
      EMFI=ZD*(RES(I,J,9)+POI*RES(I,J,8))                               TOR11690
 116  FORMAT(1X,'EMT = ',D15.6,2X,'EMFI = ',D15.6)                      TOR11700
      RES(I,J,6)=ENT/T+EMT*CZ                                           TOR11710
      RES(I,J,7)=ENT/T-EMT*CZ                                           TOR11720
      RES(I,J,8)=ENFI/T+EMFI*CZ                                         TOR11730
      RES(I,J,9)=ENFI/T-EMFI*CZ                                         TOR11740
 110  WRITE(8,26) (RES(I,J,K),K=1,10)                                   TOR11750
 26   FORMAT(1X,2F8.2,7D15.6,F8.4)                                      TOR11760
 100  WRITE(8,36)                                                       TOR11770
 36   FORMAT(1H )                                                       TOR11780
      RETURN                                                            TOR11790
      END                                                               TOR11800
C***************************** END ***********************************  TOR11810
C     LISTING FOR TORSAN EXEC                                           TOR11820
C-----------------------------------------------------------------------  TOR11830
C/*                                                                     TOR11840
C F EXEC WILL RUN A VS FORTRAN PROGRAM.                                 TOR11850
C IT IS INVOKED BY TYPING:                                              TOR11860
C       F <PROGRAM NAME> O( ONOCOMPILE" OSINGLE" ODATA=<DATA FILE NAME>"TOR11870
C                           ORESULT=<RESULT FILE NAME>"                 TOR11880
C                           OLIBRARY=<TEXT LIBRARY NAME>" "             TOR11890
C WHERE OPTIONAL ARGUMENTS ARE:                                         TOR11900
C       NOCOMPILE: USED IF A COMPILED TEXT VERSION EXISTS.              TOR11910
C       SINGLE: SPECIFIES THAT THE SINGLE PRECISION IMSL LIBRARY SHOULD TOR11920
C               BE USED. THE DEFAULT IS DOUBLE PRECISION.               TOR11930
C       DATA: GIVES THE NAME OF THE INPUT DISK FILE, OF FILETYPE DATA.  TOR11940
C             THE DEFAULT IS THE PROGRAM NAME.                          TOR11950
C       RESULT: GIVES THE NAME OF THE RESULT FILE, OF FILETYPE RESULT.  TOR11960
C               THE DEFAULT IS THE PROGRAM NAME.                        TOR11970
C       LIBRARY: GIVES THE NAME OF A USER SUPPLIED TEXT LIBRARY.        TOR11980
C IN THE FORTRAN PROGRAM, THE FILE NUMBERS USED MUST BE: 5 FOR INPUT FROTOR11990
C DISK DATA FILE; 6 FOR OUTPUT TO DISK DATA FILE; 7 FOR INPUT/OUTPUT WITTOR12000
C THE TERMINAL.                                                         TOR12010
C */                                                                    TOR12020
C PARSE UPPER ARG PROGRAMNAME '(' OP.1 OP.2 OP.3 OP.4 OP.5              TOR12030
C DATANAME=PROGRAMNAME                                                  TOR12040
C RESULTNAME=PROGRAMNAME                                                TOR12050
C IMSLLIBRARY='IMSLDLIB'                                                TOR12060
C USERLIBRARY=''                                                        TOR12070
C DO I=1 TO 5                                                           TOR12080
C    PARSE VAR OP.I OPTION '=' ARGUMENT                                 TOR12090
C   IF ABBREV('NOCOMPILE',OPTION,1) THEN COMPILE='NO'                   TOR12100
```

```
C    IF ABBREV('DATA',OPTION,1) THEN DATANAME=ARGUMENT                    TOR12110
C    IF ABBREV('RESULT',OPTION,1) THEN RESULTNAME=ARGUMENT                TOR12120
C    IF ABBREV('SINGLE',OPTION,1) THEN IMSLLIBRARY='IMSLSLIB'             TOR12130
C    IF ABBREV('LIBRARY',OPTION,1) THEN USERLIBRARY=ARGUMENT              TOR12140
C END                                                                     TOR12150
C IF COMPILE /= 'NO' THEN 'FORTVS' PROGRAMNAME '(SDUMP'                   TOR12160
C 'GLOBAL TXTLIB VLNKMLIB VFORTLIB CMSLIB' IMSLLIBRARY                    TOR12170
C 'FILEDEF 5 DISK' DATANAME 'DATA A'                                      TOR12180
C 'FILEDEF 8 DISK' RESULTNAME 'RESULT A (LRECL 130'                       TOR12190
C 'FILEDEF 6 TERMINAL'                                                    TOR12200
C /*  'ERASE' PROGRAMNAME 'LISTING'    */                                 TOR12210
C 'LOAD' PROGRAMNAME '(START'                                             TOR12220
C-------------------------------------------------------------------      TOR12230
C     LISTING FOR TORSAN DATA FILE                                        TOR12240
C-------------------------------------------------------------------      TOR12250
C$DATA                                                                    TOR12260
C     PAD LOADING USING TORSAN PROGRAM  JUNE30,1991                       TOR12270
C     51 ,25, 15,10, 1                                                    TOR12280
C     84.15, 252.45, 90., 7.1, .207D06, .3                                TOR12290
C     .0,11.25,22.5,27.5,30.,32.5,37.5,45.,52.5,57.5,60.,62.5,67.5,       TOR12300
C     78.75,90.                                                           TOR12310
C     0.,5.,15.,30.,45.,67.5,90.,120.,150.,180.                           TOR12320
C     1., 7.5, 7.5, 15., 15.                                              TOR12330
C************************END ALL************************************      TOR12340
```